The Role of Oxygen Supply in the Regulation of Neural Stem Cell Proliferation in the Brain of *Drosophila*

Bach. Martín Baccino

A thesis submitted for the Degree of

Master of biological sciences

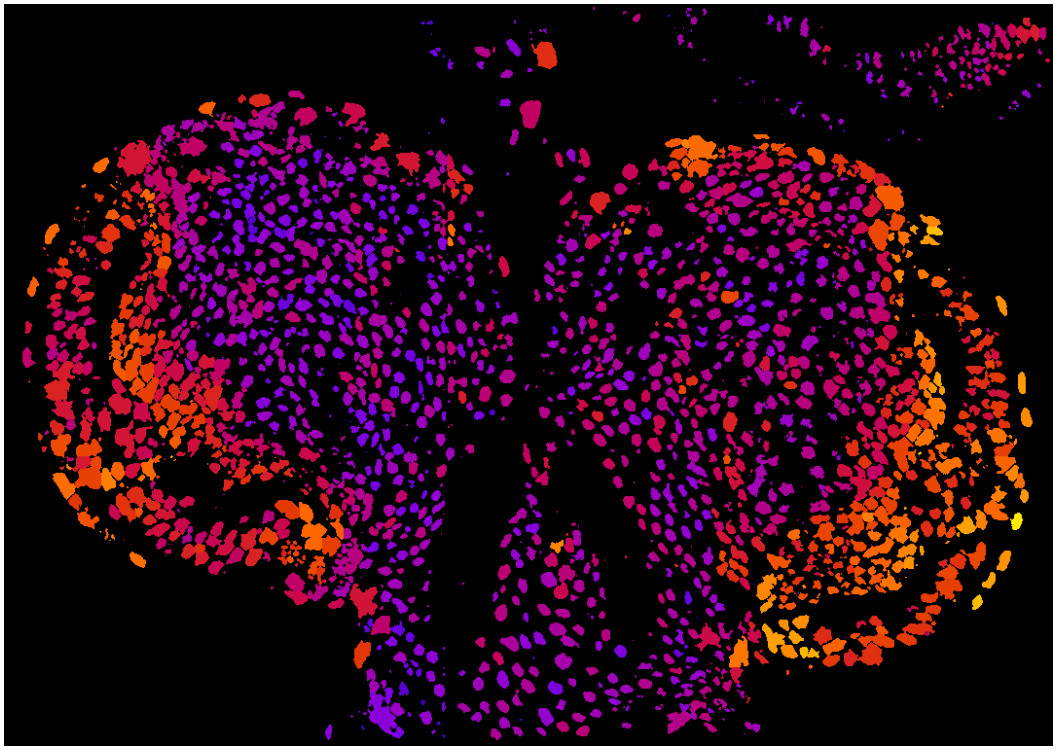

Programa de Desarrollo de Ciencias Básicas
(PEDECIBA)
Instituto de Investigaciones Biológicas Clemente Estable
(IIBCE)

2016

Thesis Supervisor: Dr. Rafael Cantera
Thesis Co-Supervisor: Dr. Boris Egger

Table of contents

Abstract 3

Resumen (Spanish) 4

Introduction..... 5

Oxygen, a metabolic double edge sword: balancing metabolic needs and toxicity ..5

Stem cells and hypoxia 7

Neural stem cells are maintained in hypoxia 10

Hypoxia protects stem cells from oxidative damage 12

The hypoxia response in mammals and insects 13

The optic lobe harbors proliferative neuroepithelial cells and it´s progeny.....16

In insects oxygen is delivered to tissues through the tracheal system.....21

The developing larval brain is differentially tracheolated 26

Hypothesis and aims of this thesis 28

Objective.....29

Specific Objectives.....29

Materials and Methods 31

Fly stocks 31

Larval staging.....31

Larval dissection and immunostainings 31

Laser confocal microscopy 32

Image analysis 32

Statistical analysis.....34

Tracheolar 3D reconstruction and measurements 34

Oxygen sensor and ratiometric analysis 35

Hyperoxia and hypoxia treatment 39

Results....40

The central brain is more densely tracheolated than the optic lobe....40

The tracheal pattern correlates with O2 availability in the brain as measured by oxygen dependent degradation of GFP-ODD....40

The sensor suggests that the asymmetry in O2 distribution is sustained throughout all stages of larval development....45

Ambient hyperoxia reduces Oxygen dependent degradation of GFP in the optic lobe and diminishes proliferation....48

Ambient hypoxia reduces oxygenation of the brain....52

Using the GAL4-UAS system to direct tracheolar growth in the optic lobe guided by bnl expression....54

Ectopic expression of *bnl* with a Bolwig nerve driver induces the growth of ectopic tracheoles into the optic lobe along the Bolwig nerve....56

Ectopic tracheolation reduces mitotic activity in the optic lobe....62

Ectopic tracheolation of the optic lobe appear not to cause malformation of the adult brain....64

Neuroblasts and neuroepithelial cells are the most hypoxic cell type in the brain.66

Discussion....69

The optic lobe is hypoxic in comparison to the central brain which correlates with the tracheal pattern in the brain....69

Possible metabolic implications of hypoxia in the optic lobe....72

Oxygenation of the optic lobe results in diminished mitotic activity, suggesting hypoxia is important for optic lobe stem cells to keep their normal rate of mitotic activity....73

Cell type specific analysis of hypoxia response activation....75

Conclusion and perspectives....78

Acknowledgements....79

References....80

Abstract

During its development, the nervous system manages to induce neuronal differentiation in certain areas while maintaining proliferation in others. The control of proliferation and differentiation within a tissue is of great biological interest and also of relevance for our understanding of pathologies like Cancer. In insects oxygen is supplied to tissues by a network of air tubes (tracheoles) that delivers oxygen to each individual cell. During larval development, the *Drosophila* brain is densely tracheolated in a region containing mostly differentiated neurons but sparsely tracheolated in a region containing neural stem cells and postmitotic cells, the optic lobe. Our main hypothesis is that this asymmetric distribution of tracheoles is important for normal brain development. We propose that in the optic lobe hypoxia promotes proliferation and/or inhibits differentiation. A novel fluorescent hypoxia sensor used here showed that sima-based hypoxia response is more activated in the optic lobe when compared with the central brain suggesting that the sparse tracheolation of the OL results in a reduced O_2 supply. Rearing larvae in hyperoxia induces a reduction of proliferation in the optic lobe that results in fewer dividing neuroepithelial cells and neuroblasts, and smaller brains. Manipulating FGF signaling using the GAL4-UAS system allowed us to guide tracheoles into the OL inducing the localized oxygenation of the optic lobe. Also this experimental approach resulted in increased supply of O_2 and a reduction of the proliferation rate of neuroepithelial cells. Finally, a cell specific analysis of O_2 distribution in the brain revealed differences in oxygenation among cell types. In conclusion, we demonstrated that the differential tracheolation of the larval brain is important for brain development and managed to establish a model system to study neural stem cell function and homeostasis in relation to O_2 availability *in vivo*.

Resumen

Durante su desarrollo, el sistema nervioso logra inducir la diferenciación neural al tiempo que mantiene otras células en estado proliferativo. El control de la proliferación y la diferenciación cellular dentro de un tejido es de gran interés y relevancia para el entendimiento de patologías como el Cáncer. En insectos el oxígeno llega a los tejidos por una compleja red de tubos llamado sistema traqueal. Durante su desarrollo, el cerebro larval de *Drosophila* está densamente traqueolado en una región que contiene principalmente neuronas diferenciadas pero escasamente traqueolado en una región que contiene células madre neurales y células postmitóticas, los lóbulos ópticos. Nuestra principal hipótesis es que la distribución asimétrica de traqueolas es importante para el desarrollo normal del cerebro. Proponemos que en los lóbulos ópticos la hypoxia o bajos niveles de oxígeno, promueve la proliferación y/o inhibe la diferenciación. Un sensor de hipoxia recientemente desarrollado y utilizado aquí mostró que la repuesta a hypoxia basada en Sima, está más activa en los lóbulos ópticos en comparación con el cerebro medio sugiriendo que la escasa traqueolación de los lóbulos ópticos resulta en bajos niveles de oxígeno. Larvas expuestas a hiperoxia muestran una disminución de la proliferación en las células neuroepiteliales de los lóbulos ópticos, un menor número de neuroblastos y cerebros más pequeños. La manipulación del desarrollo traqueal en el cerebro larval utilizando el sistema GAL4-UAS nor permitió guiar el crecimiento de traqueolas a los lóbulos ópticos induciendo una oxigenación localizada. En coherencia con el resultado anterior, este experimento resultó en una oxigenación de los lóbulos ópticos que produjo una disminución de su actividad proliferativa. Finalmente, un estudio más detallado con el sensor evidenció diferencias en la respuesta a hipoxia entre los distintos tipos celulares. En conclusión demostramos que la traqueolación asimétrica del cerebro es importante para el su desarrollo y logramos establecer un modelo para el estudio de las células madre neurales en relación a la hipoxia *in vivo*.

Introduction

Oxygen, a metabolic double edge sword: balancing metabolic needs and toxicity

Oxygen (O2) appeared on Earth 2.2 million years ago and represented one of the most significant changes in the history of life. The oxygenation of the atmosphere began when ancestors of cyanobacteria developed the capacity to fix atmospheric CO2 at the same time they liberated O2 into the atmosphere as a result of what is called oxygenic photosynthesis (De Marais, 2000; Dismukes et al., 2001; Knoll, 2003; Raymond and Segrè, 2006). Oxygen is a strong oxidizing agent and has the second-highest electronegativity of all reactive elements, second only to fluorine. It has a steep thermodynamic gradient favoring its reduction, hence, it tends to oxidize other molecules and creates reactive oxygen species (ROS), which are molecules and ions of O_2 that have an unpaired electron, thus rendering them extremely reactive (Catling et al., 2005; Koch and Britton, 2007, 2008). ROS are normally produced as a normal by-product of cellular metabolism and have the capacity to cause damage to macromolecules like proteins and DNA (Erecińska and Silver, 2001; Bruick, 2003; Busuttil et al., 2003; Raymond and Segrè, 2006) and destabilize lipid membranes. Organisms evolved at the same time that O_2 concentration produced by photosynthetic organisms increased, which served as evolutionary pressure to develop different mechanisms to cope and adapt to the increasing O_2 concentration (Raymond and Segrè, 2006; Ivanovic, 2009). Today's atmosphere exhibits a high concentration of O_2 (20.8%); 156 mm Hg, at sea level. Organisms that didn't evolve in anoxic niches developed different mechanisms that allowed them to detoxify O_2. In most cases, this adaptation was so profound that organisms became metabolically dependent on oxygen. In fact, oxidative phosphorylation is believed to have appeared in evolution as a mechanism that diminishes O_2 concentration using it as a substrate for the production of highly energetic phosphate compounds (De Marais, 2000; Dismukes et al., 2001; Ivanovic, 2009). Additionally, the evolution of parallel antioxidant reactions prevent the accumulation of damaging reactive oxygen species (ROS) deriving from incomplete reduction of O_2 (Young and Woodside, 2001). As a result of the bivalent

relationship that organisms maintain with O_2, partial pressure of oxygen became one of the key elements controlling living processes on Earth. It is believed that the diversity of multicellular complex organisms has been greatly facilitated by the transition from an inefficient anaerobic metabolism to the highly effective process of oxidative phosphorylation (Erecińska and Silver, 2001). Complete combustion of 1 mol of glucose under aerobic conditions yields 36–38 mol of ATP while breakdown to lactate, generates only 2 mol of ATP under anaerobic conditions (Erecińska and Silver, 2001). In the brain, one of the higher energy consuming organs, 95% of the total ATP synthesis occurs through oxidative phosphorylation (Erecińska and Silver, 2001).

However, oxygen remains to be toxic and its tension in tissues needs to be tightly regulated. Atmospheric O_2 is excessively high for most cells. Organisms developed complex respiratory and circulatory systems that ensure that the O_2 concentration that reaches the cells covers their metabolic needs without compromising the cells health by keeping O_2 concentration to a minimum. In humans, air enters the lungs with a O_2concentration of 156 mmHg or 21% (Panchision, 2009). When O_2 reaches circulation, its concentration drops to values between 4% to 14% which is similar to values in well irrigated organs such as the liver, kidney, and heart (Wölfle and Jungermann, 1985; Jungermann and Kietzmann, 1997; McKinley and Butler, 1999; Welch et al., 2001; Roy et al., 2003; Saltzman et al., 2003; Mik et al., 2004; Johnson et al., 2005; Wild et al., 2005). Because the brain is one of the most metabolically active tissues in the body (Hoge and Pike, 2001) O_2 levels are tightly regulated and vary from 0,5% to 7% depending on the brain area (Whalen et al., 1967; Nwaigwe et al., 2000; Erecińska and Silver, 2001; Hemphill et al., 2005; Panchision, 2009). Other tissues such as the bone marrow (Tøndevold et al., 1979; Chow et al., 2001) and the retina (1% to 5%; Buerk et al., 1993; Yu and Cringle, 2005) have different O_2 concentrations depending on their particular needs. Based on this accumulated knowledge, some authors make the precision of distinguishing atmospheric normoxia (21%) from the much lower oxygen concentration normally found in tissue that should be called in situ normoxia or physiologic normoxia (Ivanovic 2009). Due to the practical difficulties of introducing electrodes to measure O_2 (Davies and Brink, 1942) in live tissues (Oxygen microelectrodes are invasive; (Erecińska and Silver, 2001), it took

researchers many years to discover that O_2 concentrations *in vivo* were much lower than in the atmosphere (Davies and Brink, 1942; Erecińska and Silver, 2001). Hence, when using the term hypoxia, which refers to low oxygen levels and is a common feature for many cell types both in normal and pathological conditions, a distinction must be made between tissue hypoxia and atmospheric hypoxia (Guitart et al., 2010).

Stem cells and hypoxia

Stem cells reside in microenvironments called “niches”, a concept introduced by (Schofield, 1978) in 1978 (Slack, 2008). The stem cell niche refers to an anatomical compartment with cellular and acellular components integrating signals that control the homeostasis of stem cells and mediate the balanced response of stem cells to the needs of organisms (Li and Xie, 2005; Scadden, 2006; Yin and Li, 2006; Jones and Wagers, 2008; Mohyeldin et al., 2010;). Cells, blood vessels (in vertebrates and some invertebrates) or tracheoles (in Artrhopoda invertebrates), matrix glycoproteins, and the structure of the space itself provide a highly specialized microenvironment that helps maintain the combined properties of a stem cell: self-renewal and multipotency (Scadden, 2006). Oxygen concentration is an important cue that needs to be tightly regulated for the maintenance of the niche homeostasis.

Already in 1987 (Dello Sbarba et al., 1987) it was hypothesized that hypoxia at the stem-cell niche was a necessary condition for the maintenance of stem cells which is somewhat counterintuitive, given that fluctuations in oxygen availability are a major cause of cell death (Casaccia-Bonnefil, 2000; Saito et al., 2005). Tissues known to harbor stem cells keep even lower O_2 levels than other tissues (Cipolleschi et al., 1993; Braun et al., 2001; Erecińska and Silver, 2001; Mohyeldin et al., 2010). After years of research it is a widely accepted idea that hypoxia, relative to surrounding tissues, is a common feature of the environment of many stem cells such as embryonic, hematopoietic, cancer and neural stem cell (Figure 1**;** Ezashi et al., 2005; Simon and Keith, 2008; Mazumdar et al., 2010; Mohyeldin et al., 2010; Simsek et al., 2010; Takubo et al., 2010; Lee and Simon, 2012). For years oxygen was disregarded as an important cue for growing cells *in vitro*, and atmospheric normoxia was (and to this

day sometimes is) refered to as “standard culture conditions” (Ivanovic, 2009). Today, there is plentiful evidence that an oxygen concentrations below atmospheric normoxia favors survival and proliferation of stem cells *in vitro* (Csete, 2005; Mohyeldin et al., 2010).

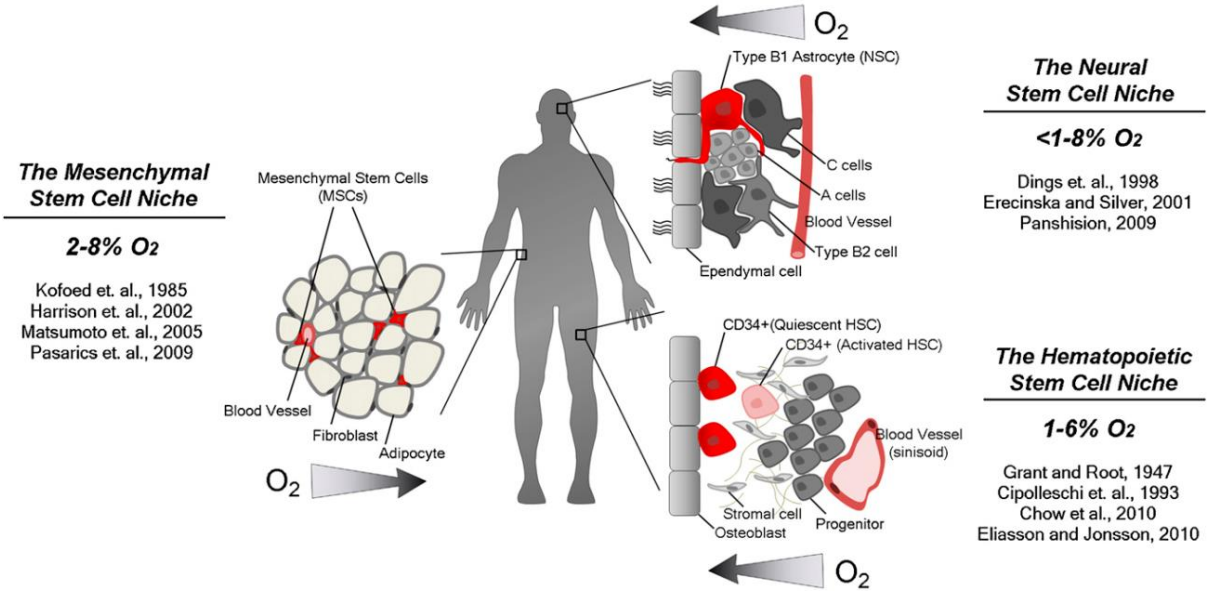

Figure 1. Low oxygen concentrations in various stem cell compartments*. Schematic models for the hematopoietic, mesenchymal and neural stem cell niches in Homo sapiens in their respective niches: bone marrow, adipose tissue, and the subventricular zone (SVZ), respectively. Red cells represent HSCs, MSCs, and NSCs. Measured or calculated* O_2 *concentrations for the different niches are specified. Image reproduced from Mohyeldin et al., 2010.*

The most well-characterized stem cell niche is that of the hematopoietic stem cells (HSC; Parmar et al., 2007; Lee and Simon, 2012) which has been described in detail (Calvi et al., 2003; Zhang et al., 2003) and has shown relative low levels of O_2 compared to other tissues (Harrison et al., 2002; Parmar et al., 2007). In 1993 Cipolleschi and collaborators (1993) used Hematopoietic stem cells in culture to study

the effect of O_2 concentration on stem cells and showed that a hypoxic environment contributes to the maintenance of an undifferentiated state. They proposed that in living tissues the distance a cell is from a blood vessel could be an indicator of its hierarchy as a stem cell. This means that a cell receiving low levels of O_2 should have higher multipotency and less fate commitment than a cell receiving more O_2. Hematopoietic stem cells are located at the lowest end of the oxygen gradient in bone marrow (Eliasson et al., 2010). Accordingly, *in vitro* incubation in severe hypoxia leads to a substantial concentration of progenitors of the highest hierarchical level (Cipolleschi et al., 1993; Eliasson et al., 2010).

Embryonic stem cells are generally derived from the inner cell mass of blastocysts produced by in vitro fertilization techniques (Thomson et al., 1998; Reubinoff et al., 2000). The environment of the mammalian reproductive tract, to which naturally conceived embryos are exposed, has an O_2 concentration between 1.5 and 5.3% (Fischer and Bavister, 1993; Aplin, 2000). Hypoxia is fundamental for the correct formation of several organs during embryonic development: heart, placenta, and bone (Dunwoodie, 2009). Cell culture experiments with embryonic stem cells in which morphological, immunohistochemical and biochemical analysis were performed showed that raising embryonic stem cells in hypoxia (1-5%) significantly reduces differentiation (Ezashi et al., 2005). The hypoxia-stem cell paradigm gained great relevance when it was also described that hypoxia was a common feature in the environment that supports cancer stem cells (Helmlinger et al., 1997; Braun et al., 2001; Brahimi-Horn et al., 2007; Bao et al., 2012). Measurements of PO_2 in tumors have been made using optical fluorescent techniques (Young et al., 1996; Helmlinger et al., 1997), hypoxia markers (Kennedy et al., 1997) and polarographic electrodes (Kruuv et al., 1967; Kallinowski et al., 1990; Dewhirst et al., 1998). It is estimated that up to 60% of locally advanced solid tumors exhibit hypoxic or anoxic conditions relative to their surrounding tissue (Favaro et al., 2011). It has been thoroughly reported that hypoxia increases tumor aggressiveness (Moulder and Rockwell, 1987; Teicher, 1994; Hockel et al., 1996; Fyles et al., 2002; Jubb et al., 2010), and approximately a three times larger radiation dose is required to kill hypoxic cells in comparison with normal cells (Tubiana et al., 1990). Hypoxia probably acts as a positive selective pressure for

cells that have lost their apoptotic response to hypoxia (Carmeliet and Jain, 2000). According to the later findings hypoxia drives tumor growth because it enhances the survival and self-renewal capacity of cancer stem cells (Ezashi et al., 2005; Gustafsson et al., 2005; Chen et al., 2007; Simon and Keith, 2008; McCord et al., 2009; Zeng et al., 2011).

Neural stem cells are maintained in hypoxia.

In 1997 the first paper reporting a functional relationship between neural precursors and hypoxia was published (Nurse and Vollmer, 1997). In that study embryonic cells of the carotid body were studied *in vitro* to test their response to hypoxia and it was found that a combination of bFGF signaling and hypoxia (6% O_2) induce cell survival and proliferation. Later, an elegant study performed *in vivo*, (Pardal et al., 2007) showed that carotid body cells proliferate in response to the exposure of mice to atmospheric hypoxia, causing the carotid body to grow in size. Once O_2 levels returned to normal, the birth of new neurons decreased (Panchision, 2009). This was also confirmed for isolated neural crest stem cells from which the carotid body is derived (Morrison et al., 2000). The carotid body shows a niche-like architecture similar to the adult brain SVZ (Kokovay and Temple, 2007); however, these particular cells are a type of very specific neuronal precursors. In the carotid body, they function as O_2-sensitive chemoreceptors that relay information to the CNS and adapt mammalian breathing responses to short term changes in O_2 in the environment, and therefore, it is expectable that they would be sensitive to variations in oxygen concentrations (Studer et al., 2000). In the mammalian CNS, interstitial tissue O_2 levels range approximately from 1 to 5% (Panchision, 2009). The first *in vitro* studies with CNS cells used embryonic day 12 rat mesencephalic precursors and showed that in lowered O_2 conditions proliferation was promoted, while apoptosis was reduced, yielding a greater number of precursors (Studer et al., 2000). Human fetal mesencephalic CNS precursor cells were expanded in an undifferentiated state for months using EGF and FGF-2 as mitogens and lowered oxygen conditions yielding a much greater proportion of TH+ (Tyrosine hydroxylase) dopamine neurons in culture

(Storch et al., 2001; Milosevic et al., 2005). Monolayer cultures of mouse fetal cortical NSCs showed that 5% O_2 permitted clonal and long-term expansion, while 20% O_2 caused a rapid induction of p53 and apoptosis (Chen et al., 2007; Panchision, 2009). Moreover, in high oxygen levels cell death occurred predominantly among multipotent stem cells and less in neuronal progenitors which are comparably inferior in the stem cell hierarchy. The authors hypothesize that oxygen could be detrimental for the expansion of multipotent cells but not neuronal progenitors; an alternative is that 20% oxygen tension inhibits the expansion of all precursors equally, but also selectively inhibits the maturation of glia (Chen et al., 2007). The same was shown for human neural stem cells derived from embryonic tissue. Low oxygen tensions specifically promoted the proliferation of nestin-positive human postnatal CNS precursors. Expansion in 5% oxygen increased the proportion of these cells with a stem cell phenotype, and the ability of the precursors to generate different CNS lineages (neurons, astrocytes and oligodendrocytes). In contrast, 20% oxygen caused precursors to differentiate into astrocytes. These results indicated that the principal response to 20% oxygen exposure is terminal differentiation of precursors to an astrocytic fate (Pistollato et al., 2007). In addition, atmospheric O_2 concentration (20%) promoted differentiation of cortical neuronal progenitors (Gustafsson et al., 2005) and terminal differentiation of human postnatal NSCs and OPCs (Pistollato et al., 2007). The central nervous system has traditionally been viewed as a system with a very limited capacity for self-renewal through addition of new cells along life (Mannello et al., 2011). However, NSCs niches active during adult life have been found in certain brain regions in vertebrates and invertebrates. In the adult mammalian brain two of those regions are the subventricular zone (SVZ) of the lateral ventricle and the subgranular zone (SGZ) of the dentate gyrus of the hippocampus. These NSCs produce neural and glial progenitors which are more fate determined and give rise to neurons and glial cells respectively

Hypoxia protects stem cells from oxidative damage

The main hypothesis explaining the tendency of stem cells to reside in hypoxic niches is that low oxygen will reduce the probability of oxidative damage of DNA, proteins and membrane lipids (Cipolleschi et al., 1993; Simon and Keith, 2008). The development and maintenance of healthy tissues depends upon appropriate stem cell regulation, therefore, it is extremely vital that they avoid damage of any kind and specially DNA damage caused by ROS (Burgess et al., 2014). Essentially all cells that use aerobic metabolism are subject to some degree of oxidative stress. The generation of ROS can damage DNA, proteins, lipids and even carbohydrates (Erecińska and Silver, 2001). A direct evidence of this is that mouse embryonic fibroblasts accumulate more mutations and senesce faster when cultured under 20% O_2 than when cultured under 3% O_2 (Busuttil et al., 2003). By residing in anatomical compartments that experience relatively low oxygen tensions stem cells may be protected from this damage.

Some research proposes that hypoxia enhances stem-cell survival by inducing a low energy state maintained mainly by glycolytic metabolism (Dello Sbarba et al., 1987; Cipolleschi et al., 1993). This represents a challenge for proliferative cells as cell division requires the production of macromolecules and ATP which is difficult to achieve in an anaerobic metabolism (Burgess et al., 2014). In some cancer cells, this may be accomplished through the Warburg effect. The Warburg effect is characterized by anaerobic glycolysis in the presence of oxygen, with some pyruvate being converted to lactate rather than entering the tricarboxylic acid (TCA) cycle (Levine and Puzio-Kuter, 2010). This allows products of glycolysis to be diverted to anabolic biosynthetic pathways rather than undergoing complete oxidation to carbon dioxide and water in the TCA cycle. The Warburg Effect has been proposed to be an adaptation mechanism to support the biosynthetic requirements of proliferation under hypoxic conditions. In this scenario, the increased glucose consumption is used as a carbon source for the anabolic processes needed to support cell proliferation (DeBerardinis et al., 2008; Vander Heiden et al., 2009; Levine and Puzio-Kuter, 2010; Cairns et al., 2011; Koppenol et al., 2011; Dang, 2012; Patra et al., 2013; Boroughs and DeBerardinis, 2015). This

excess carbon is directed into the multiple pathways that derive from glycolysis, and used for the generation of nucleotides, lipids, and proteins (Liberti and Locasale, 2016)

The hypoxia response in mammals and insects

Metazoans developed the capacity to sense oxygen concentration and to respond through rapid behavioral and long-term physiological adaptations inducing adaptive modifications that regulate oxygen delivery (Morrison et al., 2000; Mannello et al., 2011). Physiological changes in oxygen homeostasis involve the hypoxia-inducible pathway, which is well conserved along all metazoans (Branicky and Schafer, 2008).

The master regulator of the hypoxia response is the Hypoxia Inducible Factor (HIF), a heterodimeric transcription factor consisting of the regulatory HIF-alpha subunit (Wang and Semenza, 1995) and the constitutive HIF-beta subunit, both of which contain basic helix-loop-helix (bHLH) and PER-ARNT-SIM (PAS) domains (Wang and Semenza, 1995). The stability of HIF-alpha depends on oxygen concentration. HIF-alpha is degraded under physiological normoxia (Figure 2A; Huang et al., 1998; Pugh and Ratcliffe, 2003) and stabilized under hypoxia (Figure 2B). When stabilized, the factor translocates into the nucleus where it heterodimerizes with HIF-beta and binds to specific DNA recognition motifs (Maxwell et al., 1993; Firth et al., 1995) inducing the expression of target genes that mediate adaptations to hypoxia. Under normoxia prolyl hydroxylase domain (PHD) 2-oxoglutarate-dependent dioxygenases hydroxylate HIF-alpha on specific proline residues in the oxygen-dependent degradation domain (ODD; Figure 2A; Huang et al., 1998; Epstein et al., 2001; Ivan et al., 2001; Jaakkola et al., 2001). The complex formed by HIF and PHD is recognized by the von Hippel Lindau (VHL) protein, and marked for ubiquitin-mediated proteasomal degradation (Figure 2A; Berra et al., 2006; Bruick, 2003; Iwai et al., 1999; Lisztwan et al., 1999; Maxwell et al., 1993). As PHD uses 2-oxoglutarate and molecular oxygen as co-substrates, prolyl hydroxylase activity directly depends on the partial pressure of O_2 (Ivan et al., 2001; Kaelin and Ratcliffe, 2008). In mammals, but not *Drosophila*, the asparaginyl hydrosylase (FIH-1) acts on an asparaginyl residue in the c-terminal transactivation

domain of mammalian HIF-1alpha inhibiting the interaction of HIF-1alpha subunits with co-activating factors (Lando et al., 2002). The basic machinery for sensing and responding to hypoxia is evolutionary conserved. However, when compared to *Drosophila*, the mammalian system is more complex and redundant (Figure 2; Gorr et al., 2006; Romero et al., 2008). Whereas there is just one HIF-alpha in *Drosophila* which is called Sima, there are three HIF-alpha proteins in mammals (Nambu et al., 1996; Bacon et al., 1998). Likewise, there is just one PDH oxygen sensor in the fly, encoded by the gene *fatiga (fga)*, that controls Sima half-life as a function of pO_2 (Figure 2A and 2B; Lavista-Llanos et al., 2002; Centanin et al., 2005; Dekanty et al., 2005). The HIF-beta subunit of *Drosophila* is called Tango (Figure 2B). HIF acts on a number of signalling pathways controlling the expression of target genes that mediate adaptations to hypoxia, such as vascular endothelial growth factor (involved in angiogenesis) in vertebrates, and genes involved in tracheal system development in Invertebrates, as well as genes involved in cell-cycle regulation, cell survival, and cellular metabolism (Carmeliet et al., 1998; Goda et al., 2003; Eliasson et al., 2010). Some HIF target genes promote anaerobic metabolism to reduce oxygen consumption, while others ‘‘alleviate’’ hypoxia by acting non-cell-autonomously to extend and modify the surrounding vasculature (vertebrates) or tracheal system (*Drosophila* and other invertebrates; Dunwoodie, 2009). Moreover, the active HIF complex transcriptionally induces glycolytic enzymes as well as other targets to promote optimal energy utilization adapting cell metabolism to the hypoxic environment (Bruick, 2003).

There is increasing evidence that O_2 response signals interact with signals that are central to controlling neural precursor proliferation and cell fate. Two critically important developmental pathways are known to interact with the HIF signalling pathway in NSCs. One is the Notch pathway, so named because it was first described in the fly and mutations in this gene cause abnormal wing morphology, with “notchs”. Notch is a transmembrane receptor which is cleaved upon ligand binding (Delta and Jagged) and activates target genes (Gordon et al., 2008). Notch signalling acts as a stem cell self-renewal and anti-neurogenic signal during CNS development (Corbin et al., 2008). When HIF is stabilized by hypoxia, it interacts with Notch and promotes the

undifferentiated state of neural stem cells. When in physiologic normoxia, Notch is prevented from interacting with HIF allowing cells to differentiate (Gustafsson et al., 2005). An additional convergent pathway has been identified involving bone morphogenetic proteins (BMPs). These secreted ligands bind to receptor complexes that catalyse the phosphorylation and activation of the canonical SMAD proteins (Nohe et al., 2004). BMPs are well-characterized inducers of CNS stem cell differentiation (Chen et al., 2007; Panchision, 2009). Low O_2 exerts a repressive effect on BMP signalling in an HIF-dependent manner (Pistollato et al., 2007).

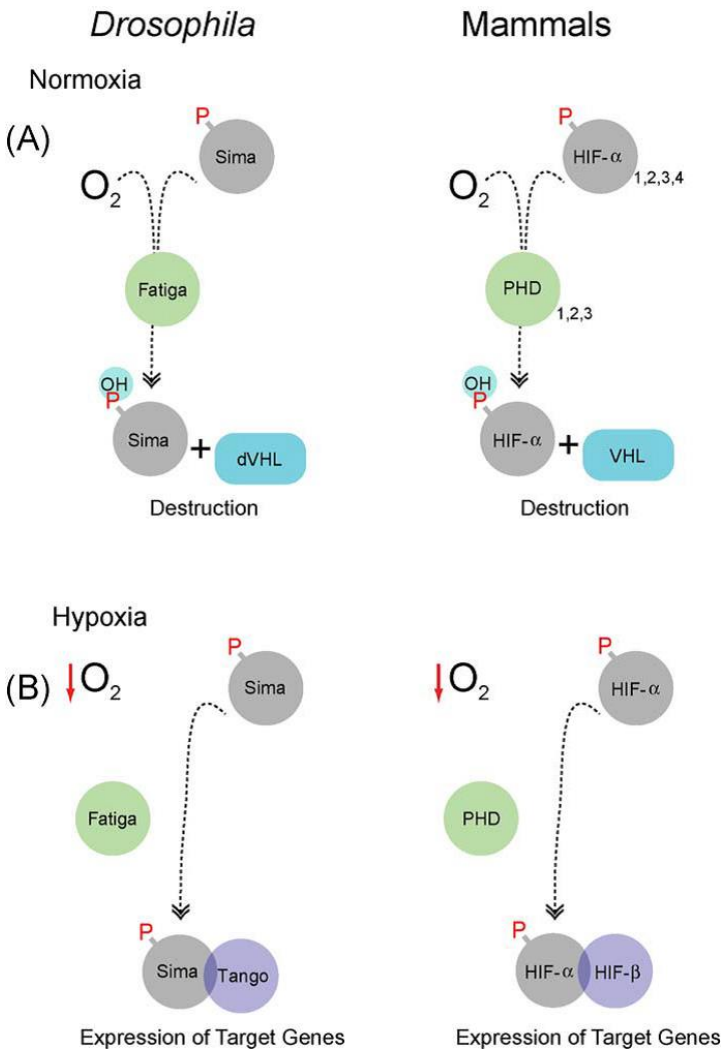

Figure 2. Oxygen-dependent regulation of the stability of HIF-a proteins. Hydroxylation of Sima (in *Drosophila*) or HIFa (in mammals) and subsequent degradation in normoxia (A) and stabilization of Sima and HIFa in hypoxia (B). Image taken from Centanin et al., 2010.

The optic lobe harbors proliferative neuroepithelial cells and it´s progeny

The study of oxygen effects on invertebrate neuronal physiology has focused mainly on cation concentrations, membrane potential and conductivity in neurons; however, practically absent are reports on neural stem cells, most of the work has been done on vertebrates (Mannello et al., 2011). *Drosophila melanogaster* is the most prominent invertebrate model organism used in research. There are many advantages in developing a system that allows the study of neural stem cell physiology in relation to O_2 homeostasis in invertebrates. *Drosophila* offers many technical advantages over vertebrate models: it is easy and inexpensive to culture in laboratory conditions, has a much shorter life cycle, a female produces large numbers of externally laid embryos and perhaps most importantly, it has enormous advantages for sophisticated and high resolution genetic manipulations (Rister et al., 2007; Gao et al., 2008; Hasegawa et al., 2011). Much of our basic knowledge about the molecular machinery controlling neural stem cell homoeostasis has been gained from Drosophila developing neural cells (Li et al., 2014). The optic lobe anlagen (optic lobe, from now on) in the larval brain (Figure 3A and 3B), the structure which gives rise to the optic lobes (visual centers) of the adult, provides an excellent model to study stem cell biology. In the past few years, a number of researchers have used the *Drosophila* optic lobe as a model to analyse the key signalling mechanisms controlling neural stem cell maintenance and the transition from symmetric to asymmetric division (Chen et al., 2014). In adult life, the optic lobe contains four neuropils were input from the retinal photoreceptors is detected and integrated: the lamina, the medulla, the lobula and the lobula plate (Meinertzhagen and Hanson, 1993). The optic lobe is a highly complex structure that contains more than a third of the total number of neurons of the fly brain (Morante and Desplan,

2004; Gold and Brand, 2014). The CNS of the freshly hatched first-instar larva already shows the morphology of the older larval brain, which consists of the two spherical brain hemispheres connected with each other and with the ventral ganglion (this last, corresponding to the entire nerve cord or ventral ganglionic chain of most invertebrates). The larval brain hemispheres can be subdivided into a region called the central brain, which contains glial cells, all differentiated neurons known to be functional in the larva and some interspaced stem cells (neuroblasts), and to each side of it the optic lobes, which harbour precursors of the optic lobe neurons in the neuroepithelial proliferation centres, it´s progeny and associated glia (Figure 3A; White and Kankel, 1978).

In holometabolous insects such as *Drosophila melanogaster* each optic lobe originates from an invagination of a small patch of ectodermal cells in the left and right sides of the head region of late-stage embryo. These are called embryonic optic placodes and soon became attached to each side of the central brain. The optic placodes are formed by approximately 40 epithelial cells that are responsible for producing all the thousands of visual interneurons of the adult optic lobes during postembryonic development (Campos-Ortega and Knust, 1990; Hofbauer and Campos-Ortega, 1990; Wang et al., 2011). Neuroepithelial cells (Figure 3C) of the optic lobe are initially in a mitotically quiescent state and only proliferate after larval hatching responding to nutritional cues (Chell and Brand, 2010; Sousa-Nunes et al., 2011; Lanet et al., 2013). During early larval stages, the optic neuroepithelium undergoes extensive proliferation as two distinct populations: the outer proliferation centre (OPC) and the inner proliferation center (IPC) (Figure 3C, D, E and F; (Egger et al., 2007; Hofbauer and Campos-Ortega, 1990; Orihara-Ono et al., 2011; Wang et al., 2013). Neuroepithelial cells have a columnar epithelial morphology, express epithelial molecular markers and epithelial junctions. During the two first (of a total of three) larval instars (stages of larval development interspaced by molts) they divide symmetrically to expand their population and later become progressively converted into neuroblasts, which have a rounded shape, lack epithelial characteristics (Figure 3F, white arrowheads and Figure 4), express the neuroblasts marker Deadpan (see Materials and Methods) and divide asymmetrically to self-renew and produce a smaller differentiating ganglion mother

cell that later produces neurons and glia (Figure 4; Hofbauer and Campos-Ortega, 1990; Egger et al., 2007; Technau, 2009; Wang et al., 2013; Apitz and Salecker, 2014).

Clonal analysis of GFP-marked cells using the FRT/FLP system firmly demonstrated that neuroepithelial cells give rise to neuroblast cells (Egger et al., 2007). The number of neuroblasts increases continuously doubling the cell number every 8-9hs (Nassif et al., 2003; Egger et al., 2007; Hayden et al., 2007). During pupal stages, almost all precursor cells differentiate into neurons and glial cells, giving rise to the mature optic lobe of the adult fly. Synaptogenesis in the optic lobe starts in the pupa halfway through metamorphosis (Melnattur and Lee, 2011). The transition from neuroepithelial cells to neuroblasts depends on the activation of the proneural gene *lethal of scute (l'sc)* in a small group of neuroepithelial cells occupying the transition zone at the edges of the neuroepithelium. *l'sc* expression is trainsient and moves across the neuroepithelium as a "proneural wave" transforming neuroepithelial cells into neuroblasts (Yasugi et al., 2008). It has been systematically proven that the gene *Notch* promotes proliferation of neuroepithelial cells and inhibits their precocious differentiation into neuroblasts. The transition is initiated by a window of downregulation of Notch signalling caused by *l´sc* activation in the transition zone. (Yasugi et al., 2008; Egger et al., 2010; Orihara-Ono et al., 2011; Wang et al., 2011; Weng et al., 2012).

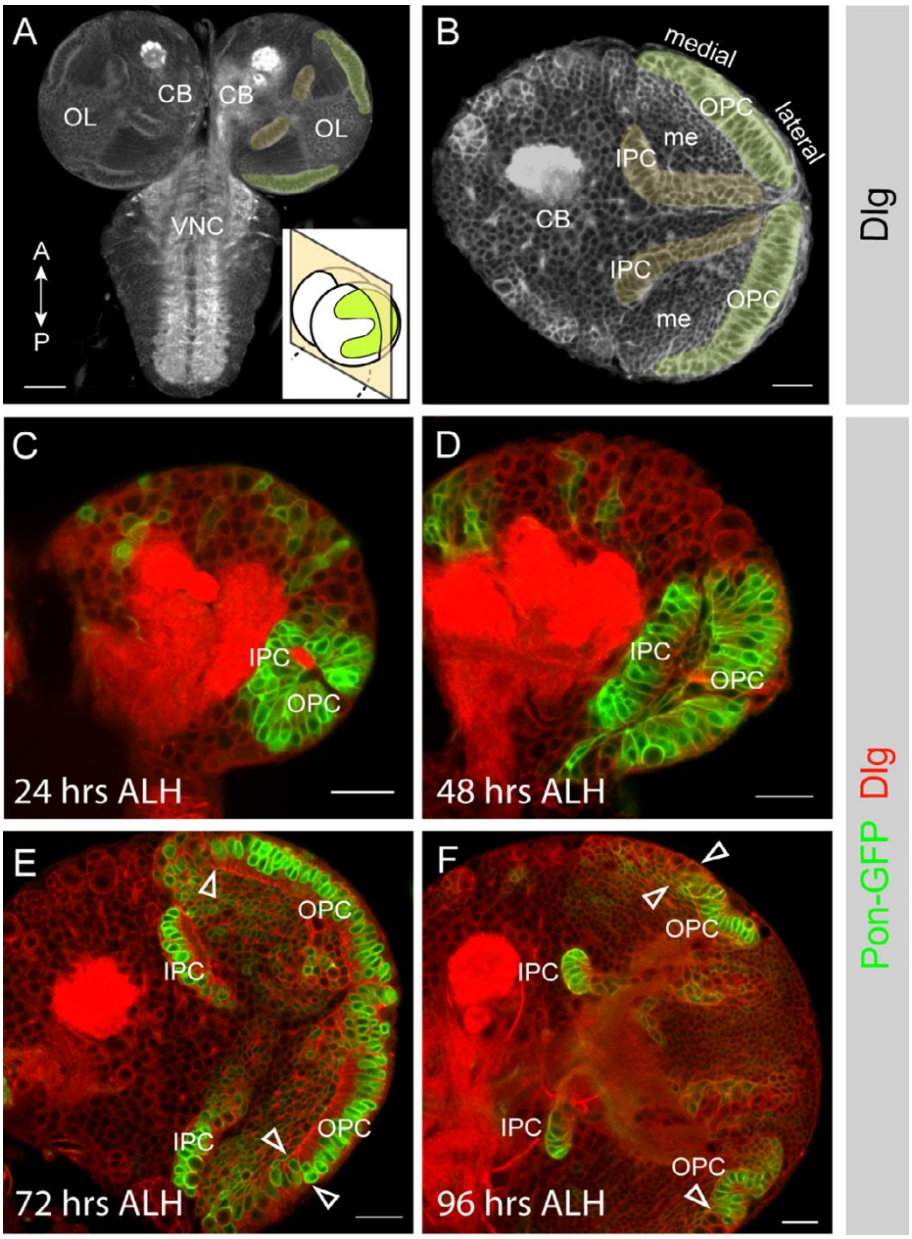

Figure 3. GAL4c855a reveals the proliferation centres of the developing optic lobe. *(A) Late third instar larval central nervous system (CNS) showing the ventral nerve cord (VNC) and the brain with its two main regions, the central brain and optic lobes. The expression of GFP in the optic lobe is directed by GAL4c855a (Green) and cell outlines are marked with anti-DLG (Red). (B) Frontal section of a brain hemisphere showing the Outer Proliferation Center (OPC) in green and the Inner Proliferation Center (IPC) in yellow. The Medulla cortex (me) is formed essentially by ganglion mother cells and is located between OPC and IPC. Anti-Disc Large (red) marks cell membranes. (C) Brain*

hemisphere with small neuroepithelial cells in green as marked by GAL4c855a driven expression of GFP. (D, E, and F) show how the optic lobe develops during larval life: IPC and OPC separate from each other and smaller progeny cells are located between the two epithelia. All images are single confocal sections, with anterior on top and lateral to the right. Scale bar is 50 µm (A) and 20 µm (B-F). Image taken from Egger et al., 2007.

Accordingly, *Notch* mutant clones of neuroepithelial cells are extruded from the neuroepithelium and differentiation occurs prematurely (Egger et al., 2010).

As noted already by Ramón y Cajal, the fly optic lobe shares structural characteristics with mammalian visual systems (Sanes and Zipursky, 2010). The Retinotopy in the optic lobe can be compared to what has been observed in the mammalian retina (Sanes and Zipursky, 2010; Egger et al., 2011). In addition to this, many of the mechanisms that have a role in optic lobe development resemble the mechanisms found in vertebrate neural development. For example, Notch signalling regulates a variety of cell fate decisions during vertebrate neural development (Louvi and Artavanis-Tsakonas, 2006) and has been repeatedly shown to be involved in cell fate decisions in a context-dependent manner (Orihara-Ono et al., 2011). Interestingly, the way neuroepithelial cells are transformed into asymmetrically dividing neuroblasts is reminiscent of the switch from neuroepithelial cells to radial glial cells in the developing mammalian cerebral cortex (Egger et al., 2010). During vertebrate embryonic development neuroepithelial cerebral cortex cells divide symmetrically to rapidly expand the stem cell pool. Later, neuroepithelial cells convert to radial glial cells, the major stem cell type contributing to cortical neurogenesis. Radial glial cells can divide asymmetrically to generate neurons either directly or via an intermediate cell type called basal progenitor cell (McConnell, 1995; Heins et al., 2002; Miyata et al., 2004; Noctor et al., 2004; Farkas and Huttner, 2008; Brand and Livesey, 2011; Homem and Knoblich, 2012; Florio and Huttner, 2014).

The versatility of *Drosophila* as a model organism and the shared homologies with mammalian nervous systems, make the larval developing optic lobe a very

interesting model to study neural stem cell physiology (Egger et al., 2011). Thus, the *Drosophila* larval brain provides a model that is simpler and easy to manipulate genetically to study the mechanisms regulating stem cell function during brain development which have shown to be shared by higher order organisms (Wang et al., 2011).

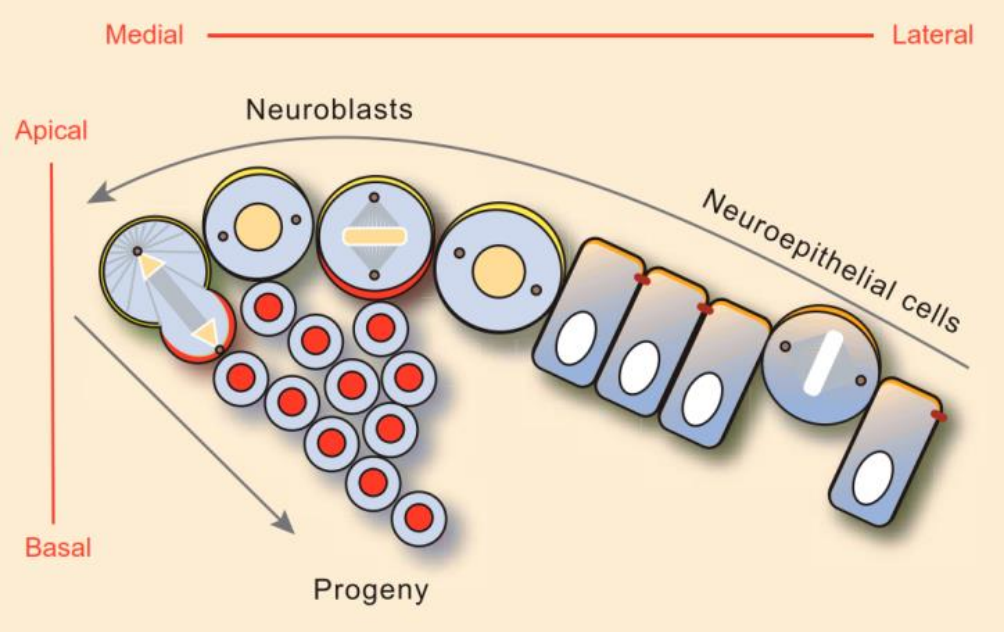

Figure 4. Model of neuroepithelial to neuroblast transition at the medial edge of the optic lobe*. At the edges of the neuroepithelium, clusters of cells disassemble their adherens junctions and undergo a transition to neuroblasts. Image taken from Egger 2007.*

<u>In insects oxygen is delivered to tissues through the tracheal system</u>

The oxygenation of the Earth's atmosphere lead to the evolution of diverse circulatory systems among animals for the transport and exchange of gases with the environment (Ivanovic, 2009). In vertebrates, the evolution of respiratory organs in the

shape of gills or lungs advanced in parallel with the evolution of a blood-based circulatory system comprising a pumping heart and a network of blood vessels for gas exchange between blood and cells. In invertebrates other respiration and respiratory systems evolved, including some with blood and capillaries. In Arhtropoda such as *Drosophila melanogaster*, gas transport and exchange is mediated mostly by the tracheal system. The *Drosophila* tracheal system is an elaborated network of air tubes that open through special openings (spiracles) on the body surface and transport air to the tissues by means of a network of air tubes with a lumen covered by a chitinous cuticle (Manning and Krasnow, 1993). Oxygen enters the network through the spiracular openings, and passes through primary, secondary and fine terminal branches (tracheoles) that end blindly inside tissues (Snodgrass, 1939; Uv et al., 2003; Affolter and Caussinus, 2008). The tracheal epithelium is a monolayer with cuticle in its luminal surface that prevents the tubes from collapsing (Noirot-Timothée et al., 1982).

The development of primary and secondary branches in the embryo depends on a genetically hardwired program of branching and tube expansion, as opposed to the development of tracheoles during postembryonic stages, which often grow in response to oxygen demands of individual targets (Ghabrial et al., 2003). The tracheal system has a metameric structure and develops from ten groups of ectodermic cells at each side of the embryo early in development. Each group invaginates and forms an epithelial sack under the body surface while still remaining connected to it (Samakovlis et al., 1996; Sutherland et al., 1996). Six branches elongate from each sack and form the primary branches, which grow in different directions with characteristic and stereotyped lengths (Samakovlis et al., 1996; Sutherland et al., 1996). Some tracheal cells generate secondary branches which bud from primary branches and are unicellular tubes formed by individual tracheal cells (Lee et al., 1996; Samakovlis et al., 1996). Terminal branching occurs in specific cells called tracheal terminal cells described by Wiggleswort (1954) as ‘‘cells at the tip of each tracheal branch’’. Terminal cells acquire a terminal cell fate during tracheogenesis (Affolter et al., 1994; Guillemin et al., 1996). Terminal branches form an intracellular lumen (Uv et al., 2003) within long cytoplasmic extensions which ramify extensively and are specialized in mediating

gas exchange with target tissues. The growth and ramification of terminal branches continues across larval stages (Samakovlis et al., 1996).

Numerous studies have aimed to describe the cellular and molecular mechanisms that direct the correct development of the tracheal system, including the formation of the primordial air sacks, the differentiation of terminal cells, the formation of the lumen, the extension of tracheoles, their growth, shape and migration (Baer et al., 2007; Chanut-Delalande et al., 2007). *Trachealess (trh)* is one of the most deeply studied genes (Isaac and Andrew, 1996; Wilk et al., 1996; Llimargas and Casanova, 1999) and it is fundamental for groups of epidermal cells to be determined to become tracheal cells. Moreover, none of the cellular activities seen during invagination of the epithelial cells occur in *trh* mutants (Wilk et al., 1996). In a recent study, mutant embryos for *trh* target genes lead to a two-step model in which *trh* induces and then organizes tracheal invagination (Brodu and Casanova, 2006). Other studied genes are *sal* (Kühnlein and Schuh, 1996), *knirps* (*kni*) and *knirps related* (*knrl)*; (Chen et al., 1998), *pruned* (Guillemin et al., 1996), decapentaplegic (*dpp*) (Vincent et al., 1997; Wappner et al., 1997), *ventral veinless* (*vvl*) (Llimargas and Casanova, 1999), and *tango* (*tgo*; Sonnenfeld et al., 1997).

Two genes, named breathless (*btl*) and branchless (*bnl*) that code for a Fibroblast Growth Factor (FGF) receptor and its ligand, an FGF homolog, have shown to be essential for the development of the tracheal system in *Drosophila* (Glazer and Shilo, 1991; Klämbt et al., 1992; Affolter et al., 1994; Reichman-Fried et al., 1994; Reichman-Fried and Shilo, 1995a; Anderson et al., 1996; Sutherland et al., 1996). Accordingly, among other functions, FGFs are potent stimulators of angiogenesis in vertebrates (Folkman and Klagsbrun, 1987). *btl* encodes a *Drosophila* homolog of the vertebrate FGF receptor (Glazer and Shilo, 1991), which is formed by five immunoglobulin domains in the extracellular region and a Tyrosine Kinase domain in the intracellular region (Klämbt et al., 1992). *btl* is expressed by all tracheal cells in every stage of development and it has been proven to be fundamental for the processes of cellular extension and migration (Reichman-Fried and Shilo, 1995b; Lee et al., 1996). In *btl* mutant embryos, tracheal cells fail to migrate out from the tracheal sacs (Klämbt et al., 1992). Btl activity is also required for the formation of secondary

and terminal branches (Reichman-Fried and Shilo, 1995b). *bnl*, a homolog of the mammalian Fibroblast Growth Factor, acts as a diffusible attractant for trachea growth acting on the Btl receptor (Sutherland et al., 1996; Shilo et al., 1997; Metzger and Krasnow, 1999). *bnl* provides inductive and guidance cues to developing tracheal cells and is dynamically expressed in every tissue that is tracheolated during larval life (Jarecki et al., 1999). During embryonic development, *bnl* is expressed at specific positions surrounding the tracheal sacs, where it induces the formation and attracts the outgrowth of primary branches. *bnl* also activates later programs of tracheal gene expression in cells that go on to form secondary and terminal branches.

In the process of terminal branching *bnl* expression is controlled by oxygen requirements and not by hardwired genetic programs (Jarecki et al., 1999). Oxygen deprivation promotes the expression of *bnl*, while excessive oxygenation represses it (Jarecki 1999). Jarecki and collaborators propose a model in which each cell senses oxygen deprivation and responds upregulating expression of *bnl* (Figure 5A; green). Bnl reaches the nearest trachea cell and through the activation of Btl induces trachea growth towards the source of Bnl (Figure 5B). When the hypoxic cell receives O_2 from the new tracheoles, it turns off the signal (Figure 5C). The process repeats itself many times due to the constantly changing balance in cell oxygen need and supply (Figure 5D). The information for the structural complexity of the tracheal system is encoded in the temporally and spatially dynamic pattern of *bnl* expression (Sutherland et al., 1996). The ectopic expression of *bnl* causes the growth of ectopic trachea to the *bnl* expressing cell. These results demonstrate that *bnl* is a localized inducer of tracheal branching and can direct outgrowth to novel positions (Sutherland et al., 1996). Interestingly, *bnl* over-expression in an ectopic location of the larva is necessary and sufficient to direct the outgrowth of tracheal terminal branches towards that particular location (Jarecki et al., 1999). In salivary glands, normally devoid of tracheae, miss-expression of *bnl* led to the colonization of the target tissue by tracheal branches. Moreover, when *bnl* is expressed in individual cells it is a sufficient signal to attract tracheal extensions from terminal cells located at a distance of several cell diameters (Jarecki et al., 1999). This process is dependent of Hif-alpha (Sima), which stabilizes under hypoxia and translocates to the nuclei where it promotes the expression of *bnl*

(in target tissue) and *btl* (in tracheal cells), among other hypoxia response genes (Centanin et al., 2008). *bnl* and *btl* are two of the hypoxia response elements sensitive to HIF induced activation. Initially, it was assumed that hypoxia response was activated in hypoxic tissues that would release *bnl* as a signal to induce tracheal growth in their direction. Surprisingly, the hypoxic reporter (Sima) is first induced in tracheal cells rather than in target tissues (Centanin et al., 2008). Terminal cells respond to hypoxia in an autonomous manner by sending cytoplasmic projections to tissues with poor oxygen supply responding to available levels of the FGF homologue Bnl, which is transcriptionally induced locally in target tissues with poor oxygenation (Centanin et al., 2008).

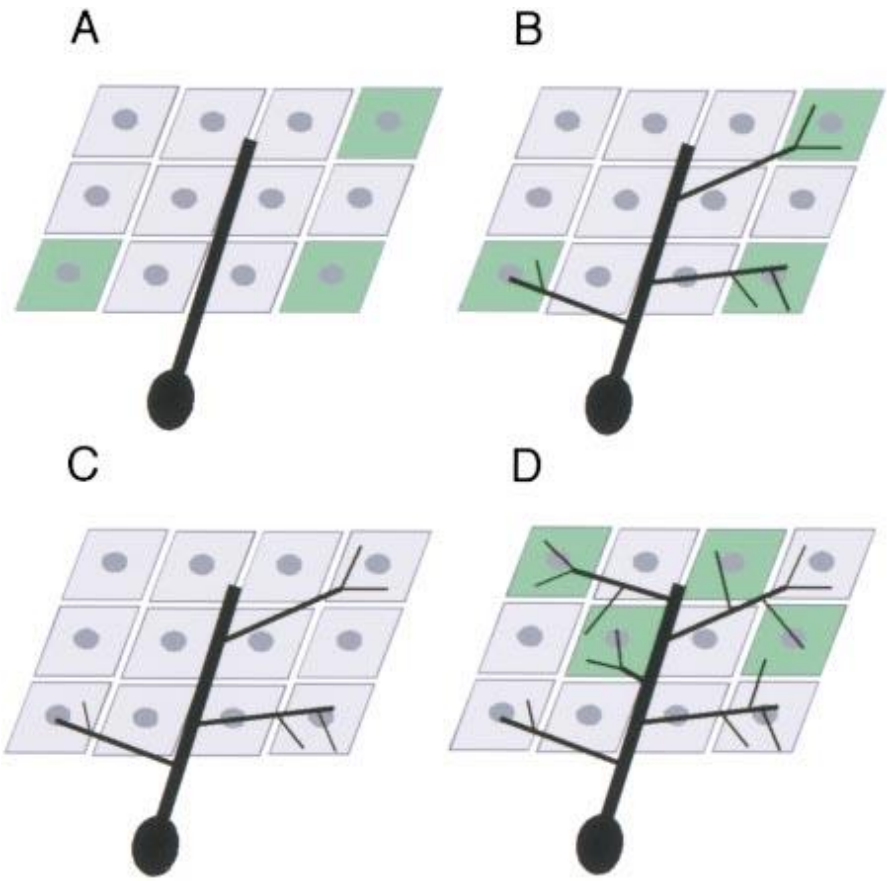

Figure 5. Model for Patterning of Terminal Branching by Bnl. *(A) Cells in a target tissue (gray) experience different degrees of hypoxia. Bnl expression is increased in the hypoxic cells (green). (B) Tracheoles grow from terminal cells towards the Bnl signalling cell. When the branch approaches the source, it begins to arborize. (C) When the new branches mature and supply oxygen to the target hypoxia is relieved and Bnl expression turns off. (D) When other cells become hypoxic the process repeats, generating dense tracheolar coverage that precisely matches tissue need. Image and legend adapted from Jarecki et al, 1999.*

The developing larval brain is differentially tracheolated

The tracheolation of the larval brain depends on the formation of the cerebral trachea (CT), a branch of the first segmental trachea. Each brain hemisphere receives one CT that enters the brain at a dorsomedial position and extends ventrally along the posterior medial neuropile surface (Figure 6; Hartenstein et al., 1993; Manning and Krasnow, 1993; Pereanu et al., 2007). In each brain hemisphere the CT ends inside the brain with 6-5 terminal cells each of which ramifies into several tracheoles in a pattern with some variability (Pereneau et al., 2007 and Leticia Couto, unpublished observations) that subsequently grow around the neuropile and develop secondary and higher order branches forming a dense tracheolar plexus in the late larval stages. All brain tracheoles grow in direct contact with glial cells compartments (Pereanu et al., 2007), which form a sheath around the tracheole and thus avoiding direct contact with neurons in analogy with the astrocytic sheath between neurons and blood vessels in mammal brains (Cantera and Trujillo-Cenoz, 1996; Pereanu et al., 2007). Glial cells restrict tracheal growth and limit the number of branches that enter the neuropile (Pereanu et al., 2007). Interestingly, only three tracheoles extend towards the larval optic lobe: The anterior optic lobe tracheole (OLTa), the lateral optic lobe tracheole (OLTl) and the posterior optic lobe tracheole (OLTp) (Pereanu et al., 2007).

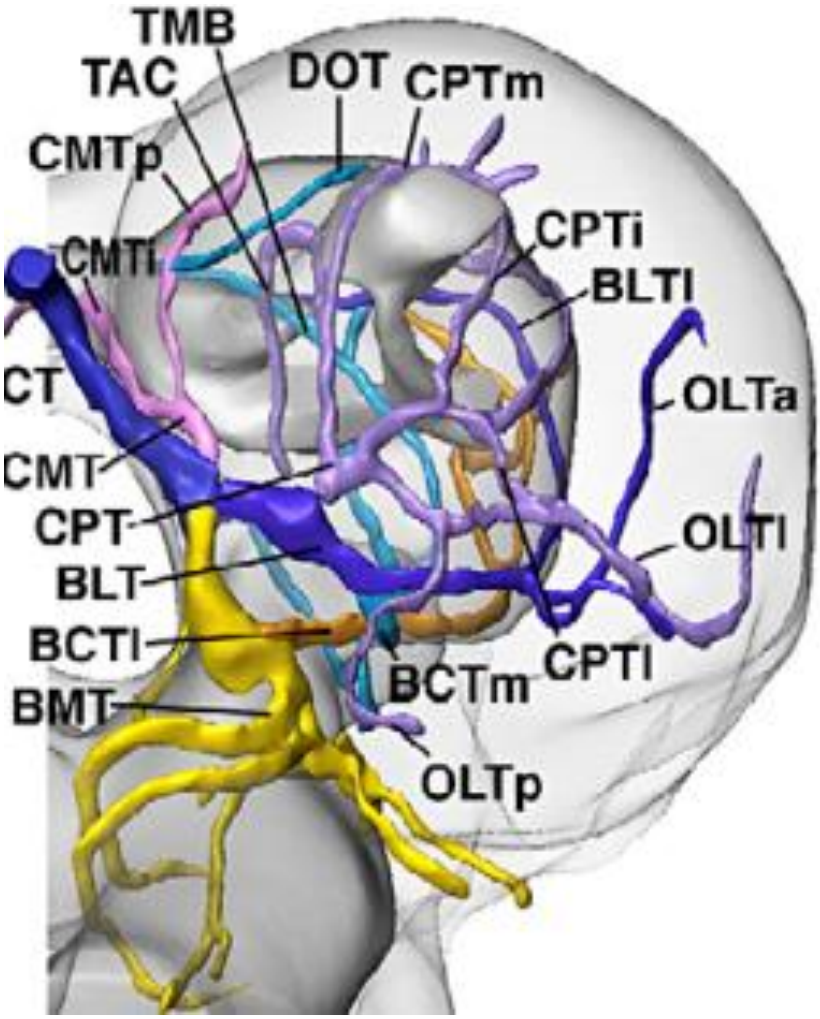

Figure 6. Pattern of brain tracheolation at mid larval stage (early third instar; 72 hrs. After Larval Hatching)*. 3D reconstruction showing a frontal view of the tracheal system in the brain. A brain hemisphere is shown in light grey, neuropile is depicted in darker gray. Three tracheoles enter the optic lobe: OLTa (anterior optic lobe tracheole), OLTp (posterior optic lobe tracheole) and OLTl (lateral optic lobe tracheole).CT is the cerebral trachea. The rest of the abbreviations should be disregarded. Image taken from Pereanu et al., 2007.*

The present Thesis originates from a striking observation regarding the tracheolation of the larval brain of *Drosophila*. While the central brain containing mostly differentiated neurons and their synapses (harboured in the neuropile), is densely tracheolated, the optic lobes which consist mainly of neuronal precursors and their progenies, are very sparsely tracheolated (Figure 7).

Hypothesis and aims of this thesis

We hypothesize that this topographic relationship has functional relevance for brain development. We propose that the sparse tracheolation of the optic lobe will result in a hypoxic condition relative to the densely tracheolated central brain. This will protect the proliferative tissue and its undifferentiated cell progenies from oxidative damage and will probably promote proliferation and prevent the differentiation of the cell progenies that only later on (During metamorphosis; reviewed in Melnattur and Lee, 2011) will differentiate.

Objective

Our main objective is to investigate the hypothesis that the relatively poor tracheolation of the optic lobe correlates with hypoxia (relative to the central brain) and that this is of functional relevance for brain development and important for the control of proliferation of stem cells.

Specific objectives:

1-To demonstrate that the sparse tracheolation of the optic lobe translates into lower O_2 levels than in the central brain, using a novel oxygen sensor.

2-To expose larvae to hypoxia and hyperoxia as a method to test the oxygen sensor and to investigate the main hypothesis.

3-To study the effect of ambient hyperoxia (Larvae kept in gas chamber) on optic lobe development by using markers specific for mitotic nuclei, neuroblasts and apoptosis.

4-To determine if a localized induction of ectopic tracheolation inside the optic lobe affects its development by using transgenic flies and markers for mitotic nuclei, neuroblasts and synapses.

5-To study the effects of ectopic tracheolation of the optic lobe during larval life, in the adult brain.

6-To study hypoxia response as reported by the oxygen sensor (and presumably O_2 concentration) in different cell types of the brain.

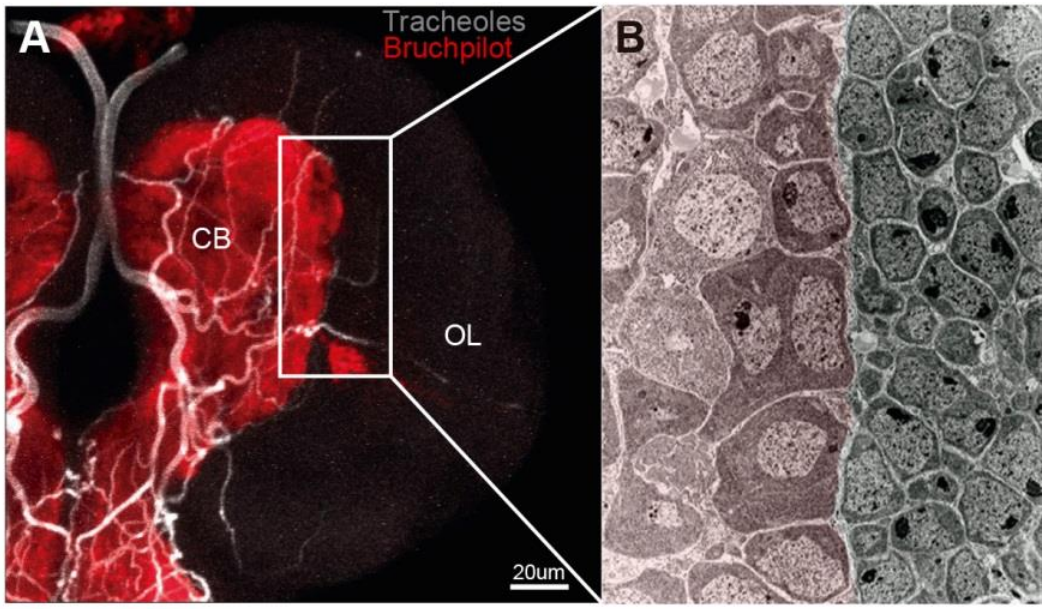

Figure 7. Topographic dichotomy of the tracheal system in the larval brain. *(A) shows the correlation between tracheal system (white) and synapses (marked by anti-Bruchpilot, red). The central brain is densely tracheolated while the optic lobe is very sparsely tracheolated. Scale bar: 20 µm. (B) TEM image of the transition zone between central brain and optic lobe (Rafael Cantera, unpublished). In this picture, a sharp interface between large, fully differentiated neurons in the central brain (pink) and smaller, undifferentiated cells in the optic lobe (grey) is evident.*

Materials and Methods

Fly stocks

Fly stocks are described in FlyBase unless mentioned otherwise. The oxygen sensor line was obtained from Dr. Stefan Luschnig: ubi-GFP-ODDD, ubi-mRFPnls in which an insertion of ubi-GFP-ODD on the second chromosome was recombined with ubi-mRFP-nls (B#34500) also in the second chromosome. Other fly lines include RH6-GAL4 (driver specific for the Bolwig's nerve), #550-GAL, P17-GAL4, svp-GAL4 (NP5606; Kyoto Stock Centre), Gliotactin-GAL4 (Sepp and Auld, 1999), UAS-bnl, UAS-CAAX-GFP and UAS-mCD8GFP. The Canton S strain was used as wild-type control. For some fly stocks a reference and origin could not be defined and is not specified.

Larval staging

Adult flies were set to lay eggs for 4 hrs in apple juice agar plates prepared according to the standard recipe. 24 hrs later larvae were collected from the agar plates and transferred to standard cornmeal medium and placed in an incubator at 25°C.

Dissection and immunostaining of larval brains

Larval brains were dissected in 4% paraformaldehyde in 0.1M Phosphate-buffered saline (PBS, pH 7.4), 0.5 mM EGTA, 5 mM MgCl and fixed for a total of 18 minutes including the dissection, washed with PBS containing 0.1% Triton-X 3 times for 5 minutes and 4 times for 15 minutes and prepared for immunostaining. The immunostaining was performed in whole-brains overnight at 4°C. The following primary antibodies were used to fluorescently mark proteins in larval and adult brains: mouse anti-Discs Large (Dlg) monoclonal antibody (4F3, DSHB; Parnas et al., 2001, 2001; 1:30) for cell cortices; rabbit polyclonal anti-Phosphohistone-3 (PH3) for mitotic nuclei (Santa Cruz Biotechnology, Inc.; 1:200); rabbit polyclonal anti-Cleaved Caspase 3

for apoptotic nuclei (Cell signalling; Asp175; 1:100); guinea pig polyclonal anti-Deadpan for neuroblasts (J. Skeath, Washington University School of Medicine, St Louis, USA; 1:1000), mouse monoclonal anti-Prospero (MR1A) for ganglion mother cells (DSHB; Campbell et al., 1994; 1:10), rat polyclonal anti-Elav for neurons (7E8A10 DSHB; O'Neill et al., 1994; 1:20), mouse anti-Dachshund for Lamina precursors (LPs; mAbdac2-3, DSHB, Mardon et al., 1994; 1:50). The chitinous cuticle lining of the tracheal lumen was visualized either under UV illumination by means of its autofluorescence or after staining with the fluorescent chitin-marker Calcofluor (1:200; Sigma). Primary antibody-binding was detected with fluorescent secondary antibodies conjugated to fluorochromes Alexa 405, Alexa488, Alexa568, or Alexa633 (1:200; Molecular Probes). Incubations with Secondary antibodies were performed overnight at 4°C. Samples were washed at room temperature and mounted in Vectashield (Vector Laboratories).

Laser confocal microscopy

Larval brains were imaged using a 60x objective on a Leica TCS SPE II confocal microscope or with a 60x objective in an Olympus Fluoview FV300. Optical sections across an entire brain hemisphere were recorded at 0.6 µm intervals for tracheal surface measurement, at 1 µm intervals for ratiometric analysis of the fluorescence emited by the oxygen sensor and at 2 µm for quantification of nuclei positive for the markers listed above.

Image analysis

Image stacks were analysed with Imaris 7.6 (Bitplane) and Fiji (Schindelin et al., 2012). Figures and illustrations were assembled using Adobe Photoshop 8.0 and Adobe Illustrator 11.0. PH3 positive (mitotic) nuclei and caspase-positive (apoptotic) nuclei were quantified manually using Image j. Neuroblast nuclei marked after the hyperoxia experiments were quantified using the software Dead Easy larval Glia developed by Dr. Alicia Hidalgo (Forero et al., 2012). Figure 8 and Table 1 show the validation for DeadEasy Larval-Glia that proves that it is appropriate for quantifying neuroblasts. For

this validation we used small stacks that were cropped out of the original ones, and represent a portion of the x, y and z extension of the original stacks obtained in the confocal microscope. This plugin is a powerful tool since it processes images in the three spatial dimensions and therefore makes possible an accurate quantification of stained nuclei. All the analyses (ratiometric analysis; mitotic nuclei, neuroblast, apoptotic nuclei, neuropile quantification, etc), whole brain stacks were analysed in which over a 100 confocal sections where made along the Z axis of a whole brain hemisphere.

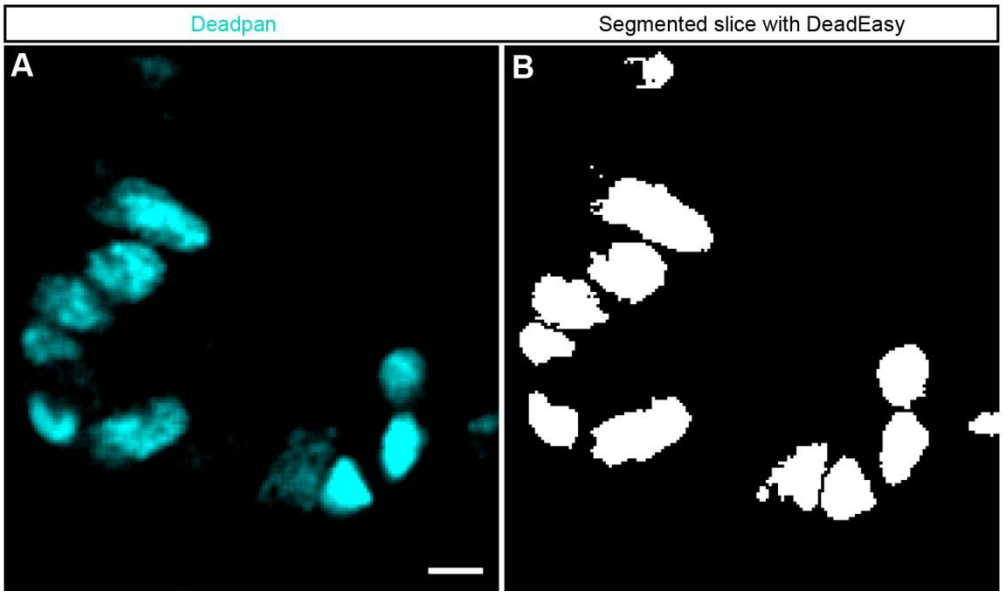

Figure 8. Quantification of neuroblast number with DeadEasy Larval-Glia. (A) a single optical section taken from one of the example cropped stacks (1), showing fluorescent nuclei of neuroblasts after immunostaining with anti-Deadpan and used for validation. (B) segmentation of the slice taken from the same image than (A) after processing for image analysis with DeadEasy Larval-Glia. Scale bar 5 µm.

Stack	Manual Count	Remove outliers (radius)	Remove outliers (threshold)	Opening (radius)	Dome 2D (height)	Minimum volume	Dead Easy count
1	19	15	15	7	5	0.5	20
2	29	15	15	7	5	0.5	27
3	62	15	15	7	5	0.5	60
4	57	15	15	7	5	0.5	54

Table1. DeadEasy Larval-Glia validation*. The Table shows four representative examples of the results of manual count of neuroblasts nuclei parameters and automatic counts obtained with DeadEasy Larval-Glia in cropped stacks.*

Statistical analysis

All the data analysis and graphs were done using R. For the optic lobe and central brain Ratio values a Boxplot Histogram was created in such a way that each boxplot contains the normalized frequency values for the seven replicates in a given bin. Student t-tests were performed when assumptions for parametric test were accomplished (normality using Shapiro-Wilk test and homoscedasticity using Levene´s test). If these assumptions were not achieved, nonparametric Mann-Whitney U tests were performed instead. Statistical significance was set at 0.05, 0.01 and 0.001.

Tracheolar 3D reconstruction and measurements

Measurements of tracheolar surfaces were done separately in the optic lobe and in the central brain. TrackEM in Fiji was used to segment the two areas to be compared (optic lobe and central brain) in images of one brain hemisphere per larva (n=12 larvae), following the neuroanatomical borders outlined by anti-Dlg staining. Subsequently, Imaris 7.6 was used to segment and quantify the surfaces of all tracheoles in each of the two regions.

Oxygen sensor and ratiometric analysis

The construction of the oxygen sensor was the aim of the PhD Thesis of Tvisha Misra under the supervision of Dr. Stefan Luschnig in Zürich. We (Baccino, Cantera and Egger) contributed to the first set of experiments designed to explore the potential of the sensor. The results of this collaboration will be published soon as a scientific paper presenting the sensor to the scientific community (Misra et al., submitted) and given the importance of this tool for this Thesis, and that it is yet not published, we will give here a brief presentation.

To construct a sensor which reflects the O_2-dependent dynamics of Sima, the Oxygen-dependent Degradation Domain (ODD, aa 692-863; Lavista-Llanos et al., 2002) of Sima was fused to the C-terminus of Green Fluorescent Protein (GFP-ODD) and placed under the control of the ubiquitin-69E (ubi) promoter for constitutive expression in all cells throughout development. Changes in GFP-ODD intensity reflect the behaviour of full-length Sima protein under changing ambient O_2 concentrations. However, besides regulating the stability of the GFP-ODD protein, changing O_2 concentrations influence gene expression in *Drosophila* (Liu et al., 2006; Azad et al., 2009), as well as maturation of the GFP fluorophore (Heim et al., 1994). Thus, in order to detect even subtle O_2-dependent changes in GFP-ODD levels, and to exclude confounding effects of O_2 conditions on gene expression and on fluorophore maturation, a second protein was co-expressed whose stability is not influenced by changing O_2 levels: a monomeric red fluorescent protein with a nuclear localization signal (mRFP-nls) under the control of the same *ubi* promoter to normalize GFP-ODD signal intensity. O_2-dependent changes in gene expression (transcription, translation) should equally affect the expression of ubi-GFP-ODD and ubi-mRFP-nls. Thus, at a given O_2 concentration and in any cell type, changes in the ratio between GFP-ODD and mRFP-nls signals should only depend on the O_2-triggered degradation of GFP-ODD. Hence, this ratio should provide a measure for Sima degradation independent of absolute protein levels and of cell type-specific expression of the hypoxia sensor (Misra et al, submitted). A customized plugin was developed in Fiji (Schindelin et al., 2012) by Dr. Egger and Felix Meyenhofer (University of Fribourg) to perform the ratiometric

analysis. The nuclear mRFP-nls signal (Figure 9A) was used to segment nuclei. Prior to segmentation, background subtraction was performed on a neighbourhood of 40 pixels using the rolling ball algorithm (Figure 9D). To de-noise, the images were smoothened using an average filter on a 3 × 3 neighbourhood (Figure 9E). To obtain ROIs corresponding to nuclei in each confocal section, Autothreshold segmentation was applied (default method; Figure 9F) and regions were subsequently separated using the Watershed algorithm (Figure 9G). In each ROI the ratiometrics plugin calculates the average pixel intensity for the reference signal (mRFP-nls) and the sensor signal (GFP-ODD). These values were used to calculate the GFP-ODD/mRFP-nls signal ratio for each nucleus. In the segmentation mask each nuclear ROI was false-coloured according to its mean ratio value using a heat-map lookup-table (Figure 9I). Figures 8H and 8I show the ratiometric macro (H) and plugin layout (I). Ratio values shown on images and graphs were scaled to the mean value of all nuclei. To quantify mean ratios and the frequency distribution of different brain regions, the central brain and optic lobe regions were manually separated using TrackEM in Fiji based on the neuroanatomy revealed by the anti-Dlg staining. Graphs were prepared using R studio software. For the cell specific study of ratio values we used different antibodies to obtain a cell specific signal for segmentation (anti-Deadpan, anti-Dachshund, anti-Prospero, anti-Repo anti-Elav). For the brains stained for Prospero or Dachshund, we used DeadEasy Larval-Glia to segment the nuclei (Forero et al 2012). When the ratiometric analysis was perfomed more than a 100 confocal sections per brain were analzed covering the whole larval hemisphere.

Acquisition of confocal stacks

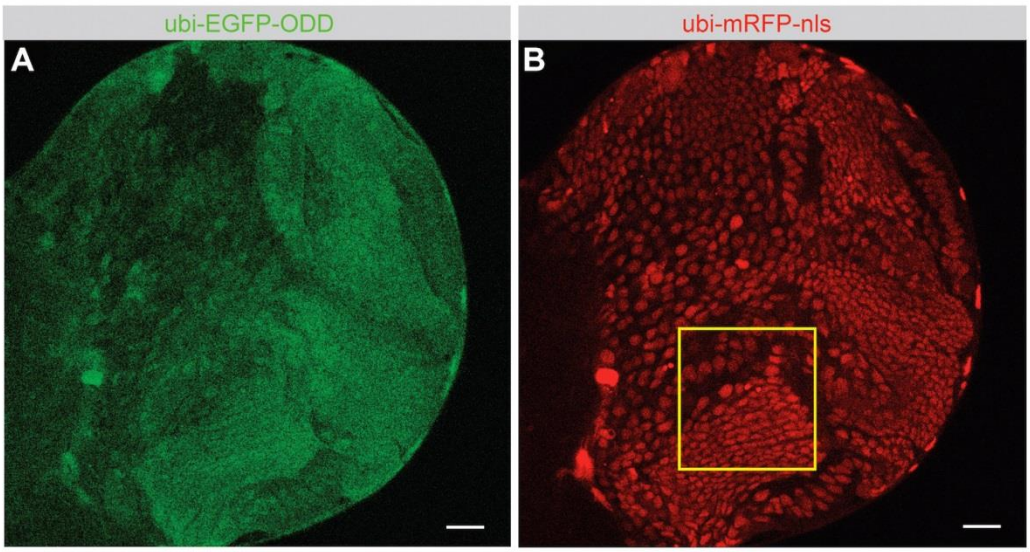

Nuclei Segmentation with Macro Language in Fiji

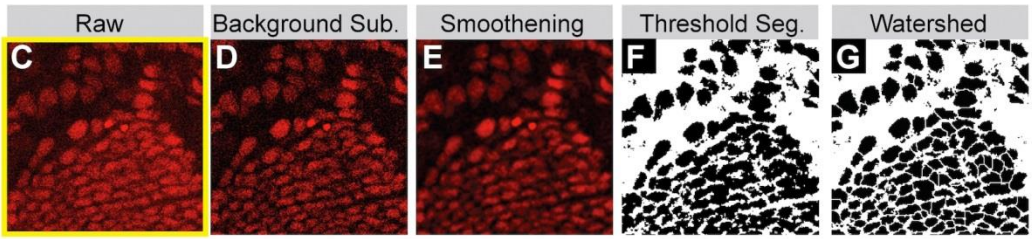

Analysis with Ratiometric Plugin in Fiji

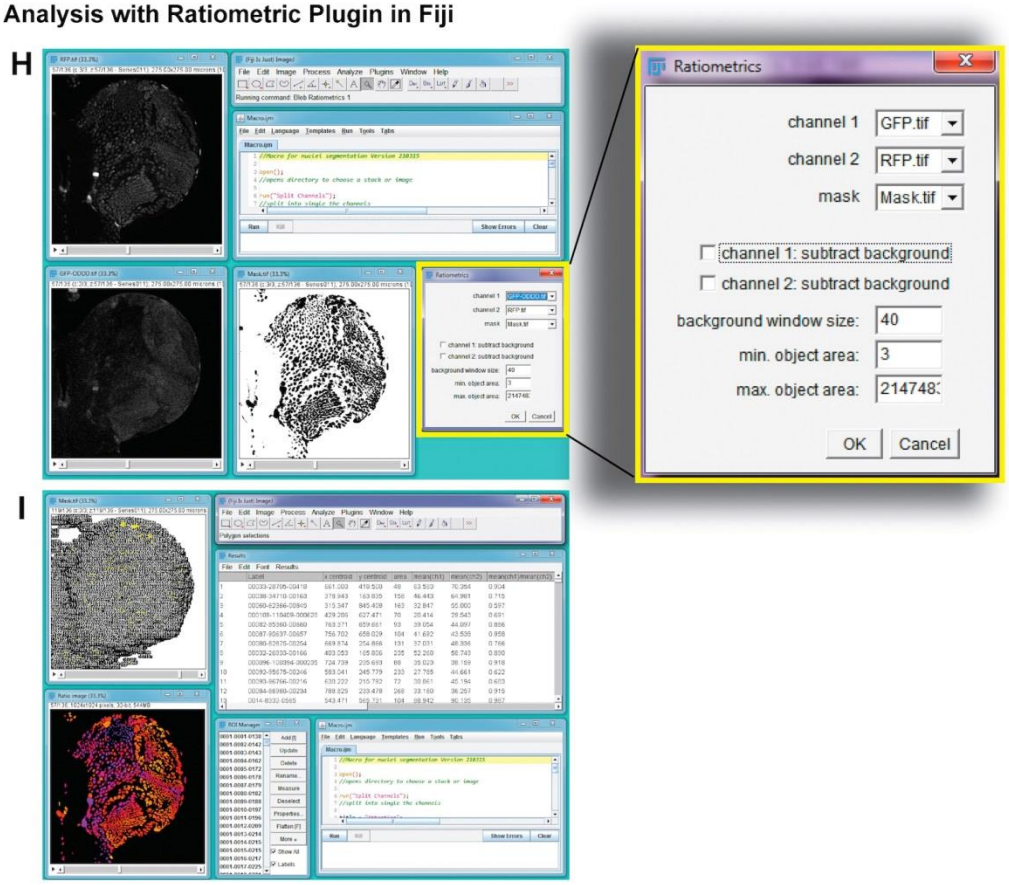

Figure 9. Overview of the working steps for the image segmentation and ratiometric analysis used in this Thesis. *A single confocal section of a brain hemisphere from a larva of age 96h After Larval Hatching shows the oxygen-sensitive signal in green (ubi-GFP-ODD, A) and the oxygen-independent red nuclear signal emited by ubi-mRFP-nls (B). Prior to segmentation of nuclei, raw confocal image stacks of the red channel (C) were subjected to background subtraction (D) and smoothening (E). Nuclei were segmented with Autothreshold (F) and Watershed (G) algorithms. A plugin was developed in Fiji to perform the ratiometric analysis (Egger and Meyenhofer). A screenshot of Fiji is shown before (H) and after (I) running the ratiometric analysis. In the ratiometric plugin interface GFP, RFP and segmented mask image stacks are selected. The plugin also allows the user to specify parameters for background subtraction, as well as for minimum and maximum size of segmented objects.*

Hyperoxia and hypoxia treatment

Embryos were collected for two hrs at 25°C on apple juice-agar plates and transferred into plates with standard medium. For hyperoxia treatment, at 24 hrs ALH (after larval hatching) they were placed in a Modular Incubator Chamber (MIC-101; Billups-Rothenberginc.), which was flushed with pre-mixtures of 60% O_2 in N (PanGas). At 96 hrs ALH, when larvae where in the wandering stage, they were dissected as described before. The O_2 Analyzer/Monitor (Vascular Technology VTI-122 Disposable Polarography Oxygen Cell Catalog No. 100122) was used to measure O_2 concentration when chambers were flushed. For the hypoxia experiments, larvae were collected at 72 hrs ALH and placed in the incubation chamber previously flushed with 5% O_2 pre-mixtures in N for one day. In a set of pilot experiments we tested different durations of hypoxia and hyperoxia treatments on larvae of different ages. Stem cells of the optic lobe divide in all stages of larval development, therefore, we used a long lasting hyperoxia treatment. In hypoxia, larvae tend to escape the medium, refrain from feeding and have a delay in development (Callier et al., 2013; Wong et al., 2014; Bailey et al., 2015). For this reason, we decided to use a short treatment which was enough to observe a change in brain oxygenation with the bio-sensor.

Results

The central brain is more densely tracheolated than the optic lobe

In the insect brain, the central nervous system is organized in such a way that cell bodies locate mostly in the periphery, called the cortex, while neurites grow inwards into a region called "neuropile" where motoneurons, sensory neurons and interneurons form synapses with each other. In the larval brain of Drosophila, this organization is observed in the central brain. Since in the insect CNS synapses on cell bodies are very rare, most synapses are located in the neuropil region. Bruchpilot is a protein found in synapses, that can be used as a marker for the neuropile (see for example; Cachero et al.,2010). By correlating the fluorescence emitted from tracheoles and that corresponding to anti-Brp we observed that there is a tight topographic correlation between brain synapses and the densely tracheolated region of the larval brain (Figure 7A). Transmission electron microscopy (Rafael Cantera, unpublished data) disclosed also the existence of a sharp interface between central brain and optic lobe regions. In the central brain region we found relatively large cells with voluminous cytoplasm corresponding to the fully differentiated, synapse forming neurons of the larval brain. In the optic lobe, facing the interface with the central brain, we found relatively small cells with a very small cytoplasm that correspond to the undifferentiated, non-synaptogenic progenies formed by larval proliferation in more superficial regions of the optic lobe (Figure 7B).

The tracheal pattern correlates with O_2 availability in the brain as measured by oxygen dependent degradation of GFP-ODD

The difference in tracheolation density between central brain and optic lobe had not been explicitly formulated at the beginning of this Thesis and because it is an important premise for the Thesis we decided to confirm it through a detailed quantification. We performed a comparison of the total surface area of trachea in the central brain and the optic lobe by producing 3D models of the brain tracheolation in

wandering larvae (96 hrs ALH; Figure 10A). This revealed that the tracheal surface is 5.7 times larger in the central brain than in the optic lobe (Figure 10B; mean=24437.9 μm^2 for the central brain, mean=4312.1 μm^2 for the optic lobe; n=12 brains; student's t-test, p=0.0009) and confirmed our previous observations. We hypothesized that the scarce tracheolation of the optic lobe should result in a weaker oxygenation of this region relative to the more densely tracheolated central brain. Hence, lower O_2 levels in the optic lobe relative to the central brain should translate into less oxygen-dependent degradation of GFP-ODD in the optic lobe.

Nevertheless, the presence of tracheoles in a volume of tissue is not sufficient evidence to assume that oxygen is being delivered as some newly formed tracheoles are perhaps not functional (Ghabrial et al., 2003) and it is known that cerebral tracheoles grow more or less continuously during larval life (Pereanu et al., 2007). Furthermore, oxygen distribution may not only be determined by the tracheal pattern alone. It has been proven that in vertebrate tissues, oxygenated by blood capillaries, oxygen diffuses up to 150 µm away from its source (Folkman et al., 2000; Gatenby and Gillies, 2004), which is within the range of distance relevant for this Thesis. Moreover, some Aquaporines have been proposed as a factor regulating cell permeability to O_2, which would mean possible existence of pathways through which O_2 diffuses more easily among cells that express those molecules in a given tissue (Panchision, 2009). To validate the basis of our hypothesis, it was imperative to implement a method to study oxygen distribution in the brain with enough spatial resolution to test our hypothesis that the topographic dichotomy in the tracheolation of the larval brain correlates with different oxygen levels.

To test this hypothesis, we used the ratiometric analysis pipeline based on a custom imageJ plugin developed by Boris Egger and Felix Meyenhoffer (see Materials and Methods) and measured the ratio of GFP-ODD and mRFP-nls mean intensities in every segmented cell nucleus of one larval brain hemisphere per studied larva. This analysis provided a portrayal of O_2 distribution at the single-cell level in the brain by representing the GFP-ODD/mRFP-nls ratio in every nucleus using a heat map (Fig. 10C, E). We observed striking differences between central brain and optic lobe indicating that oxygen levels are indeed lower in the optic lobe relative to the central brain.

Whereas most central brain nuclei showed low GFP-ODD/mRFP-nls ratios, presumably reflecting high oxygenation, optic lobe nuclei displayed, in general, markedly higher ratios, consistent with lower oxygenation of this region (Fig. 10F and G). Strikingly, the range of GFP-ODD/mRFP-nls ratios correlated with the differential tracheolation pattern in the developing brain (Fig. 10C-E). To quantify this topographic correlation we measured the GFP-ODD/mRFP-nls ratios on each confocal slice throughout the brain and plotted the distribution of ratio frequencies (Fig. 10F, n=7 brains). Indeed, the histogram showed a significant shift in the frequency distribution towards higher ratios for optic lobe nuclei as compared to central brain nuclei (Fig. 10F). The average ratio for nuclei in the optic lobe was significantly higher than in the central brain (Figure 10G; mean: 1.11 in optic lobe vs. 0.83 in central brain; n=7, student's t-test, p=1.256e-06). The correlation between tracheal tubes and the ratiometric signal was most prominent in the region called inner cell plug (Hofbauer and Campos-Ortega, 1990). Cells of the inner cell plug are generated by the inner proliferation center of the optic lobe. These cells show lower ratios compared to cells of the neighboring Medulla cortex (Fig. 10C and D, arrows). They are in close vicinity of the optic lobe tracheoles (OLTl) that run from the central brain trough the inner cell plug of the optic lobe (Pereanu et al., 2007). The results validate the applicability of the hypoxia sensor (Misra et al 2016; submitted) as a tool to visualize tissue oxygenation in vivo and illustrate that the spatial resolution provided by our method is sufficient to detect differences in the hypoxia response within a single tissue and at the level of individual cells.

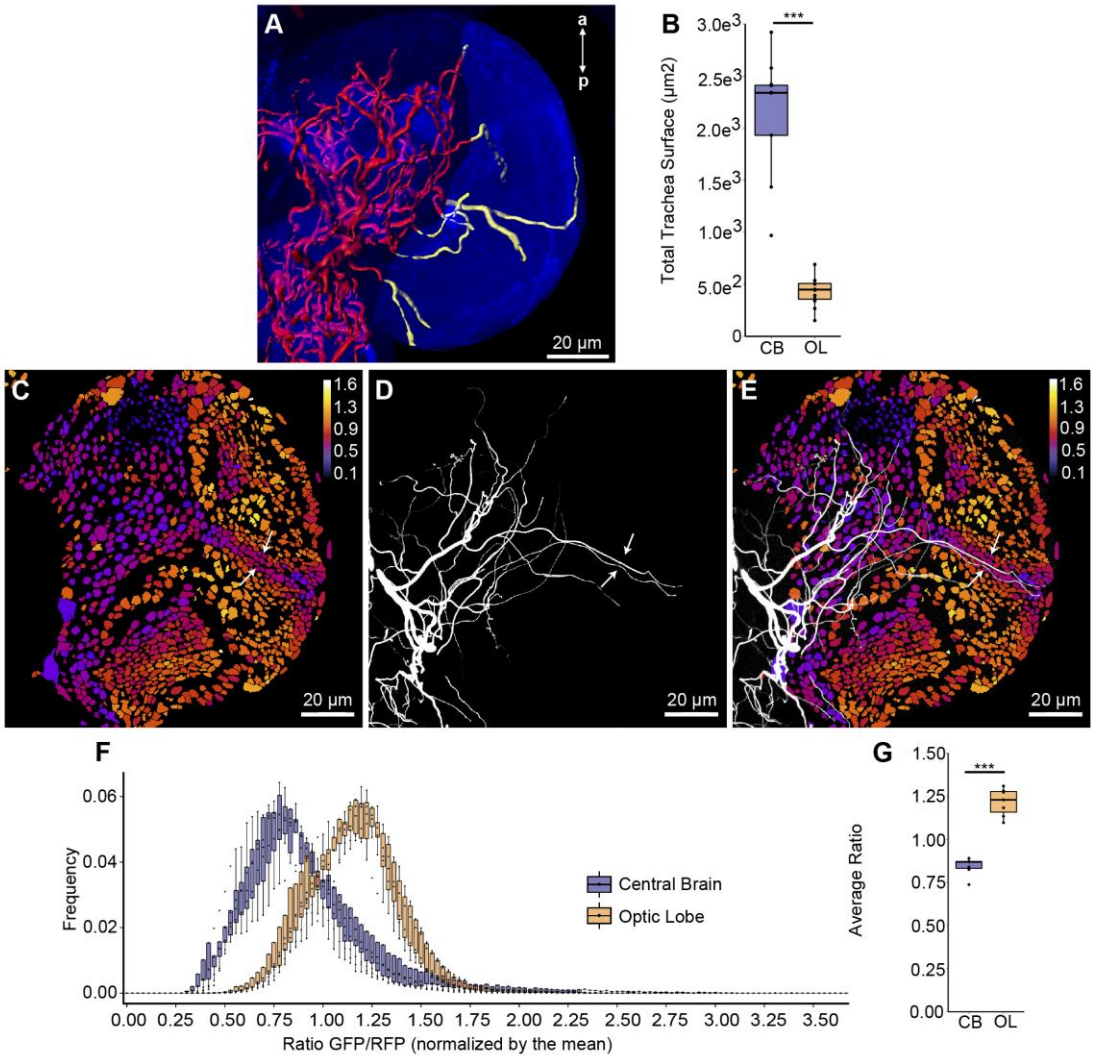
A
a
p
20 µm
B
***
Total Trachea Surface (µm2)
3.0e3
2.5e3
2.0e3
1.5e3
1.0e3
5.0e2
0
CB
OL
C
D
E
1.6
1.3
0.9
0.5
0.1
20 µm
F
Frequency
0.06
0.04
0.02
0.00
0.00 0.25 0.50 0.75 1.00 1.25 1.50 1.75 2.00 2.25 2.50 2.75 3.00 3.25 3.50
Ratio GFP/RFP (normalized by the mean)
Central Brain
Optic Lobe
G
Average Ratio
1.50
1.25
1.00
0.75
0.50
0.25
0.00
CB
OL

Figure 10. Different tracheolation densities within the brain appear to correlate with different oxygen availability. *(A) 3D surface reconstruction of the tracheal system in a single brain lobe of a larva at 96 hrs ALH. The 3D reconstruction is superimposed on a maximum intensity projection of an anti-Dlg antibody staining (blue) to visualize cell outlines and neuropil. Tracheoles in the central brain are coloured in red and those in the optic lobe are coloured in yellow. The midline of the brain is to the left. Anterior (a) and posterior (p) are indicated by the double arrow on the top right corner. (B) Box plot showing quantification of total tracheal surface within the central brain (red) compared to the optic lobe (yellow). The box plot shows maximum and minimum observation, upper and lower quartile, and median. n=5 brain hemispheres. (C) shows a single frontal confocal section of a brain hemisphere of a larva at 96 hrs ALH expressing ubi-GFP-ODD and ubi-mRFP-nls. The colour code (upper right corner) indicates average ratios between GFP-ODD and mRFP-nls for each nucleus. (D) Maximal intensity projection of the brain's tracheal system stained with Calcofluor, shown in white. (E) Superposition of the images shown in (C) and (D) to illustrate the topographical correlation between the differential tracheolation of central brain and optic lobe regions and their different hypoxic state. Low ratios correlate with central brain regions that are densely tracheolated. Higher ratios are observed in the sparsely tracheolated optic lobe region. Note the lateral tracheoles that enter the optic lobe through the inner cell plug (arrows). Cell nuclei adjacent to these tracheoles exhibit lower ratios, consistent with* O_2 *diffusion across a few cell diameters. (F) Histogram representing the frequency distribution of ratio values for the central brain and the optic lobe, showing a clear separation. n=7 brain hemispheres.* ***(****G****)*** *Box plot showing that cell nuclei in the optic lobe display significantly higher average ratios compared to cell nuclei in the central brain. The box plot shows maximum and minimum observation, upper and lower quartile, and median. n=7 brain hemispheres. Scale bars, 20 µm.*

As a proof of principle to show that presence of tracheoles translates into higher oxygen delivery, we measured the ratiometric values in single cells located at the immediate vicinity of the OLTl tracheole and measured also the distance between the cell and the OLTl tracheole (Fig 11A). This analysis showed that cells that reside at a greater distance from a tracheole receive less oxygen and vice à versa (Figure 11B).

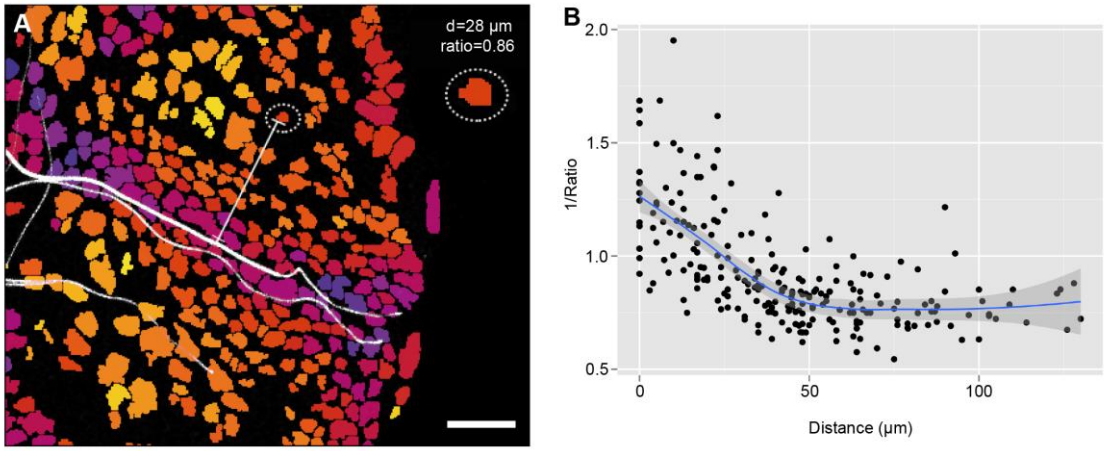

Figure 11. Changes in ratio values from the oxygen sensor correlate with the distance between the cells and the OLTl tracheole in the optic lobe. *(A) shows an amplification of Figure 10C in the area that the OLTl enters the optic lobe. (B) Distance from OLTl and ratios were measured for a number of randomly chosen nuclei in each brain (n=6). Ratios increased with increased distance to the OLTl (the opposite is true for multiplicative inverse: 1/Ratio). Non-linear trend line is blue. Grey area indicates Standard Error of the mean. Scale bar is 10 µm.*

Asymmetry in O_2 distribution is sustained throughout all stages of larval development

After we had documented that it is possible to use the hypoxia sensor to visualize oxygen availability inside the brain at 96 hrs of larval development we decided to apply this method to larvae of different ages because it was important for the investigation of our main hypothesis to define if this situation is maintained along larval

development. By using the O_2 biosensor and the ratiometric analysis pipeline we studied oxygen distribution in the brain throughout larval development (at 24hrs, 36hrs, 48hrs, 60 hrs, 72hrs and 84hrs ALH). The results showed that the unequal distribution of oxygen between central brain and optic lobe is present at all larval stages, although with some variability. This is shown by the ratiometric images presented in Figures 12A´, B´, C´, D´, E´, F´ and the corresponding histograms for frequency distribution of the ratiometric values (Figures 12A, B, C, D, E, F). Figure 12G shows the mean ratio value for each brain compartment in every larval stage studied (24 hrs mean: 1.13 in optic lobe vs. 0.96 in central brain; n=5, student's t-test, p=0.007; 36 hrs mean: 1.23 in optic lobe vs. 0.90 in central brain; n=6, student's t-test, p=6.956e-06; 48 hrs mean: 1.13 in optic lobe vs. 0.93 in central brain; n=6, student's t-test, p=0.002; 60 hrs mean: 1.3 in optic lobe vs. 0.88 in central brain; n=6, student's t-test, p=0.002; 72 hrs mean: 1.13 in optic lobe vs. 0.89 in central brain; n=7, student's t-test, p=0.00058; 84 hrs mean: 1.11 in optic lobe vs. 0.82 in central brain; n=7, student's t-test, p=1.256e-06). Figure H depicts the differences between central brain and optic lobe in each larval stage. This consistency suggests that the lower O_2 supply of the optic lobe, relative to that of the central brain, is an important mechanism that accompanies optic lobe neural stem cells throughout larval development.

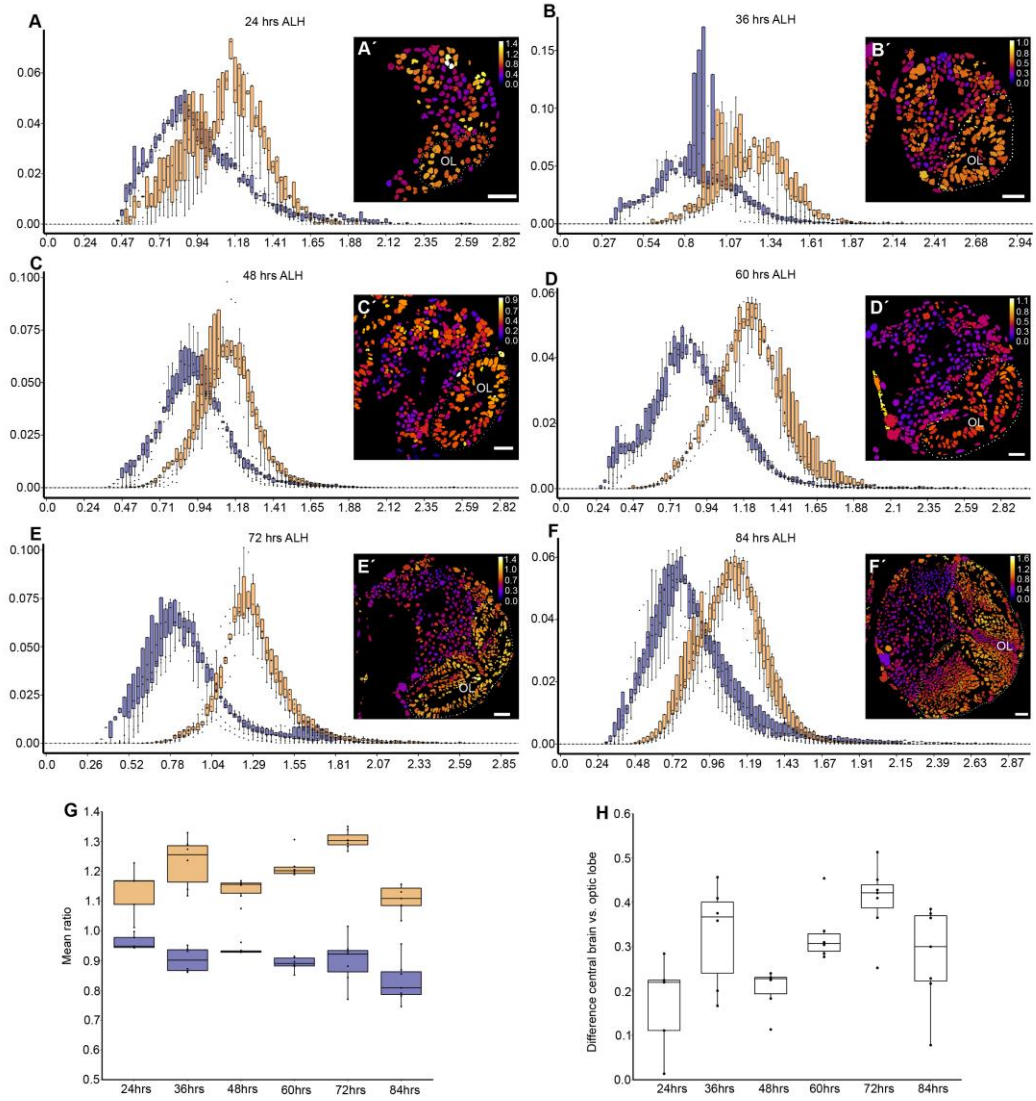

Figure 12. The sensor suggests that O_2 is asymmetrically distributed in the brain throughout larval development. *(A) to (F) shows distribution of central brain and optic lobe ratio values for each studied timepoint at 12-hrs intervals, starting at 24 hrs ALH. For each stage, a single slice of the ratiometric stack illustrates the difference in oxygenation between central brain and optic lobe. Dotted line depicts the optic lobe. Scale bar is 20 µm. (G) shows mean ratio values for central brain (blue) and optic lobe (orange) at every timepoint. In all cases the mean ratio for the optic lobe was significantly higher than that of the central brain. (H) shows the difference between mean ratios between central brain and optic lobe for each timepoint. OL stands for optic lobe and CB stands for central brain.*

Ambient hyperoxia oxygenates the optic lobe and diminishes proliferation

Hypoxia has been shown *in vitro* to induce cell proliferation and to maintain an undifferentiated cellular state. Conversely, hyperoxia can have the opposite effect; it inhibits cell proliferation and in some cases induces differentiation (Lange et al., 2016). We subjected larvae to hyperoxia to test whether cell division is arrested and whether cell differentiation is stimulated. Larvae where exposed to 60% O_2 from 24 hrs ALH until the end of larval life. With this experimental setup the central brain appeared to be saturated with oxygen and oxygenation of the optic lobe increased. We found an increase in O_2 dependent degradation of GFP in the optic lobe. The distribution of Ratio frequencies showed that optic lobe values were shifted towards central brain values in the brains of larvae in hyperoxia (Figure 13A and C) when compared with brains from larvae kept in normoxia (Figure 12B). The frequency histogram was built by normalizing the ratios against the average value in each brain to more adequately represent the difference between central brain and optic lobe and reduce the noise created by individual variability. The difference between average central brain and optic lobe oxygenation found in normoxic larvae is significantly reduced in hyperoxia as attested by student t test (figure 13E; difference between means in optic lobe and central brain in normoxia: 0.29 and hyperoxia: 0.05, p value= $7.892e^{-5}$, n=7).

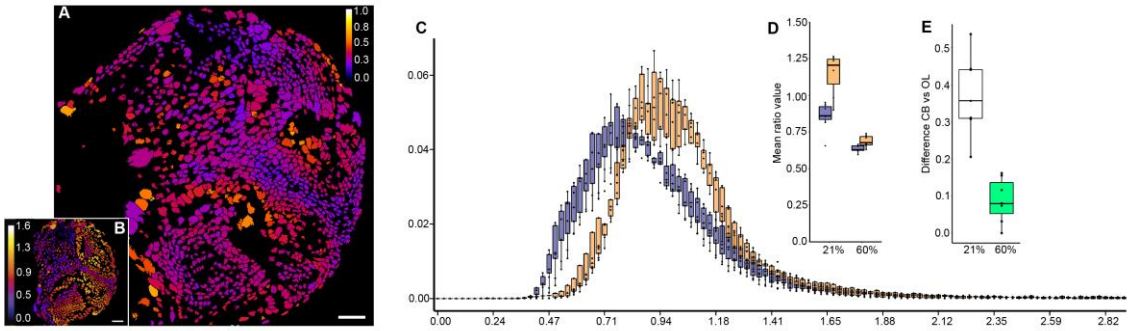

Figure 13. Ambient hyperoxia changes ratiometric values distribution in the brain. *(A) Ratiometric analysis revealed a presumably higher oxygenation of the optic lobe in larvae reared in hyperoxia when compared to larvae reared in normoxia (B). The distribution of frequencies for experimental brains showed a shift of optic lobe values towards central brain values (C) when compared to the normoxic brain in Figure 10C. Optic lobe mean ratio is reduced in 60%* O_2 *(D) as well as the difference between optic lobe and central brain mean ratio values (E).*

This result gave us an opportunity to test the consequences for brain development of increased oxygenation of the optic lobe. Using confocal microscopy we generated full reconstructions of brain hemispheres of experimental and control larvae immunostained with anti-Dlg, which outlines the brain, optic lobe and neuroepithelium, as well as markers for mitosis, apoptosis and neuroblasts (Figure 14A, B and C).

Ambient hyperoxia significantly reduced brain size (Figure 14D; 3.7 e^6 µm3 for normoxia vs. 2.7e^6 µm3 for hyperoxia, n=6; Mann Whitney U test, 0.002), and optic lobe size (Figure 14E; 1.9 e^6 µm3 for normoxia vs. 1.1 e^6 µm3 for hyperoxia, n=6; Mann Whitney U test, p value=0.04). In order to quantify mitotic activity we manually counted the number of cells stained for anti-PH3 in the entire optic lobe. Mitotic profiles (PH3 positive) among neuroepithelial cells showed a reduction in number in brains exposed to hyperoxia (Figure 14F; student t test, p value=0.019). Interestingly, brains exposed to hyperoxia showed smaller proliferation centres and also a smaller proportion of cells undergoing mitosis (Figure 14J; Student t test, p value=0,002).

Coherently, the number of neuroblasts in the optic lobe was significantly reduced (Figure 14G; mean: 1145 for normoxia vs. 842 for hyperoxia, Student t test, p value=$3.5e^{-5}$), however, the proportion of neuroblasts undergoing mitosis showed no significant differences suggesting that the decreased number of neuroblasts responds to a reduced mitotic activity among neuroepithelial cells (Figure 14K; Mann Whitney U test, p value=0.06). The effect on reduced brain size is apparently not a cause of increased cell death, as apoptotic nuclei where actually more scarce in larvae exposed to hyperoxia (Figure 14I; mean: 209 in normoxia vs 163 in hyperoxia, student t test, p value=0.048).

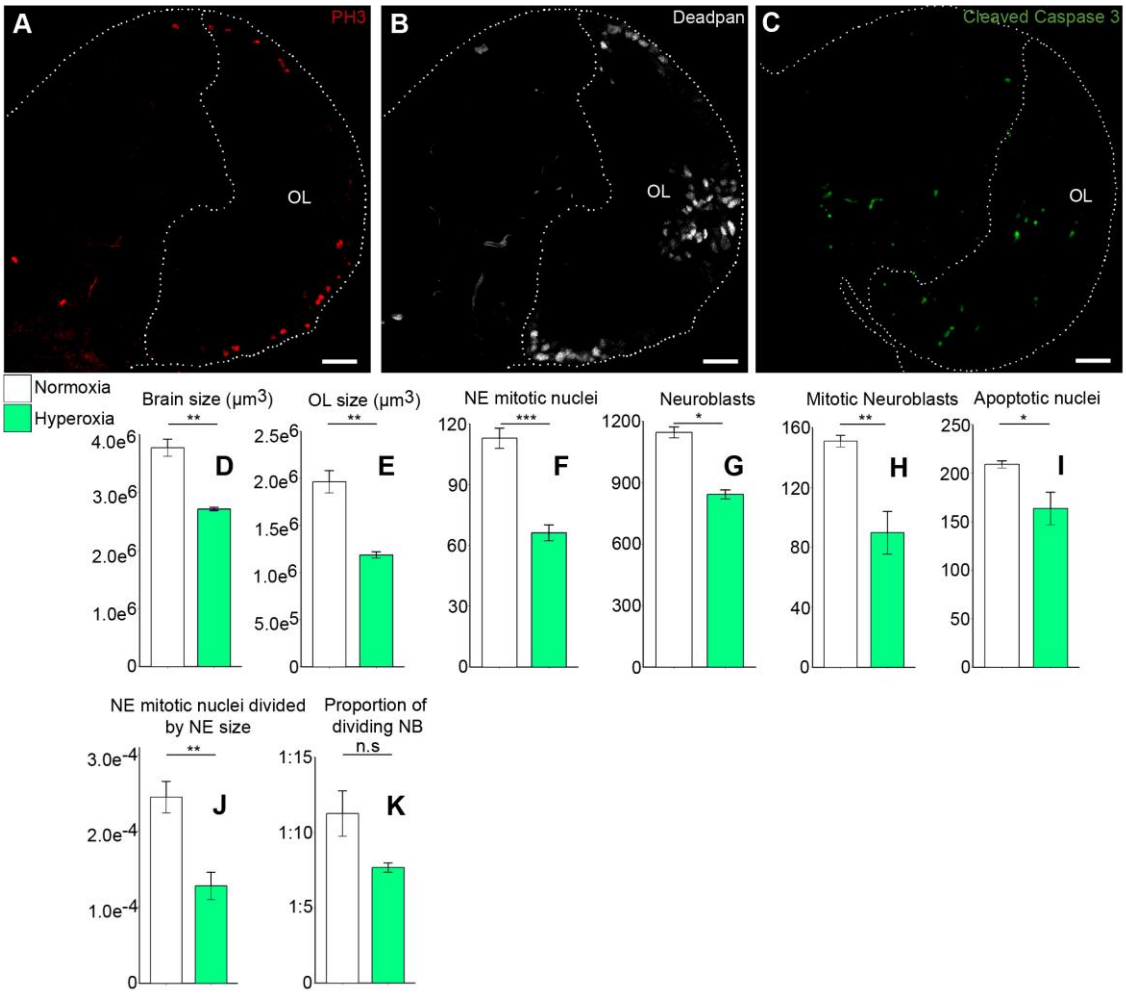

Figure 14. Ambient hyperoxia reduces mitotic activity in the optic lobe and results in smaller brains. *(A, B and C) show horizontal sections of brain lobes stained for mitotic nuclei, neuroblasts and apoptotic nuclei, respectively for control brainas (experimental brains are very similar and not shown here). Brains subjected to hyperoxia were smaller (D) and had smaller optic lobes (E). The number of neuroepithelial cells undergoing mitosis was reduced in hyperoxia (F) and when normalized against neuroepithelial size, brains exposed to hyperoxia showed fewer mitotic nuclei per volume of neuroepithelium compared to brains exposed to normoxia (J). Both the number of neuroblasts as well as the number of neuroblasts undergoing mitosis was reduced in larvae exposed to hyperoxia (G and H). However, the proportion of neuroblasts undergoing mitosis did not show a significant difference in either treatment (K). (I)*

shows that brains reared in hyperoxia had fewer cells undergoing apoptosis than control brains.

Ambient hypoxia reduces oxygenation of the brain

Next we exposed the larvae to ambient hypoxia to investigate if the sensor is able to show decreased O_2 availability in the brain. Larvae where exposed to hypoxic air with 5% O_2 from 72 hrs ALH until the end of larval life. We observed an increase in ratio values in both central brain and optic lobe which reflects a higher activated hypoxia response, probably meaning lower O_2 availability (Figure 15D). Figure 15C shows frequency distributions for ratio values normalized against the mean in each brain illustrating that the difference between central brain and optic lobe is increased. The difference between average central brain and optic lobe oxygenation found in normoxic larvae is significantly increased in hypoxia as attested by student t test (figure 15E; difference between means in optic lobe and central brain in normoxia: 0.36 and hypoxia: 0.60, p value= 0.008, n=6). Although we managed to diminish O_2 in the optic lobe, we chose not to study the effects of hypoxia in the optic lobe further because larvae reared in hypoxia abandon the food and also experience dramatic metabolic and growth effects that would make our results difficult to interpret (Bailey et al., 2015; Callier et al., 2013; Wong et al., 2014).

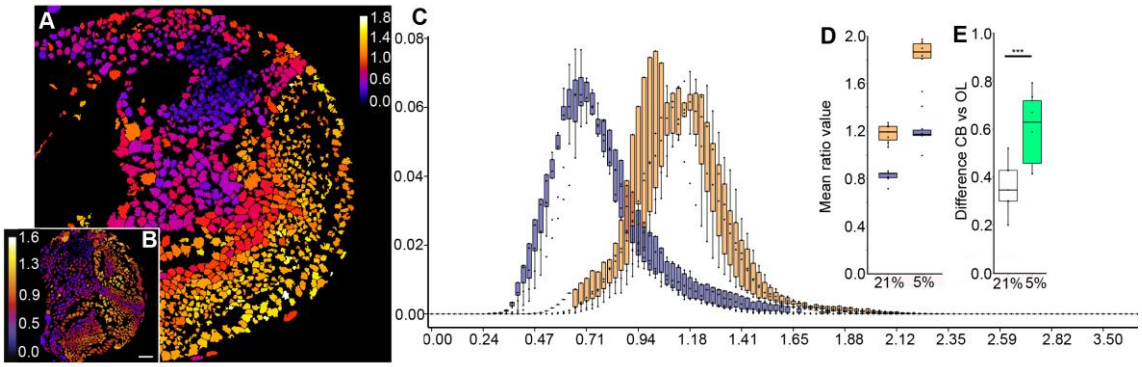

Figure 15. Ambient hypoxia reduces oxygen supply in the brain. *(A) Ratiometric analysis revealed a reduced oxygenation of the optic lobe in larvae reared in hypoxia when compared to larvae reared in normoxia (B). Frequency histogram shows distributions of values normalized by the mean (C). Without normalization, optic lobe and central brain ratios show a reduction in 5% O_2 (D) and the difference between optic lobe and central brain mean ratio was increased showing that the OL is even less oxygenated than in larvae raised in normoxia (E).*

Using the GAL4-UAS system to direct tracheolar growth in the optic lobe guided by *bnl* expression

The two most important factors in tracheal system development are encoded by the genes *bnl* and *btl*. The localized expression of *bnl* directs tracheolar growth to specific locations in the tissue by activating the BTL receptor in the tracheal cells. *btl* is active in brain tracheolar cells during embryonic and larval development (Pereanu et al., 2007). Due to the lack of antibodies for Btl and Bnl we resorted to the GAL4-UAS system to study *bnl* and *btl* expression patterns. Using *bnl-GAL4* and *btl-GAL4* to drive the expression of *UAS-GFP* we discovered that the *bnl* promoter is active in the perineurial glia surrounding the brain (Figure 16A, B and C show 36, 60 and 84 hrs. ALH respectively) and confirmed that *btl* is expressed in the tracheal system throughout larval development (Figure 16D, E and F show 36, 60 and 84 hrs ALH respectively). As larval life proceeds, the brain grows rapidly in size and the tracheal system must account for the increasing demand of O_2 by growing itself. It is likely that Btl and Bnl interact during larval life structuring and guiding the growth of the tracheal system to account for the increasing oxygen needs (Centanin et al., 2008). It is worth noting that *bnl* expression seems to be weaker and in some cases appeared to be much weaker in the perineurial glia at the surface of the optic lobe (Figure 16A and B, arrowhead).

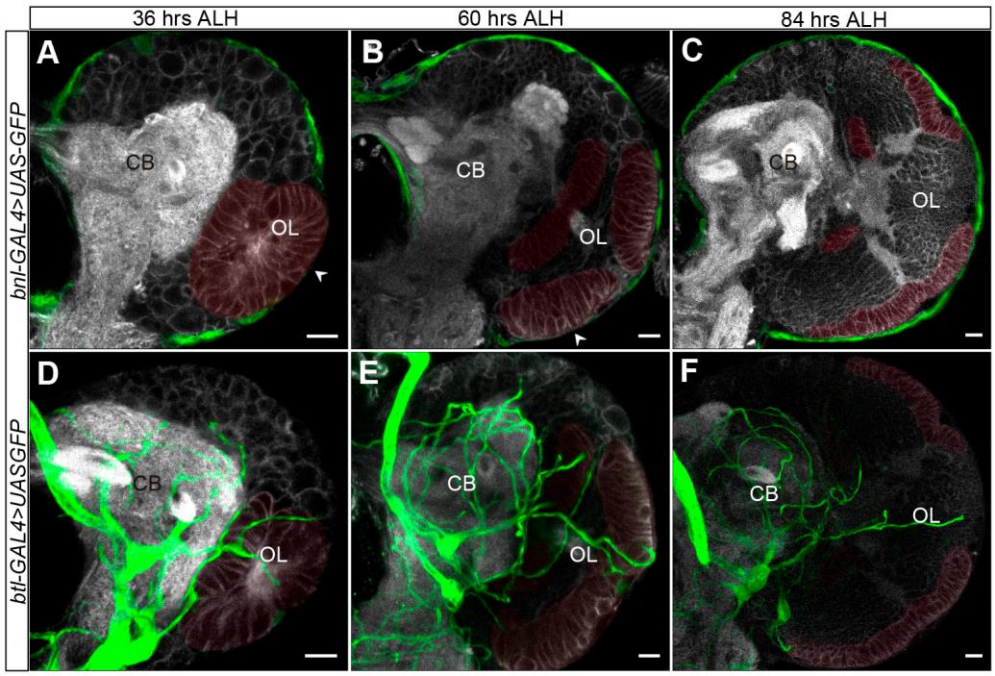

Figure 16. btl and bnl expression in the larval brain. *Confocal frontal sections of brain hemispheres showing the central brain and optic lobe stained for GFP (green) and Dlg (gray) to outline cells and the neuropile, respectively. The lateral half of each brain hemisphere comprises cells that form the developing optic lobe. (A, B and C) show the expression pattern of bnl (as evidenced by bnl-GAL4 activity) in green for 36 (A), 60 (B), and 84 (C) hrs ALH. (D, E and F) show the expression pattern of btl (as evidenced by btl-GAL4 activity) in green for 36 (D), 60 (E), and 84 (F) hrs ALH. bnl expression is restricted to the perineurial glia and it seems to be downregulated in the surface of the optic lobe. Btl is expressed in the tracheal system in every stage of development studied. Scale bar 10µm.*

Ectopic expression of *bnl* with a Bolwig nerve driver induces the growth of ectopic tracheoles into the optic lobe along the Bolwig nerve.

During larval development, the *bnl* enhancer is only active in glial cells. Therefore, we used the GAL4-UAS system and a number of Glial-cell drivers to induce the growth of trachea in the optic lobe (Figure 17). With this approach we were unable to induce a significant number of tracheoles to grow into the optic lobe, regardless of the driver. The optic lobe appears to be almost completely impervious to tracheolar growth except for the inner cell plug through which tracheoles did grow at least with one of the drivers used (Figure 17C and G). This result suggested that the majority of the optic lobe is reluctant to trachea growth while directed by a driver with a broad glial expression and thus we determined to use a driver that can direct *bnl* expression along the inner cell plug. After these pilot experiments we decided to use only the RH6 driver, which has the enhancer from the gene encoding Rhodopsin 6 and is expressed in larval photoreceptor axons entering the brain along the Bolwig nerve, along the optic stalk of the eye imaginal disk (Melamed and Trujillo-Cenóz, 1975). After entering the brain the Bolwig nerve follows the Inner cell plug and the terminals of the axons carried by this nerve are restricted to a very small brain neuropile (the Larval Optic Center) making this driver very convenient to obtain tracheoles in a very localized, small volume of the optic lobe. With this type of localized *bnl* missexpression we found that tracheoles external to the optic lobe (originating from the central brain) were induced to follow the Bolwig nerve centripetally and grow ectopically into the optic lobe in a localized bundle (Figure 18). The phenotype was extreme at later stages of development meaning that most of the trachea and tracheoles in the brain were pressed in a bundle following the Bolwig nerve, and therefore we decided to study early larvae at 36 hrs (Figure 18A, B and C) and 60 hrs ALH (Figure 18D, E and F).

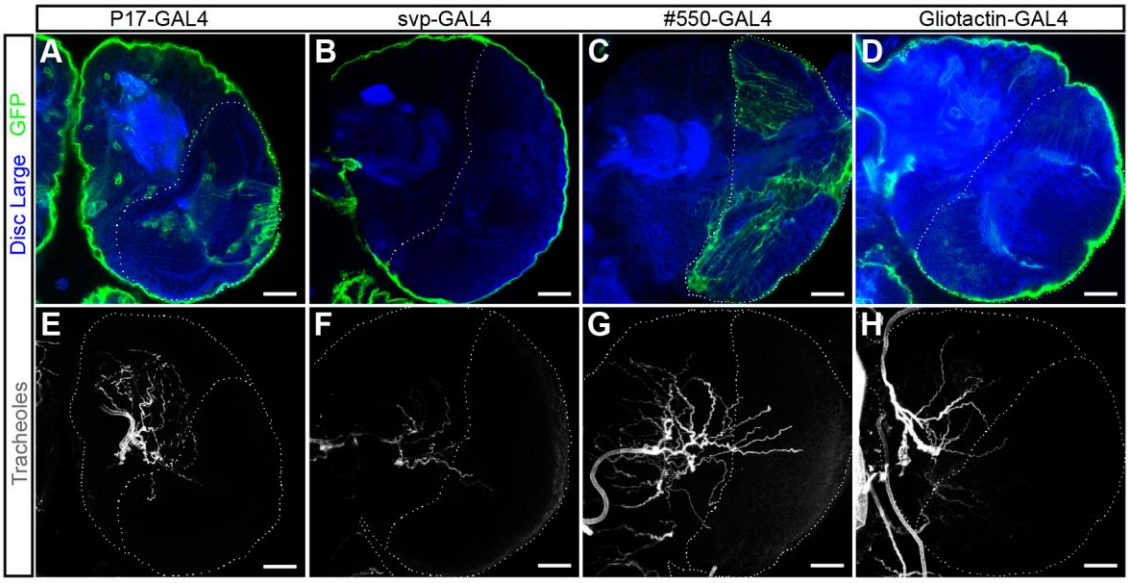

Figure 17. Four different glial-specific GAL4 drivers used to attempt the induction of ectopic tracheolation into the optic lobe. *(A), (B), (C) and (D) show bnl expression pattern (Green) when driven by P17-GAL4, NP5606-GAL4, #550-GAL4 and Glioactin-GAL4 respectively. Anti-Dlg was used to mark the cell membrane (Blue). (E), (F), (G) and (H) show the resulting tracheal pattern (maximum projection of a complete hemisphere). Scale bars, 20 µm.*

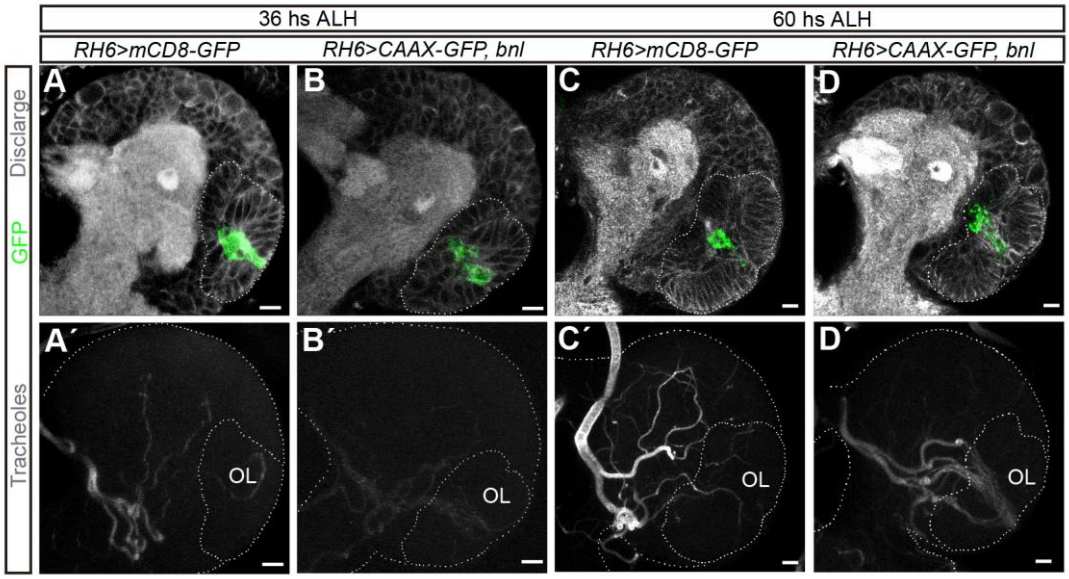

Figure 18. Ectopic expression of bnl with the RH6 driver induces growth of tracheoles into the optic lobe. *The directed expression of bnl with the RH6-GAL4 driver induced tracheoles to grow in a bundle into the optic lobe. 36 and 60 hrs ALH individuals were analysed and shown here. The spatial pattern of expression of the RH6 driver is evidenced by expression of CAAX-GFP which marks the cell membrane (green). In (A) and (C) GFP reports where this driver induced the expression of bnl. In (B) and (D) UAS-mCD8GFP served as a control for UAS-bnl. Disc Large depicts the cell membrane in (A,B C and D). (A´, B´, C´and D´) show a maximum intensity projection of the tracheal system of the brain. (A´) and (C´) show control brains (RH6-GAL4; UAS-mcD8GFP). (B´) and (D´) show tracheoles entering the optic lobe in a bundle in brains in which ectopic expression of bnl was induced (RH6-GAL4; UAS-CAAX-GFP, UAS-bnl). Notice that the ectopic expression of bnl appears to recruit tracheoles from the central brain to the optic lobe. Scale bar: 20 µm (A, B, A´, B´) and 10µm (C, D, C ´, D´).*

Using the ratiometric analysis, we confirmed that at 36 hrs ALH, ectopic tracheoles entering the optic lobe manage to carry O_2 and to increase the oxygenation of the optic lobe significantly (Figure 19; difference between the ratiometric values for optic lobe and central brain: 0.33 in the control vs. 0.09 with ectopic trachea, n=6, student t test, p value=0.002). There is a small increase in ratio values for the central brain when ectopic tracheolation is induced. This means that the central brain receives less oxygen, suggesting that part of the tracheoles that grow into the optic lobe belong originally to the central brain. However, the change observed in the difference of oxygenation between central brain and optic lobe in brains with ectopic tracheolation comes predominantly from a reduction in optic lobe values, and not from an increase of central brain values. For the 60 hrs ALH brain ectopic tracheoles did not induce significant changes in O_2 distribution (Figure 20, difference between the ratiometric values for optic lobe and central brain: 0.33 in the control vs. 0.37 with ectopic trachea, n=7, Mann Whitney U test, p value=0.18).

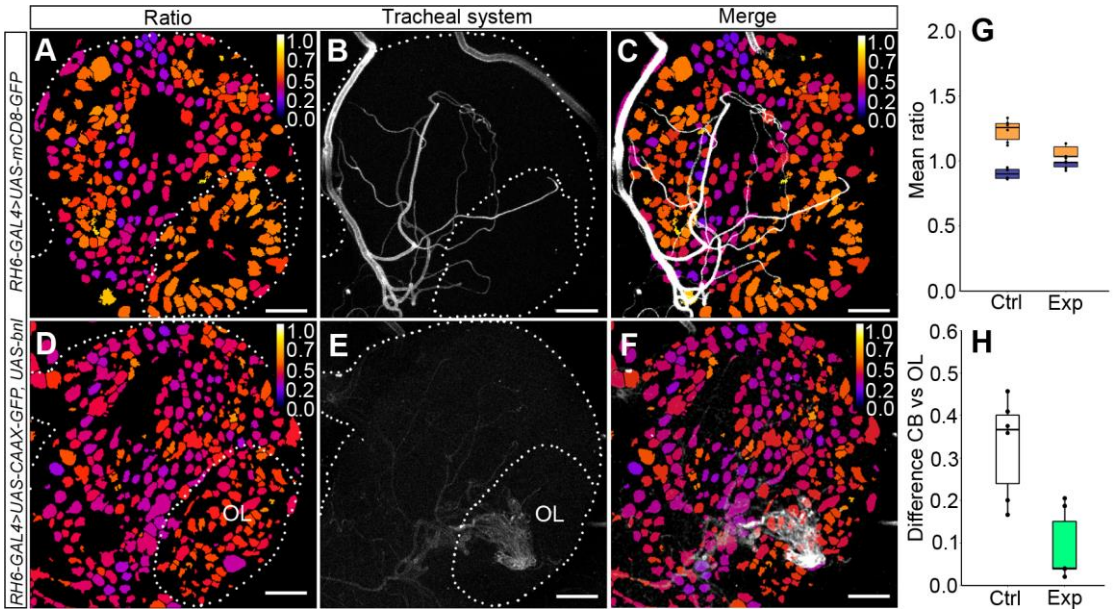

Figure 19. The sensor suggests that ectopic tracheolation significantly increases oxygen levels in the optic lobe. *(A, C, D and F) show single slices of ratiometric values measured in stacks. (B and E) show maximum projections of the tracheal system autofluorescence as recorded with 405 nm laser. Upper row (A, B, and C) show control brains (ubi-GFP-ODD, ubi-mRFPnls; RH6-GAL4/UAS-mCD8-GFP) and lower row (D, E and F) shows brains with ectopic tracheolation in the optic lobe (C: ubi-GFP-ODD, ubi-mRFPnls; RH6-GAL4/UAS-bnl). (G) depicts mean ratio for each brain compartments (central brain and optic lobe). Oxygen dependent degradation of GFP-ODD was increased by ectopic tracheolation of the optic lobes which is evidenced by lower ratio values. (H) shows a decrease in the difference of oxygenation of central brain and optic lobe for the brains with ectopic tracheolation. Scale bar: 20µm.*

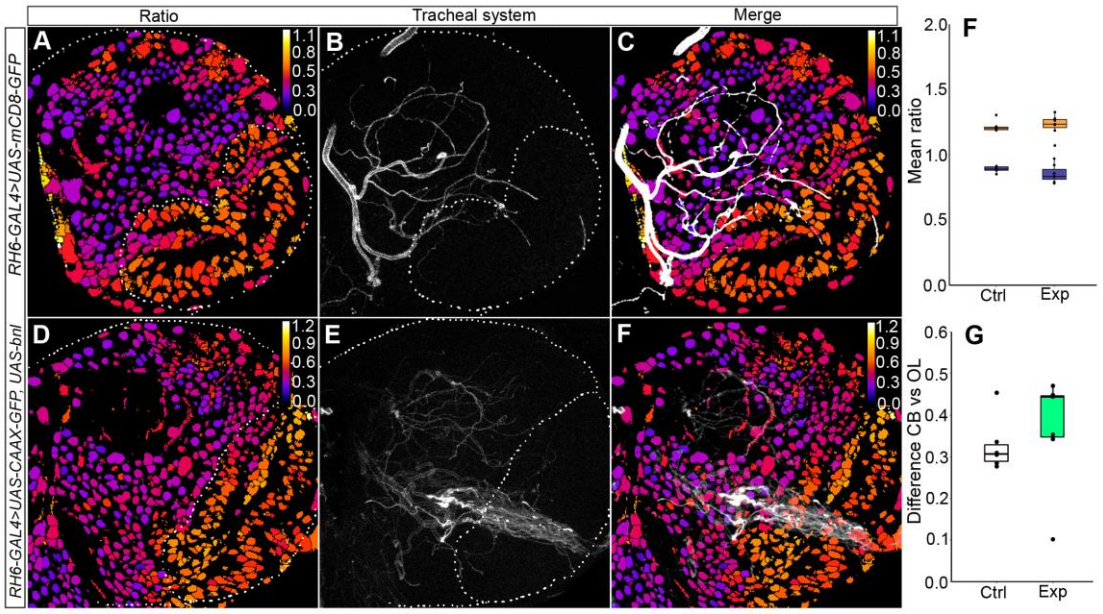

Figure 20. Ectopic tracheolation significantly increases oxygenation in the optic lobe. *(A, C, D and F) show single slices of ratiometric stacks. (B and E) show maximum projections of the tracheal autofluorescence as recorded with a 405 nm laser. Upper row (A, B, and C) show control brains (ubi-GFP-ODD, ubi-mRFPnls; RH6-GAL4/UAS-mCD8-GFP) and lower row (D, E and F) shows brains with ectopic tracheolation in the optic lobe (C: ubi-GFP-ODD, ubi-mRFPnls; RH6-GAL4/UAS-bnl). (G) depicts mean ratio for each brain compartment (central brain and optic lobe). Oxygen dependent degradation of GFP-ODD is increased by ectopic trahceolation of the optic lobes which is evidenced by lower ratio values. (H) shows a decrease in the difference of oxygenation of central brain and optic lobe for the brains with ectopic tracheolation. Scale bar: 20µm.*

Ectopic tracheolation reduces mitotic activity in the optic lobe

If cell proliferation is reduced by increased O_2 then ectopic tracheolation might also slow down mitotic activity and perhaps also produce smaller brains or brains with smaller optic lobe as observed in larvae kept in ambient hyperoxia. We measured control and ectopic tracheolated brain and optic lobe volumes at different larval stages. We found no significant changes at 36 hrs ALH (Figure 21G and H; brain mean: $2.77e^5$ μm^3 for the control vs. $3.00e^5$ μm^3 for ectopic trachea, n=21, student t test, p value=0.14, optic lobe mean: $3.4e^4$ μm^3 for the control vs. $3.9e^4$ μm^3 for ectopic trachea, n=21, student t test, p value=0.08) or at 60 hrs ALH (Figure 21G and H; brain mean: $6.28e^5$ μm^3 for the control vs. $7.36e^5$ μm^3 for ectopic trachea, n=24, student t test, p value=0.06, optic lobe mean: $1.5e^5$ μm^3 for the control vs. $1.7e^5$ μm^3 for ectopic trachea, n=24, Mann Whitney U test, p value=0.24). After [3t-I] thymidine incubation of brains of freshly hatched larvae no labelled nuclei are found in the precursor cells of the optic lobes. However, from the 1^{st} and 2^{nd} larval instar on, mitotic cells appear in the optic lobe (Hofbauer and Campos-Ortega; 1990). We used an anti-PH3 antibody to mark mitotic nuclei as a method to measure the rate of cell proliferation (Figure 21A and D). The results showed that at 36 hrs ALH, there are fewer mitotic nuclei in the Neuroepithelium of brains with ectopic tracheoles (Figure 21I; 27 for control vs. 21 for ectopic tracheoles, n=11, student t test, p value=0.0085). This difference was however smaller than what was found in larvae kept under atmospheric hyperoxia, which probably responds to the fact that the additional oxygenation that ectopic tracheoles induced in the experimental optic lobe is mild (Figure 19). No change was observed at 60 hrs ALH (Figure 21I; mean: 86 for control vs. 81 for ectopic trachea, n=12, student t test, p value=0.21).

To test if the transition from neuroepithelial cells to neuroblasts was affected, or if the proliferation rate of neuroblasts was altered, we used anti-Deadpan to mark and quantify the number of neuroblasts (Figure 21B and E). No change was evident in neuroblasts number either at 36 hrs ALH or at 60 hrs ALH (Figure 21J; 36 hrs mean: 22 for control vs. 21 for brain with ectopic trachea, n=10, student t test, p value=0.33; 60 hrs mean: 37 for control vs. 34 for ectopic tracheoles, n=10, student t test, p value=0.35, respectively). Finally, we tested if neural differentiation was induced by

ectopic tracheoles in the optic lobe by using anti-Bruchpilot to mark synapses (Figure 21C and F). we found no differences between control and experimental brains in neuropil size (anti-BRP positive regions of the brain) at 36 hrs ALH or at 60 hrs ALH (Figure 21K; 36 hrs mean: 27758 μm^3 for control vs. 34201 μm^3 for ectopic trachea, n=10, Mann Whitney U test, p value=0.35; 60 hrs mean: $1.0e^5$ μm^3 for control vs. $1.1e^5$ μm^3 for ectopic tracheoles, n=10, student t test, p value=0.38, respectively).

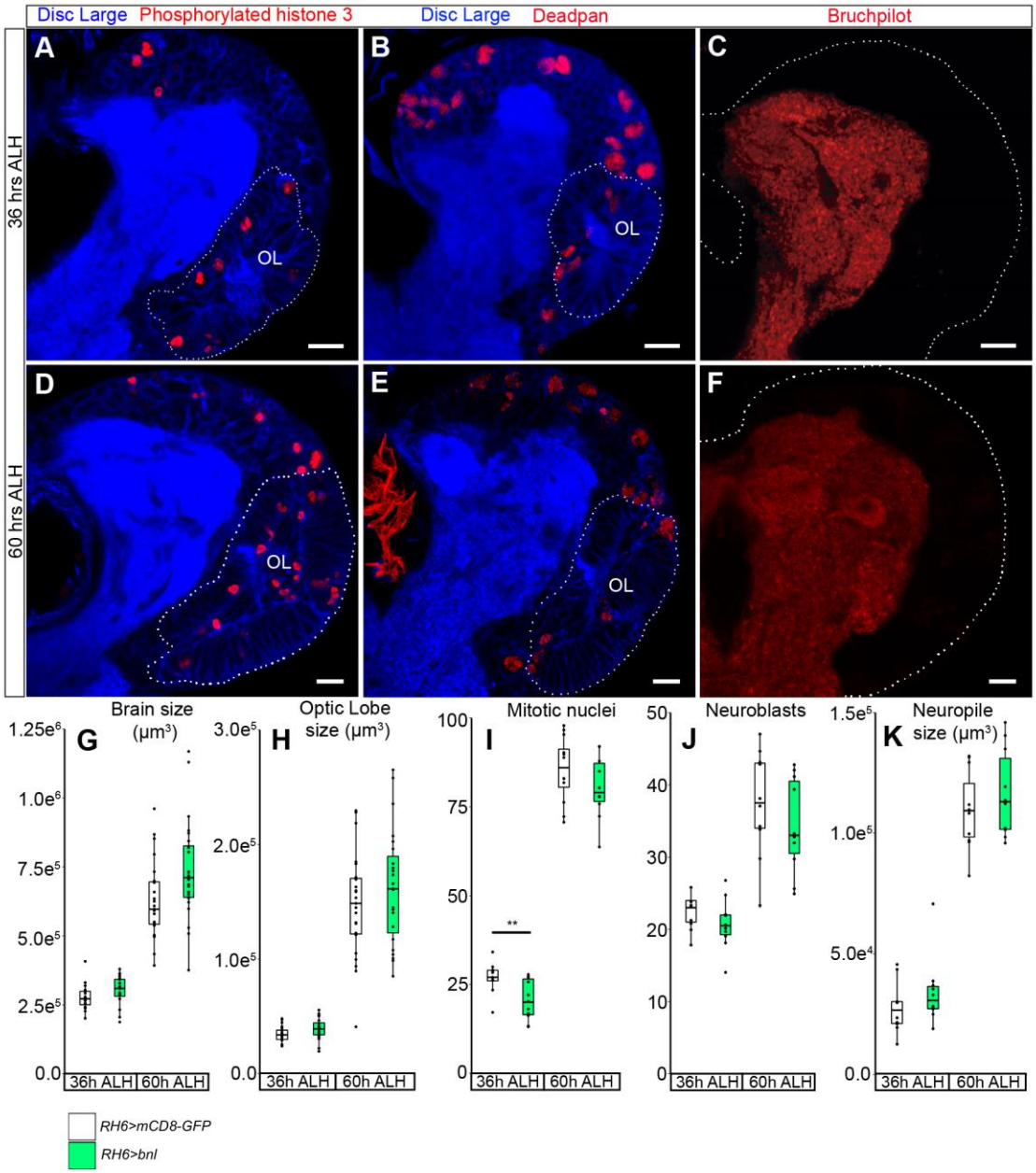

Figure 21. Ectopic tracheolation reduces mitotic activity in the optic lobe at 36 hrs ALH*. (A to F) are confocal frontal sections of the larval brain. (A and D) show brains stained for PH3 (mitotic nuclei) and Disc Large. (B and E) show brains stained for Deadpan (Neuroblasts) and Disc Large. (C and F) show brains stained for Bruchpilot (synapses). Using whole brain stacks we quantified Brain size (G), Optic Lobe size (H), mitotic nuclei (I), Neuroblasts (J) and Neuropile size (K) at 36 hrs and 60 hrs ALH. The only difference observed was a decrease in mitotic activity at 36 hrs ALH. Scale bar 10 µm.*

<u>Ectopic tracheolation of the optic lobe appear not to cause malformation of the adult brain.</u>

Lastly we tested if the ectopic tracheolation of the optic lobe in the larval brain leads to gross neuroanatomical defects in the adult optic neuropiles. We used anti-Dlg to mark the cell membranes and Track EM in Imagej to quantify the volumes of three main optic neuropiles (Figure 22A and B; Lamina, Medulla and Lobulla). We found no differences in the volume of any of the measured samples (Figure 22C, D and E. Lamina (mean): 614150 μm^3 for control vs. 664291 μm^3 for ectopic trachea, n=8, Mann Whitney U test, p value=0.84; Medulla (mean): 1215547 μm^3 for control vs. 1372693 μm^3 for ectopic trachea, n=12, Mann Whitney U test, p value=0.07; Lobula (mean): 619633 μm^3 for control vs. 684533 μm^3 for ectopic trachea, n=12, Mann Whitney U test, p value=0.18).

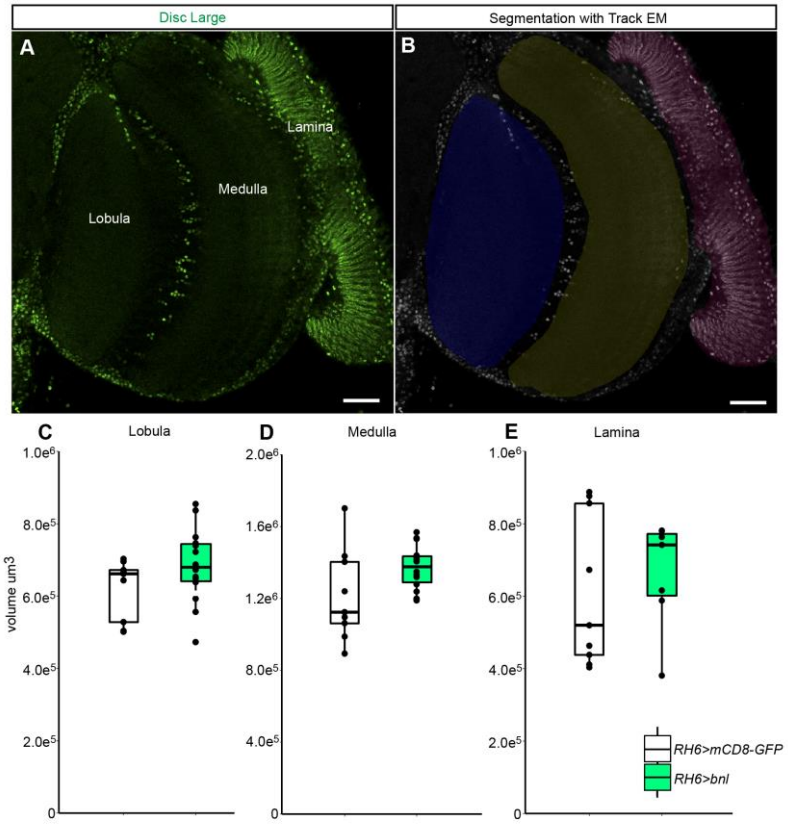

Figure 22. Ectopic tracheolation during larval optic lobe development does not affect the size of optic neuropiles in adult flies. *(A) shows an adult brain hemisphere stained for Disc Large to mark cell membranes. Optic neuropiles were measured by 3D reconstruction after segmentation with Track EM (B). (C), (D) and (E) show Lobula, Medulla and Lamina volumes respectively in control brains and brains which experienced ectopic tracheolation of the optic lobes during larval life. Scale bar 20 µm.*

Neuroblasts and neuroepithelial cells are the most hypoxic cell type in the brain

The division of central brain and optic lobe to compare ratiometric values was suitable to test that there should be a differential distribution of O_2 in the brain when comparing the two compartments. However, different cell types reside in each of these compartments, and, even though there are not fully defined niches or border lines that separate cell types within the compartments, there are nonetheless stereotyped positions for different cell types that could determine variable O_2 availability among them. It will be interesting to know whether the method employed here based in the hypoxia sensor and its ratiometric analysis could be used to investigate the possibility that different cell types exhibit different degrees of hypoxia response. For this approach we combined the sensor with antibodies used as cell-specific markers to perform the ratiometric analysis in identified cell types. The following primary antibodies were used: Anti-Deadpan for neuroblasts (Figure 23A), anti-Repo for glial cells (Figure 23B), anti-Prospero for ganglion mother cells (Figure 23C; Weng y Cohen, 2015), anti-Elav for neurons (Figure 23D) and anti-Dachshund for Lamina precursors (Figure 23E). Stacks obtained for stainings with these markers served as the primal image to produce cell type specific mask-like/binary stacks for the ratiometric analysis (Figure 23A´, B´, D´).

In the case of brains stained for Prospero and Dachshund, the macro used to segment the other stainings failed to produce a good enough binary image. We found that the DeadEasy Larval-Glia plugin for imagej provided the means to obtain a superior binary image than the one produced by the macro (Figure 23C´, E´). To investigate possible differences in the ratiometric values of each cell type depending on whether the cells are located in the central brain or the optic lobe we used the same method used before for the manual segmentation of these two regions.

We found differences among several cell types and also between cells of the same type depending on whether they were located in the central brain or the optic lobe. In the central brain, neuroblasts appeared to be more hypoxic than any other cell type, and this difference was statistically significant (Figure 23F; mean: 0.96 for neuroblasts, 0.68 for ganglion mother cells, student t test, p value= $1.28e^{-7}$, 0.78 for Glial cells, p value= $1.52e^{-5}$, 0.80 for neurons, student t test, p value= 0.0015). On the

other hand, ganglion mother cells appeared to be more hyperoxic than any other cell type including neurons and glial cells (Figure 23F; mean: 0.68 ganglion mother cell, 0.78 for Glial cells, p value=$5.41e^{-4}$; 0.80 neurons, p value= 0.0018, student t test). Interestingly, neuroblasts appeared also to be the most hypoxic cell type in the optic lobe together with neuroepithelial cells (Figure 23F; mean: 1.29 for neuroblasts, 1.11 for ganglion mother cells, student t test, p value= $3.09e^{-12}$, 1.14 for Glial cells, student t test, p value= $8.50e^{-8}$, 1.1 for LPs, student t test, p value= $6.97e^{-5}$). The IPC and OPC were segmented using Track EM in imagej and the ratio values of these two proliferative centres were among the most hypoxic in the brain. The OPC showed no significant difference with neuroblasts of the optic lobe. In summary, neuroblasts are apparently the most hypoxic cell type in the central brain and optic lobe (in the optic lobe they share this characteristic with OPC cells). Neuroblasts are more hypoxic than IPC cells (Figure 23F; mean: 1.29 for neuroblasts and 1.21 for IPC cells, p value=0.01; Man Whitney U test). Ganglion mother cells appeared to be the most hyperoxic cell type in the central brain and are among the most hyperoxic cell type in the optic lobe. The different cell types have stereotypical positions in the brain and therefore, the differences in mean ratio values could be accounted for by the distance from cells to the tracheal system.

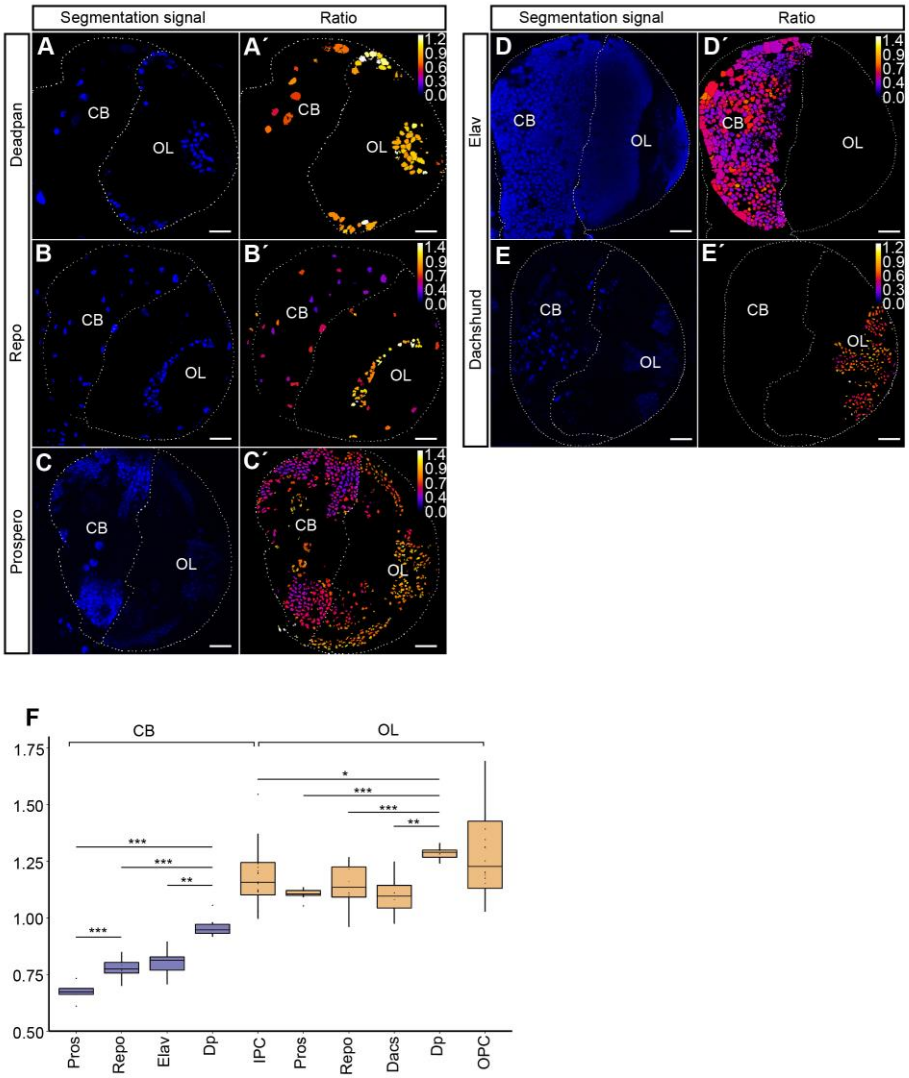

Figure 23. The state of the hypoxia response varies among different cell types in the brain. *Specific staining for neuroblasts, glial cells, neurons, ganglion mother cells and Lamina precursors (A to E) was used to perform a cell specific study of hypoxia response and presumably* O_2 *distribution using the ratiometric analysis. The segmentation signal used to create the ratio image (F-J) was the cell specific staining. Mean ratio for central brain and optic lobe for each cell type is represented in (F). Every cell type in the Optic Lobe is more hypoxic than any cell type belonging to the Central Brain (K). Neuroblasts appear to be the most hypoxic cell type when compared against other cell types both in the Central Brain or the Optic Lobe (K). Pros stands for cells marked with anti-Prospero antibody, Repo with anti-repo antibody, Elav with anti-Elav antibody, Deadpan with anti-Deadpan and Dacs with anti-Dacshund. Scale bar 20 µm.*

Discussion

The optic lobe is hypoxic in comparison to the central brain which correlates with the tracheal pattern in the brain

The hypoxia sensor used for this Thesis (Misra et al., submitted) is a genetic construct consisting of a fusion protein with the Oxygen-Degradation-Dependent domain of Sima fused to GFP and co-expressed with a non-oxygen dependent RFP. The GFP signal is degraded in the presence of O_2. When compared to the O_2 insensitive signal (nlsRFP) a ratio value is obtained which indicates the level of activation of the hypoxia response of the cell and presumably its O_2 levels because the ratio value is inversely proportional to the oxygen dependent degradation of GFP-ODD. Hence, the relatively low ratio values observed in the optic lobe of 96 hrs brains where tracheoles are almost completely absent indicates that the sparse tracheolation of the optic lobe translates into lower O_2 levels. The oxygen gradient observed in the vicinity of the OLTl tracheole(s) is a powerful example evidencing the spatial resolution produced by our biosensor combined with our ratiometric analysis.

To our knowledge this is the first time that it has been shown that the distribution of tracheoles correlates with O_2 availability in a tissue and hence one of the most important advances of our work.

This approach provides several specific advantages when compared to other methods to monitor hypoxia response or oxygen availability. Firstly, it reveals spatial information at a single-cell resolution, which is lost in whole-animal transcriptomic and proteomic analyses, in mass spectrometry (Seylaz and Pinard, 1978). These methods employ a relatively large tissue probe, providing an 'average' rather than a highly localised measurement (Erecińska and Silver, 2001). Good spatial resolution is also difficult to obtain with microelectrodes (Clark, 1959) which are invasive and would not allow as many measurements as this method provides, in which virtually every cell in an entire brain could be accounted for. Porphyrin Phosphorescence Methods (Shonat et al., 1992, 1995; Shonat and Johnson, 1997) need injection of the fluorophore and the signal is distorted by oxygen consumption as phosphorescence decays. Secondly, this system detects changes directly at the level of the cellular O_2 sensor, rather than

downstream transcriptional responses, and therefore avoids the delay associated with transcriptional reporters, such as *ldh-GAL4-UAS-GFP (ldh* stands for lactate dehydrogenase*)*or other hypoxia-responsive element (HRE) derived drivers (Lavista-Llanos et al., 2002; Erapaneedi et al., 2016). Transcriptional reporters get stably induced by a hypoxic episode, but do not, or only with a significant delay, report the dynamics of the response, such as equilibration after re-oxygenation. Thirdly, the hypoxia reporter used here is compatible with a variety of genetic manipulations including other transgenic constructs, mutations, RNAi, and over-expression, and thus provides a versatile tool for a wide range of approaches to examine hypoxia signalling and its relation to physiological and pathological conditions.

One of the most important findings in this work is that the asymmetric tracheolation of the larval brain corresponds with relative lower level of O_2 in the optic lobe compared to the central brain. This suggests that undifferentiated cells in the optic lobe exist in a relatively hypoxic niche when compared to the more oxygenated differentiated cells in the central brain, which is in agreement with the extensive literature describing the relationship between hypoxia and stem cells (as reviewed in Mohyeldin et al., 2010) and more specifically, between hypoxia and neural stem cells (Panchision, 2009). The novelty of these finding is that this is the first time that a hypoxic neural stem cell niche is described for *Drosophila*. The relevance of this is that *Drosophila* is an excellent model for most of the scientific research oriented to understand stem cell biology and now it can be used to study the functional relationship between stem cells and hypoxia.

As previously described, during early larval stages (1^{st} and 2^{nd} instar) the optic lobe consists exclusively of neuroepithelial cells. Later on, the population of neuroepithelial cells, neuroblasts, ganglion mother cells and their postmitotic progenies increases dramatically which completely reshapes the structure and the cellular constitution of the optic lobe. Our results suggest that this asymmetric O_2 distribution between central brain and optic lobe is already present as early as 24 hrs into larval development and remains so throughout larval development. The result suggests that hypoxia is an important condition for the maintenance of neural stem cells in the optic lobe during all stages of larval development. In further experiments,

we must determine the mechanisms that maintain the difference in oxygenation between central brain and optic lobe seemingly constant with the rapid increase in optic lobe volume.

The imaginal disks are another tissue that is deprived of tracheoles where cells are born but do not differentiate until metamorphosis. It is possible that in these tissues, similar mechanisms to the ones in the optic lobe are in play. The study of imaginal disks *in vitro* or *in vivo* in hypoxic and hyperoxic conditions could reveal similar mechanisms and therefore be a good model to validate our results. If the cells in the imaginal discs benefit from hypoxic conditions as cells in the optic lobe do, then hyperoxia should reduce proliferation and maybe induce premature differentiation, and hypoxia should do the opposite.

In the context of the previous findings our results obtained for *btl* and *bnl* expression patterns are worth discussing. *btl* is expressed in tracheal cells and *bnl* is mostly expressed in perineurial glia, especially in the central brain. *bnl* expression seems to be weaker and in some cases shows some gaps in perineurial glia at the surface of the optic lobe (Figure 16A and B, arrowhead). Tracheoles never reach the Perineurial glia where *bnl* is expressed, which suggests that *bnl* expression probably serves a function different from attracting tracheal growth, which has been previously shown (Dossenbach et al., 2001). Another interpretation is that while Bnl is being released from the perineurial glia, and inducing tracheolar growth, an additional inhibitory signal prevents trachea from growing into the optic lobe and reaching the glial layer. For instance, Archipielago (*ago*) was shown to act as an antagonist of the physiologic response to low oxygen (hypoxia). Reducing Ago activity in larval muscle cells elicits enhanced branching of nearby tracheal terminal cells in normoxia (Mortimer and Moberg, 2013). In this sense, *ago* is a possible candidate as inhibitory signal preventing trachea to grow into the optic lobe. This would be an interesting area into which the future of our research could be directed. Interestingly, it has been shown that *ago* is expressed in neuroepithelial cells of the optic lobe (Southall et al., 2013).

Possible metabolic implications of hypoxia in the optic lobe

Our results indicate that stem cells in the larval optic lobe are adapted to a fairly hypoxic state compared with other brain regions. Evidently, survival in hypoxia requires adaptations that include metabolic adjustments. In the absence of O_2, cells have a metabolism based on glycolysis, mostly avoiding mitochondrial respiration (oxidative phosphorylation) which is O_2 dependent. However, some authors suggest that the energy produced by a glycolytic metabolism is not sufficient to sustain the energetic costs of cell proliferation (Tannock, 1968; Olivotto and Paoletti, 1981; Olivotto et al., 1984; Cipolleschi et al., 1993). Others propose that only extreme hypoxia drives cells into a quiescent state, while mild hypoxia (3%) allows cells to proliferate (Cipolleschi et al., 1993; Eliasson et al., 2010). In the 1920s, Otto Warburg described what was later called the Warburg effect based on observations made on glucose consumption by tumors. It was found that glucose uptake in tumor cells was higher when compared to surrounding tissue due to a high rate of fermentation even in the presence of O_2 (Warburg 1925; Liberti and Locasale, 2016). A glycolytic metabolism is far less efficient in terms of energy production when compared to mitochondrial respiration. However, it is worth noting that while the Warburg effect yields a smaller ATP production, it is faster in producing energy than the complete combustion of glucose through oxidative phosphorylation (Shestov 2014). The Warburg Effect is believed to be an adaptation mechanism to support the biosynthetic requirements for rapid proliferation (Liberti and Locasale, 2016). With the incomplete combustion of glucose, this process yields a great amount of excess carbon that can be diverted into the multiple anabolic branching pathways that emanate from glycolysis, and to be used for the generation of nucleotides, lipids, and proteins. Additionally, proliferating cells are in greater need of reducing equivalents in the form of NADPH than of ATP. The great uptake of glucose allows for the production of NADPH in the oxidative branch of pentose phosphate pathway and used in biosynthesis (Vander Heiden et al., 2009; Ward and Thompson, 2012). Tennessen and collaborators (2011) describe a model in which *Drosophila* larval growth depends on a form of aerobic glycolysis that is similar to the Warburg effect and that is dependent of estrogen-

related receptors (ERRs; Tennessen et al., 2011). The trehalase gene in *Drosophila* encodes a hydrolase that generates energy by hydrolysing threhalose into two glucose molecules (Chen et al., 2014). In the *Drosophila* optic lobe, the loss of the threhalase gene causes neuroepithelial disintegration and premature generation of medulla neuroblasts. The authors propose that Threhalase controls neuroepithelial cells stem cells maintenance supressing differentiation. However, since they were not able to rescue the mutant phenotype by raising the larvae in high-glucose diet these authors propose that perhaps the protein Trehalase does not contribute to optic lobe development by its trehalase enzymatic activity but through other, unknown function (Chen et al., 2014). Another option is that Trehalase works as a trehalase enzyme but the addition of glucose to the diet is not sufficient to make a difference big enough that would rescue the phenotype.

In the context of the aforementioned findings, it is possible that metabolic adaptations similar to the Warburg effect are in place in the *Drosophila* optic lobe allowing cells to rapidly divide during larval development producing the great amount of progeny needed to structure the adult optic neuropiles despite the fact that they reside in a brain region almost devoid of tracheoles and under relative hypoxia. Cells avoid the need of O_2 to cover the enormous metabolic need of this process and in doing so, manage to protect the precious stem cells from ROS-induced damage.

Oxygenation of the optic lobe results in diminished mitotic activity, suggesting that hypoxia is important for optic lobe stem cells to keep their normal rate of mitotic activity.

Once we had obtained results reinforcing the idea that the sparse tracheolation of the optic lobe correlates with lower oxygen levels relative to the central brain, an important hypothesis to be tested during this work was whether this feature is necessary for normal brain development. We expected that reducing hypoxia in the optic lobe would result in a decreased rate of proliferation in all or some of the precursor cells. We tested this hypothesis by incrementing oxygen levels in the optic lobe with two different experimental approaches. Larvae reared in hyperoxia had

fewer neuroepithelial cells undergoing mitosis, as well as fewer neuroblasts compared with control larvae, reared in normoxia. It is interesting that while the number of neuroepithelial cells undergoing mitosis was reduced when the larvae were kept in ambient hyperoxia, the proportion of neuroblasts undergoing mitosis was not significantly reduced. This indicates that the smaller number of neuroblasts in hyperoxia is probably a response to the reduced mitotic activity of neuroepithelial cells. As a consequence fewer neuroepithelial cells undergo the transition to neuroblasts. The reduction of mitotic activity results in smaller brains and smaller optic lobes. This is probably a response to the hyper-oxygenation of the optic lobe as reported by the ratiometric analysis. However, it is possible that this phenotype responds to an alteration of development and metabolism caused by the increased oxygen concentration and therefore, the reduced rate in cell division we observed could be a response to a systemic effect of hyperoxia and not a direct effect of oxygen concentration on neuroepithelial cells. Our second approach proves that this is probably not the case since a localized change in O_2 delivery induced by the ectopic growth of tracheoles into the optic lobe also appeared to slow down mitotic activity. The use of the ratiometric analysis of the fluorescence emitted by the oxygen sensor allowed us to test whether the ectopic tracheoles managed to increase O_2 levels locally. Our results were consistent with the hypothesis that ectopic optic lobe tracheolation does increment oxygen levels in the optic lobe and showed a similar result to that obtained by incubation of larvae in 60% oxygen. We observed a small decrease in neuroepithelial cells proliferation but we did not observed changes in neuroblasts number. Interestingly, the effect was observed only at 36 hrs ALH but not at 60 hrs ALH. This could have several explanations. One possibility is that during the time from 36 to 60 hrs ALH a compensatory mechanism is responsible for recovering cell mitosis in the experimental brains. Additionally, it could be that our method was not able to detect a decrease of mitosis by the localized delivery of O_2 provided by ectopic trachea when the optic lobes (but not the ectopic trachea) grow larger.

Thus, both approaches had a negative effect on mitotic rate but the exposure of the entire larvae to 60% oxygen during several days had clearly a stronger effect than incrementing oxygen locally by ectopic tracheolation in larvae kept in normoxia.

Additionally, by exposing the larvae to hyperoxia we found a decrease in neuroblasts number which we don´t find by inducing ectopic tracheolation. This could have different explanations. First, neuroblasts appear in the larval optic lobe during the second instar and it is possible that the time between appearance of neuroblasts and dissection time was not enough for the ectopic tracheolation to induce a significant effect. Also, there is a possibility that neuroblasts are less sensitive to hyperoxia than neuroepithelial cells, and therefore, the small amount of extra O_2 provided by the ectopic tracheoles was perhaps not sufficient to affect their division rate, while the amount provided by a hyperoxic environment is. Taken together, these results show that hypoxia in the optic lobe relative to the central brain is a required condition for normal brain development, and that a reduction of this condition results in reduced mitotic activity, fewer cells and smaller brain.

Interestingly, a recent publication indicates that the same occurs in a neurogenic tissue in mammals. Lange and collaborators (2016) tested the very same hypothesis in mammals and found that in early neurogenic regions of the CNS, absence of blood vessels result in relatively low oxygen levels which in turn keep the neurogenic region in a proliferative state (radial glia amplification). Later on, angiogenesis leads to higher oxygen which switches cell fate to intermediate precursor division (asymmetric divisions) and neuronal differentiation. They used staining with pimonidazole as hypoxia marker, and looked at mutants without correct vascularization. Exposure to increased oxygen levels (80%) rescued NSC differentiation in mutants without correct vascularization and increased it further in WT embryos.

<u>Cell type specific analysis of hypoxia response activation</u>

Using specific cell markers in combination with measuring the green and red fluorescence of the oxygen sensor to calculate the mean ratio of each cell type revealed that the hypoxia response shows quantitative differences among different cell types. We selected a set of antibodies to identify every step in the differentiation process of cells in the optic lobe (neuroepithelial cells, neuroblasts, ganglion mother cells, lamina precursors, glial cells and neurons). Our results suggest that this is indeed

the case since we found differences indicative of different degrees of hypoxia response in some cell types. Neuroblasts and neuroepithelial cells appeared to be the most hypoxic cell types of the brain, suggesting that hypoxia is a condition that favours more undifferentiated cell types, which are multipotent, as documented by other studies (Eliasson et al., 2010). Also in our studies more committed progenitors (ganglion mother cells), neurons and glial cells, appeared to have a less activated hypoxia response. Possibly these cells receive less oxygen, suggesting that cells that are more advanced in the differentiation process prefer a more normoxic environment. However, all our heat maps indicated that in each brain there are some cells with substantially different ratiometric values although they are located very close to each other. This prompts the question of how cells manage to regulate their O_2 availability when they co-exist in the same niche and are located very closely to each other. It is likely that different cells are exposed to variable O_2 concentrations by different mechanisms, of which the most simple and obvious will be their distance to tracheoles. This mechanism, however, needs to be elucidated by a more detailed structural analysis including careful measurements of 3D reconstructions.

An alternative explanation could be cell-specific facilitation of oxygen diffusion or transport, or different oxygen binding properties. Aquaporines have been proposed as a factor regulating cell permeability to O_2 (Panchision, 2009), which means that there are pathways through which O_2 diffuses more easily in a given tissue virtually allowing the possibility of existence of more or less oxygenated microenvironments within the same niche or tissue compartment. However, very little is known about aquaporing-mediated gas transport into cells in *Drosophila*.

Another possibility could be cell-specific differences in proteasome activation, enzymatic activity or in the expression of proteins of the hypoxia response other than Sima. It is important to remember that the degradation of GFP-ODD, which depends principally upon O_2 availability (Misra et al., submitted and the present study), can be also affected by other factors as the activity of Tango, which forms dimers with Sima and the prolyl hydroxylase (Fatiga) and dVhl. Southall and collaborators (2013) showed that the expression of the genes encoding Tango and dVhl is particularly higher in neuroblasts when compared to neuroepithelial cells, while the expression of *fatiga* is

higher in neuroepithelial cells. In the “classic” hypoxia response all of these three genes contribute to the degradation of Sima, and therefore differences in their level of expression among cell types could affect the degradation of GFP-ODD. A differential activity of the proteasome among different cell types in the larval brain could mean that degradation of GFP-ODD is not only a function of O_2 availability and therefore depends on other factors as well. However, it is still safe to say that the sensor reflects the state of activation of hypoxia response in a given cell and we conclude that neuroblasts and neuroepithelial cells are more sensitive to O_2 than ganglion mother cells, glial cells or neurons. This means that less committed progenitors (neuroepithelial cells and neuroblasts) are apparently more sensitive to O_2 and need a more hypoxic environment to thrive, at least in comparison to more committed progenitor cells such as ganglion mother cells, or fully committed cells such as neurons and glia. This is not the first time that such a model has been proposed. Cipolessci et al proposed that the distance a cell is away from a blood vessel in a stem cell hematopoietic niche could be an indicator of its hierarchy as a stem cell. Meaning that, a cell receiving low levels of O_2 should have higher multipotency and less fate commitment than a cell receiving more O_2. A model similar to the one observed in the hematopoietic stem cell niche could be in place in the Drosophila larval optic lobe, where primary progenitor cells are protected from oxidative damage by existing in a more hypoxic microenvironment, which become gradually more oxygenated as they advance in the differentiation process.

Conclusion and Perspectives

In this Thesis we investigated if the sparse tracheolation of the larval optic lobes in Drosophila melanogaster has functional relevance for the development of the brain. Using a novel genetic tool, a fluorescent protein biosensor, we showed that the optic lobe receives less oxygen than the central brain, which is densely tracheolated. Using a ratiometric analysis of the signals emitted by the biosensor to map oxygen availability throughout the brain of larvae exposed to higher oxygen levels, and throughout brains in which the normal oxygen distribution had been manipulated by means of ectopic tracheolation of the optic lobe, we showed that the hypoxic condition of this brain region is necessary for normal brain development. With both experimental approaches, elevated oxygen levels resulted in slower mitotic activity among proliferating neuroepithelial cells.

We have thus shown that the Drosophila brain can be used as a novel system to study stem cell homeostasis in relation to O2 concentration in vivo. Given that this model organism offers countless sophisticated genetic tools and experimental advantages, we propose that this model has a promising future in advancing the study of hypoxia and neural stem cell function.

In a near future, it would be interesting to investigate the molecular mechanisms that sense the increase of O2 tension in the optic lobe and convey the signal to neuroepithelial cells to reduce their proliferative rate. It is possible that HIF is involved in this process and probably other hypoxia-pathway related genes such as *fatiga*, *dvhl* and *tango*. By down-regulation or up-regulation of these genes, it might be possible to rescue the phenotype produced by ambient hyperoxia in stem cell proliferation. Other proteins, such as Trehalase which regulates metabolism and is necessary for the correct development of the optic lobe could also be regulated in it´s expression by the hypoxia pathway genes. It would be interesting to investigate if these two pathways are connected and to discover other relationships between the hypoxia pathway and metabolism in the optic lobe.

It will also be important to clarify the mechanism that limits the growth of tracheoles into the optic lobes. Archipielago is a possible candidate and down-

regulation of Archipielago protein levels with ago RNA interference, using the GAL4-UAS system, might induce trachea to grow into the optic lobe.

Finally, Egger (2013) published a protocol to perform primary neural cell culture in Drosophila. It will be interesting to apply this method to study the effect of hypoxia and hyperoxia in culture using cell cultures that express the sensor. Additionally, this will allow us to correlate GFP-ODD levels with absolute values of O2 concentration.

Acknowledgements

I am very greatful to Rafael Cantera and Boris Egger for their supervision. I thank ANII for financial support (Fondo Clemente Estable and Master Scholarship), PEDECIBA and Clemente Estable Institute. Stefan Luschnig and Tvisa Misra produced the bio-sensor used in this work. I also appreciate Dr. Santiago Ruiz´s help and advice in the beginning of my work. During this Thesis I did two internships in the Department of Biology in the University of Fribourg, for which I thank the Institution for welcoming me, Boris Egger, the Swiss National Foundation and the Swiss University Conference.

References

Affolter, M. and Caussinus, E. (2008). Tracheal branching morphogenesis in Drosophila: new insights into cell behaviour and organ architecture. Dev. Camb. Engl. *135*, 2055–2064.

Affolter, M., Montagne, J., Walldorf, U., Groppe, J., Kloter, U., LaRosa, M. and Gehring, W.J. (1994). The Drosophila SRF homolog is expressed in a subset of tracheal cells and maps within a genomic region required for tracheal development. Dev. Camb. Engl. *120*, 743–753.

Anderson, M.G., Certel, S.J., Certel, K., Lee, T., Montell, D.J. and Johnson, W.A. (1996). Function of the Drosophila POU domain transcription factor drifter as an upstream regulator of breathless receptor tyrosine kinase expression in developing trachea. Dev. Camb. Engl. *122*, 4169–4178.

Apitz, H. and Salecker, I. (2014). A challenge of numbers and diversity: neurogenesis in the Drosophila optic lobe. J. Neurogenet. *28*, 233–249.

Aplin, J.D. (2000). Hypoxia and human placental development. J. Clin. Invest. *105*, 559–560.

Azad, P., Zhou, D., Russo, E. and Haddad, G.G. (2009). Distinct mechanisms underlying tolerance to intermittent and constant hypoxia in Drosophila melanogaster. PloS One *4*, e5371.

Bacon, N.C., Wappner, P., O'Rourke, J.F., Bartlett, S.M., Shilo, B., Pugh, C.W. and Ratcliffe, P.J. (1998). Regulation of the Drosophila bHLH-PAS protein Sima by hypoxia: functional evidence for homology with mammalian HIF-1 alpha. Biochem. Biophys. Res. Commun. *249*, 811–816.

Baer, M.M., Bilstein, A. and Leptin, M. (2007). A clonal genetic screen for mutants causing defects in larval tracheal morphogenesis in Drosophila. Genetics *176*, 2279–2291.

Bailey, A.P., Koster, G., Guillermier, C., Hirst, E.M.A., MacRae, J.I., Lechene, C.P., Postle, A.D. and Gould, A.P. (2015). Antioxidant Role for Lipid Droplets in a Stem Cell Niche of Drosophila. Cell *163*, 340–353.

Bao, B., Azmi, A.S., Ali, S., Ahmad, A., Li, Y., Banerjee, S., Kong, D. and Sarkar, F.H. (2012). The biological kinship of hypoxia with CSC and EMT and their relationship with deregulated expression of miRNAs and tumor aggressiveness. Biochim. Biophys. Acta *1826*, 272–296.

Berra, E., Ginouvès, A. and Pouysségur, J. (2006). The hypoxia-inducible-factor hydroxylases bring fresh air into hypoxia signalling. EMBO Rep. *7*, 41–45.

Boroughs, L.K. and DeBerardinis, R.J. (2015). Metabolic pathways promoting cancer cell survival and growth. Nat. Cell Biol. *17*, 351–359.

Brahimi-Horn, M.C., Chiche, J. and Pouysségur, J. (2007). Hypoxia and cancer. J. Mol. Med. Berl. Ger. *85*, 1301–1307.

Brand, A.H. and Livesey, F.J. (2011). Neural stem cell biology in vertebrates and invertebrates: more alike than different? Neuron *70*, 719–729.

Branicky, R.S. and Schafer, W.R. (2008). Oxygen homeostasis: how the worm adapts to variable oxygen levels. Curr. Biol. CB *18*, R559-560.

Braun, R.D., Lanzen, J.L., Snyder, S.A. and Dewhirst, M.W. (2001). Comparison of tumor and normal tissue oxygen tension measurements using OxyLite or microelectrodes in rodents. Am. J. Physiol. Heart Circ. Physiol. *280*, H2533-2544.

Brodu, V. and Casanova, J. (2006). The RhoGAP crossveinless-c links trachealess and EGFR signaling to cell shape remodeling in Drosophila tracheal invagination. Genes Dev. *20*, 1817–1828.

Bruick, R.K. (2003). Oxygen sensing in the hypoxic response pathway: regulation of the hypoxia-inducible transcription factor. Genes Dev. *17*, 2614–2623.

Buerk, D.G., Shonat, R.D., Riva, C.E. and Cranstoun, S.D. (1993). O2 gradients and countercurrent exchange in the cat vitreous humor near retinal arterioles and venules. Microvasc. Res. *45*, 134–148.

Burgess, R.J., Agathocleous, M. and Morrison, S.J. (2014). Metabolic regulation of stem cell function. J. Intern. Med. *276*, 12–24.

Busuttil, R.A., Rubio, M., Dollé, M.E.T., Campisi, J. and Vijg, J. (2003). Oxygen accelerates the accumulation of mutations during the senescence and immortalization of murine cells in culture. Aging Cell *2*, 287–294.

Cachero, S., Ostrovsky, A.D., Yu, J.Y., Dickson, B.J. and Jefferis, G.S. (2010). Sexual dimorphism in the fly brain. Curr. Biol. CB 20, 1589-1601.

Cairns, R.A., Harris, I.S. and Mak, T.W. (2011). Regulation of cancer cell metabolism. Nat. Rev. Cancer *11*, 85–95.

Callier, V., Shingleton, A.W., Brent, C.S., Ghosh, S.M., Kim, J. and Harrison, J.F. (2013). The role of reduced oxygen in the developmental physiology of growth and metamorphosis initiation in Drosophila melanogaster. J. Exp. Biol. *216*, 4334–4340.

Calvi, L.M., Adams, G.B., Weibrecht, K.W., Weber, J.M., Olson, D.P., Knight, M.C., Martin, R.P., Schipani, E., Divieti, P., Bringhurst, F.R., et al. (2003). Osteoblastic cells regulate the haematopoietic stem cell niche. Nature *425*, 841–846.

Campbell, G., Göring, H., Lin, T., Spana, E. andersson, S., Doe, C.Q. and Tomlinson, A. (1994). RK2, a glial-specific homeodomain protein required for embryonic nerve cord condensation and viability in Drosophila. Dev. Camb. Engl. *120*, 2957–2966.

Campos-Ortega, J. A. and Hartenstein, V. (1985). The embryonic development of Drosophila melanogaster. In The Development of Drosophila melanogaster (ed. Bate M. and Martinez-Arias A.). Cold Spring Harbor, New York: Cold Spring Harbor Laboratory Press. pp. 1363–1492.

Campos-Ortega, J.A. and Knust, E. (1990). Molecular analysis of a cellular decision during embryonic development of Drosophila melanogaster: epidermogenesis or neurogenesis. Eur. J. Biochem. FEBS *190*, 1–10.

Cantera, R. and Trujillo-Cenoz, O. (1996). Glial cells in insect ganglia. Microsc. Res. Tech. *35*, 285–293.

Carmeliet, P. and Jain, R.K. (2000). Angiogenesis in cancer and other diseases. Nature *407*, 249–257.

Carmeliet, P., Dor, Y., Herbert, J.M., Fukumura, D., Brusselmans, K., Dewerchin, M., Neeman, M., Bono, F., Abramovitch, R., Maxwell, P., et al. (1998). Role of HIF-1alpha in hypoxia-mediated apoptosis, cell proliferation and tumour angiogenesis. Nature *394*, 485–490.

Casaccia-Bonnefil, P. (2000). Cell death in the oligodendrocyte lineage: a molecular perspective of life/death decisions in development and disease. Glia *29*, 124–135.

Catling, D.C., Glein, C.R., Zahnle, K.J. and McKay, C.P. (2005). Why O2 is required by complex life on habitable planets and the concept of planetary "oxygenation time." Astrobiology *5*, 415–438.

Centanin, L., Ratcliffe, P.J. and Wappner, P. (2005). Reversion of lethality and growth defects in Fatiga oxygen-sensor mutant flies by loss of hypoxia-inducible factor-alpha/Sima. EMBO Rep. *6*, 1070–1075.

Centanin, L., Dekanty, A., Romero, N., Irisarri, M., Gorr, T.A. and Wappner, P. (2008). Cell autonomy of HIF effects in Drosophila: tracheal cells sense hypoxia and induce terminal branch sprouting. Dev. Cell *14*, 547–558.

Chanut-Delalande, H., Jung, A.C., Lin, L., Baer, M.M., Bilstein, A., Cabernard, C., Leptin, M. and Affolter, M. (2007). A genetic mosaic analysis with a repressible cell marker screen to identify genes involved in tracheal cell migration during Drosophila air sac morphogenesis. Genetics *176*, 2177–2187.

Chell, J.M. and Brand, A.H. (2010). Nutrition-responsive glia control exit of neural stem cells from quiescence. Cell *143*, 1161–1173.

Chen, C.K., Kühnlein, R.P., Eulenberg, K.G., Vincent, S., Affolter, M. and Schuh, R. (1998). The transcription factors KNIRPS and KNIRPS RELATED control cell migration and branch morphogenesis during Drosophila tracheal development. Dev. Camb. Engl. *125*, 4959–4968.

Chen, H.-L., Pistollato, F., Hoeppner, D.J., Ni, H.-T., McKay, R.D.G. and Panchision, D.M. (2007). Oxygen tension regulates survival and fate of mouse central nervous system precursors at multiple levels. Stem Cells Dayt. Ohio *25*, 2291–2301.

Chen, X., Quan, Y., Wang, H. and Luo, H. (2014). Trehalase regulates neuroepithelial stem cell maintenance and differentiation in the Drosophila optic lobe. PloS One *9*, e101433.

Chow, D.C., Wenning, L.A., Miller, W.M. and Papoutsakis, E.T. (2001). Modeling pO(2) distributions in the bone marrow hematopoietic compartment. I. Krogh's model. Biophys. J. *81*, 675–684.

Cipolleschi, M.G., Dello Sbarba, P. and Olivotto, M. (1993). The role of hypoxia in the maintenance of hematopoietic stem cells. Blood *82*, 2031–2037.

Clark, L.C. (1959). Electrochemical device for chemical analysis. US Patent 2,913,386.

Corbin, J.G., Gaiano, N., Juliano, S.L., Poluch, S., Stancik, E. and Haydar, T.F. (2008). Regulation of neural progenitor cell development in the nervous system. J. Neurochem. *106*, 2272–2287.

Csete, M. (2005). Oxygen in the cultivation of stem cells. Ann. N. Y. Acad. Sci. *1049*, 1–8.

Dang, C.V. (2012). Links between metabolism and cancer. Genes Dev. *26*, 877–890.

Davies, P.W. and Brink, F. (1942). Microelectrodes for Measuring Local Oxygen Tension in Animal Tissues. Rev. Sci. Instrum. *13*, 524–533.

De Marais, D.J. (2000). Evolution. When did photosynthesis emerge on Earth? Science *289*, 1703–1705.

DeBerardinis, R.J., Lum, J.J., Hatzivassiliou, G. and Thompson, C.B. (2008). The biology of cancer: metabolic reprogramming fuels cell growth and proliferation. Cell Metab. *7*, 11–20.

Dekanty, A., Lavista-Llanos, S., Irisarri, M., Oldham, S. and Wappner, P. (2005). The insulin-PI3K/TOR pathway induces a HIF-dependent transcriptional response in Drosophila by promoting nuclear localization of HIF-alpha/Sima. J. Cell Sci. *118*, 5431–5441.

Dello Sbarba, P., Cipolleschi, M.G. and Olivotto, M. (1987). Hemopoietic progenitor cells are sensitive to the cytostatic effect of pyruvate. Exp. Hematol. *15*, 137–142.

Dewhirst, M.W., Braun, R.D. and Lanzen, J.L. (1998). Temporal changes in PO2 of R3230AC tumors in Fischer-344 rats. Int. J. Radiat. Oncol. Biol. Phys. *42*, 723–726.

Dismukes, G.C., Klimov, V.V., Baranov, S.V., Kozlov, Y.N., DasGupta, J. and Tyryshkin, A. (2001). The origin of atmospheric oxygen on Earth: the innovation of oxygenic photosynthesis. Proc. Natl. Acad. Sci. U. S. A. *98*, 2170–2175.

Dossenbach, C., Röck, S. and Affolter, M. (2001). Specificity of FGF signaling in cell migration in Drosophila. Dev. Camb. Engl. *128*, 4563–4572.

Dunwoodie, S.L. (2009). The role of hypoxia in development of the Mammalian embryo. Dev. Cell *17*, 755–773.

Egger, B., Boone, J.Q., Stevens, N.R., Brand, A.H. and Doe, C.Q. (2007). Regulation of spindle orientation and neural stem cell fate in the Drosophila optic lobe. Neural Develop. *2*, 1.

Egger, B., Gold, K.S. and Brand, A.H. (2010). Notch regulates the switch from symmetric to asymmetric neural stem cell division in the Drosophila optic lobe. Dev. Camb. Engl. *137*, 2981–2987.

Egger, B., Gold, K.S. and Brand, A.H. (2011). Regulating the balance between symmetric and asymmetric stem cell division in the developing brain. Fly (Austin) *5*, 237–241.

Egger, B., van Giesen, L., Moraru, M., and Sprecher, S.G. (2013). In vitro imaging of primary neural cell from Drosophila. Nat. Protoc. 8, 958–965.

Eliasson, P., Rehn, M., Hammar, P., Larsson, P., Sirenko, O., Flippin, L.A., Cammenga, J. and Jönsson, J.-I. (2010). Hypoxia mediates low cell-cycle activity and increases the proportion of long-term-reconstituting hematopoietic stem cells during in vitro culture. Exp. Hematol. *38*, 301–310.e2.

Epstein, A.C., Gleadle, J.M., McNeill, L.A., Hewitson, K.S., O'Rourke, J., Mole, D.R., Mukherji, M., Metzen, E., Wilson, M.I., Dhanda, A., et al. (2001). C. elegans EGL-9 and mammalian homologs define a family of dioxygenases that regulate HIF by prolyl hydroxylation. Cell *107*, 43–54.

Erapaneedi, R., Belousov, V.V., Schäfers, M. and Kiefer, F. (2016). A novel family of fluorescent hypoxia sensors reveal strong heterogeneity in tumor hypoxia at the cellular level. EMBO J. *35*, 102–113.

Erecińska, M. and Silver, I.A. (2001). Tissue oxygen tension and brain sensitivity to hypoxia. Respir. Physiol. *128*, 263–276.

Ezashi, T., Das, P. and Roberts, R.M. (2005). Low O2 tensions and the prevention of differentiation of hES cells. Proc. Natl. Acad. Sci. U. S. A. *102*, 4783–4788.

Farkas, L.M. and Huttner, W.B. (2008). The cell biology of neural stem and progenitor cells and its significance for their proliferation versus differentiation during mammalian brain development. Curr. Opin. Cell Biol. *20*, 707–715.

Favaro, E., Lord, S., Harris, A.L. and Buffa, F.M. (2011). Gene expression and hypoxia in breast cancer. Genome Med. *3*, 55.

Firth, J.D., Ebert, B.L. and Ratcliffe, P.J. (1995). Hypoxic regulation of lactate dehydrogenase A. Interaction between hypoxia-inducible factor 1 and cAMP response elements. J. Biol. Chem. *270*, 21021–21027.

Fischer, B. and Bavister, B.D. (1993). Oxygen tension in the oviduct and uterus of rhesus monkeys, hamsters and rabbits. J. Reprod. Fertil. *99*, 673–679.

Florio, M. and Huttner, W.B. (2014). Neural progenitors, neurogenesis and the evolution of the neocortex. Dev. Camb. Engl. *141*, 2182–2194.

Folkman, J. and Klagsbrun, M. (1987). Angiogenic factors. Science *235*, 442–447.

Folkman, J., Hahnfeldt, P. and Hlatky, L. (2000). Cancer: looking outside the genome. Nat. Rev. Mol. Cell Biol. *1*, 76–79.

Fyles, A., Milosevic, M., Hedley, D., Pintilie, M., Levin, W., Manchul, L. and Hill, R.P. (2002). Tumor hypoxia has independent predictor impact only in patients with node-negative cervix cancer. J. Clin. Oncol. Off. J. Am. Soc. Clin. Oncol. *20*, 680–687.

Gao, S., Takemura, S.-Y., Ting, C.-Y., Huang, S., Lu, Z., Luan, H., Rister, J., Thum, A.S., Yang, M., Hong, S.-T., et al. (2008). The neural substrate of spectral preference in Drosophila. Neuron *60*, 328–342.

Gatenby, R.A. and Gillies, R.J. (2004). Why do cancers have high aerobic glycolysis? Nat. Rev. Cancer *4*, 891–899.

Ghabrial, A., Luschnig, S., Metzstein, M.M. and Krasnow, M.A. (2003). Branching morphogenesis of the Drosophila tracheal system. Annu. Rev. Cell Dev. Biol. *19*, 623–647.

Glazer, L. and Shilo, B.Z. (1991). The Drosophila FGF-R homolog is expressed in the embryonic tracheal system and appears to be required for directed tracheal cell extension. Genes Dev. *5*, 697–705.

Goda, N., Ryan, H.E., Khadivi, B., McNulty, W., Rickert, R.C. and Johnson, R.S. (2003). Hypoxia-inducible factor 1alpha is essential for cell cycle arrest during hypoxia. Mol. Cell. Biol. *23*, 359–369.

Gold, K.S. and Brand, A.H. (2014). Optix defines a neuroepithelial compartment in the optic lobe of the Drosophila brain. Neural Develop. *9*, 18.

Gordon, W.R., Arnett, K.L. and Blacklow, S.C. (2008). The molecular logic of Notch signaling--a structural and biochemical perspective. J. Cell Sci. *121*, 3109–3119.

Gorr, T.A., Gassmann, M. and Wappner, P. (2006). Sensing and responding to hypoxia via HIF in model invertebrates. J. Insect Physiol. *52*, 349–364.

Guillemin, K., Groppe, J., Ducker, K., Treisman, R., Hafen, E., Affolter, M. and Krasnow, M.A. (1996). The pruned gene encodes the Drosophila serum response factor and regulates cytoplasmic outgrowth during terminal branching of the tracheal system. Dev. Camb. Engl. *122*, 1353–1362.

Guitart, A.V., Hammoud, M., Dello Sbarba, P., Ivanovic, Z. and Praloran, V. (2010). Slow-cycling/quiescence balance of hematopoietic stem cells is related to physiological gradient of oxygen. Exp. Hematol. *38*, 847–851.

Gustafsson, M.V., Zheng, X., Pereira, T., Gradin, K., Jin, S., Lundkvist, J., Ruas, J.L., Poellinger, L., Lendahl, U. and Bondesson, M. (2005). Hypoxia requires notch signaling to maintain the undifferentiated cell state. Dev. Cell *9*, 617–628.

Harrison, J.S., Rameshwar, P., Chang, V. and Bandari, P. (2002). Oxygen saturation in the bone marrow of healthy volunteers. Blood *99*, 394.

Hartenstein, V. (1993.a). Development of the Drosophila tracheal system. In The Development of Drosophila melanogaster (ed. Bate M. and Martinez-Arias A.). Cold Spring Harbor, New York: Cold Spring Harbor Laboratory Press. pp. 609–685.

Hasegawa, E., Kitada, Y., Kaido, M., Takayama, R., Awasaki, T., Tabata, T. and Sato, M. (2011). Concentric zones, cell migration and neuronal circuits in the Drosophila visual center. Dev. Camb. Engl. *138*, 983–993.

Hayden, M.A., Akong, K. and Peifer, M. (2007). Novel roles for APC family members and Wingless/Wnt signaling during Drosophila brain development. Dev. Biol. *305*, 358–376.

Heim, R., Prasher, D.C. and Tsien, R.Y. (1994). Wavelength mutations and posttranslational autoxidation of green fluorescent protein. Proc. Natl. Acad. Sci. U. S. A. *91*, 12501–12504.

Heins, N., Malatesta, P., Cecconi, F., Nakafuku, M., Tucker, K.L., Hack, M.A., Chapouton, P., Barde, Y.-A. and Götz, M. (2002). Glial cells generate neurons: the role of the transcription factor Pax6. Nat. Neurosci. *5*, 308–315.

Helmlinger, G., Yuan, F., Dellian, M. and Jain, R.K. (1997). Interstitial pH and pO2 gradients in solid tumors in vivo: high-resolution measurements reveal a lack of correlation. Nat. Med. *3*, 177–182.

Hemphill, J.C., Smith, W.S., Sonne, D.C., Morabito, D. and Manley, G.T. (2005). Relationship between brain tissue oxygen tension and CT perfusion: feasibility and initial results. AJNR Am. J. Neuroradiol. *26*, 1095–1100.

Hockel, M., Schlenger, K., Aral, B., Mitze, M., Schaffer, U. and Vaupel, P. (1996). Association between tumor hypoxia and malignant progression in advanced cancer of the uterine cervix. Cancer Res. *56*, 4509–4515.

Hofbauer, A. and Campos-Ortega, J.A. Proliferation pattern and early differentiation of the optic lobes in Drosophila melanogaster.

Hoge, R.D. and Pike, G.B. (2001). Oxidative metabolism and the detection of neuronal activation via imaging. J. Chem. Neuroanat. *22*, 43–52.

Homem, C.C.F. and Knoblich, J.A. (2012). Drosophila neuroblasts: a model for stem cell biology. Dev. Camb. Engl. *139*, 4297–4310.

Huang, L.E., Gu, J., Schau, M. and Bunn, H.F. (1998). Regulation of hypoxia-inducible factor 1alpha is mediated by an O2-dependent degradation domain via the ubiquitin-proteasome pathway. Proc. Natl. Acad. Sci. U. S. A. *95*, 7987–7992.

Isaac, D.D. and Andrew, D.J. (1996). Tubulogenesis in Drosophila: a requirement for the trachealess gene product. Genes Dev. *10*, 103–117.

Ivan, M., Kondo, K., Yang, H., Kim, W., Valiando, J., Ohh, M., Salic, A., Asara, J.M., Lane, W.S. and Kaelin, W.G. (2001). HIFalpha targeted for VHL-mediated destruction by proline hydroxylation: implications for O2 sensing. Science *292*, 464–468.

Ivanovic, Z. (2009). Hypoxia or in situ normoxia: The stem cell paradigm. J. Cell. Physiol. *219*, 271–275.

Iwai, K., Yamanaka, K., Kamura, T., Minato, N., Conaway, R.C., Conaway, J.W., Klausner, R.D. and Pause, A. (1999). Identification of the von Hippel-lindau tumor-suppressor protein as part of an active E3 ubiquitin ligase complex. Proc. Natl. Acad. Sci. U. S. A. *96*, 12436–12441.

Jaakkola, P., Mole, D.R., Tian, Y.M., Wilson, M.I., Gielbert, J., Gaskell, S.J., von Kriegsheim, A., Hebestreit, H.F., Mukherji, M., Schofield, C.J., et al. (2001). Targeting of HIF-alpha to the von Hippel-Lindau ubiquitylation complex by O2-regulated prolyl hydroxylation. Science *292*, 468–472.

Jarecki, J., Johnson, E. and Krasnow, M.A. (1999). Oxygen regulation of airway branching in Drosophila is mediated by branchless FGF. Cell *99*, 211–220.

Johnson, P.C., Vandegriff, K., Tsai, A.G. and Intaglietta, M. (2005). Effect of acute hypoxia on microcirculatory and tissue oxygen levels in rat cremaster muscle. J. Appl. Physiol. Bethesda Md 1985 *98*, 1177–1184.

Jones, D.L. and Wagers, A.J. (2008). No place like home: anatomy and function of the stem cell niche. Nat. Rev. Mol. Cell Biol. *9*, 11–21.

Jubb, A.M., Buffa, F.M. and Harris, A.L. (2010). Assessment of tumour hypoxia for prediction of response to therapy and cancer prognosis. J. Cell. Mol. Med. *14*, 18–29.

Jungermann, K. and Kietzmann, T. (1997). Role of oxygen in the zonation of carbohydrate metabolism and gene expression in liver. Kidney Int. *51*, 402–412.

Kaelin, W.G. and Ratcliffe, P.J. (2008). Oxygen sensing by metazoans: the central role of the HIF hydroxylase pathway. Mol. Cell *30*, 393–402.

Kallinowski, F., Zander, R., Hoeckel, M. and Vaupel, P. (1990). Tumor tissue oxygenation as evaluated by computerized-pO2-histography. Int. J. Radiat. Oncol. Biol. Phys. *19*, 953–961.

Kennedy, A.S., Raleigh, J.A., Perez, G.M., Calkins, D.P., Thrall, D.E., Novotny, D.B. and Varia, M.A. (1997). Proliferation and hypoxia in human squamous cell carcinoma of the cervix: first report of combined immunohistochemical assays. Int. J. Radiat. Oncol. Biol. Phys. *37*, 897–905.

Klämbt, C., Glazer, L. and Shilo, B.Z. (1992). breathless, a Drosophila FGF receptor homolog, is essential for migration of tracheal and specific midline glial cells. Genes Dev. *6*, 1668–1678.

Knoll, A.H. (2003). The geological consequences of evolution. Geobiology *1*, 3–14.

Koch, L.G. and Britton, S.L. (2007). Evolution, atmospheric oxygen, and complex disease. Physiol. Genomics *30*, 205–208.

Koch, L.G. and Britton, S.L. (2008). Aerobic metabolism underlies complexity and capacity. J. Physiol. *586*, 83–95.

Kokovay, E. and Temple, S. (2007). Taking neural crest stem cells to new heights. Cell *131*, 234–236.

Koppenol, W.H., Bounds, P.L. and Dang, C.V. (2011). Otto Warburg's contributions to current concepts of cancer metabolism. Nat. Rev. Cancer *11*, 325–337.

Kruuv, J., Inch, W.R. and McCredie, J.A. (1967). Effects of breathing gases containing oxygen and carbon dioxide at 1 and 3 atmospheres pressure on blood flow and oxygenation of tumors. Can. J. Physiol. Pharmacol. *45*, 49–56.

Kühnlein, R.P. and Schuh, R. (1996). Dual function of the region-specific homeotic gene spalt during Drosophila tracheal system development. Dev. Camb. Engl. *122*, 2215–2223.

Lando, D., Peet, D.J., Gorman, J.J., Whelan, D.A., Whitelaw, M.L. and Bruick, R.K. (2002). FIH-1 is an asparaginyl hydroxylase enzyme that regulates the transcriptional activity of hypoxia-inducible factor. Genes Dev. *16*, 1466–1471.

Lanet, E., Gould, A.P. and Maurange, C. (2013). Protection of neuronal diversity at the expense of neuronal numbers during nutrient restriction in the Drosophila visual system. Cell Rep. *3*, 587–594.

Lange, C., Turrero Garcia, M., Decimo, I., Bifari, F., Eelen, G., Quaegebeur, A., Boon, R., Zhao, H., Boeckx, B., Chang, J., et al. (2016). Relief of hypoxia by angiogenesis promotes neural stem cell differentiation by targeting glycolysis. EMBO J. *35*, 924–941.

Lavista-Llanos, S., Centanin, L., Irisarri, M., Russo, D.M., Gleadle, J.M., Bocca, S.N., Muzzopappa, M., Ratcliffe, P.J. and Wappner, P. (2002). Control of the hypoxic response in Drosophila melanogaster by the basic helix-loop-helix PAS protein similar. Mol. Cell. Biol. *22*, 6842–6853.

Lee, K.E. and Simon, M.C. (2012). From stem cells to cancer stem cells: HIF takes the stage. Curr. Opin. Cell Biol. *24*, 232–235.

Lee, T., Hacohen, N., Krasnow, M. and Montell, D.J. (1996). Regulated Breathless receptor tyrosine kinase activity required to pattern cell migration and branching in the Drosophila tracheal system. Genes Dev. *10*, 2912–2921.

Levine, A.J. and Puzio-Kuter, A.M. (2010). The control of the metabolic switch in cancers by oncogenes and tumor suppressor genes. Science *330*, 1340–1344.

Li, L. and Xie, T. (2005). Stem cell niche: structure and function. Annu. Rev. Cell Dev. Biol. *21*, 605–631.

Li, S., Wang, H. and Groth, C. (2014). Drosophila neuroblasts as a new model for the study of stem cell self-renewal and tumour formation. Biosci. Rep. *34*.

Liberti, M.V. and Locasale, J.W. (2016). The Warburg Effect: How Does it Benefit Cancer Cells? Trends Biochem. Sci. *41*, 211–218.

Lisztwan, J., Imbert, G., Wirbelauer, C., Gstaiger, M. and Krek, W. (1999). The von Hippel-Lindau tumor suppressor protein is a component of an E3 ubiquitin-protein ligase activity. Genes Dev. *13*, 1822–1833.

Liu, G., Roy, J. and Johnson, E.A. (2006). Identification and function of hypoxia-response genes in Drosophila melanogaster. Physiol. Genomics *25*, 134–141.

Llimargas, M. and Casanova, J. (1999). EGF signalling regulates cell invagination as well as cell migration during formation of tracheal system in Drosophila. Dev. Genes Evol. *209*, 174–179.

Louvi, A. and Artavanis-Tsakonas, S. (2006). Notch signalling in vertebrate neural development. Nat. Rev. Neurosci. *7*, 93–102.

Mannello, F., Medda, V. and Tonti, G.A. (2011). Hypoxia and neural stem cells: from invertebrates to brain cancer stem cells. Int. J. Dev. Biol. *55*, 569–581.

Manning, G. and Krasnow, M.A. (1993). Development of the Drosophila tracheal system. In The Development of Drosophila melanogaster (ed. Bate M. and Martinez-Arias A.). Cold Spring Harbor, New York: Cold Spring Harbor Laboratory Press. pp. 609–685.

Mardon, G., Solomon, N.M. and Rubin, G.M. (1994). dachshund encodes a nuclear protein required for normal eye and leg development in Drosophila. Dev. Camb. Engl. *120*, 3473–3486.

Maxwell, P.H., Pugh, C.W. and Ratcliffe, P.J. (1993). Inducible operation of the erythropoietin 3' enhancer in multiple cell lines: evidence for a widespread oxygen-sensing mechanism. Proc. Natl. Acad. Sci. U. S. A. *90*, 2423–2427.

Mazumdar, J., O'Brien, W.T., Johnson, R.S., LaManna, J.C., Chavez, J.C., Klein, P.S. and Simon, M.C. (2010). O2 regulates stem cells through Wnt/β-catenin signalling. Nat. Cell Biol. *12*, 1007–1013.

McConnell, S.K. (1995). Constructing the cerebral cortex: neurogenesis and fate determination. Neuron *15*, 761–768.

McCord, A.M., Jamal, M., Shankavaram, U.T., Shankavarum, U.T., Lang, F.F., Camphausen, K. and Tofilon, P.J. (2009). Physiologic oxygen concentration enhances the stem-like properties of CD133+ human glioblastoma cells in vitro. Mol. Cancer Res. MCR *7*, 489–497.

McKinley, B.A. and Butler, B.D. (1999). Comparison of skeletal muscle PO2, PCO2, and pH with gastric tonometric P(CO2) and pH in hemorrhagic shock. Crit. Care Med. *27*, 1869–1877.

Meinertzhagen, I.A. and Hanson, T.E. (1993). The development of the optic lobe. In The Development of Drosophila melanogaster (ed. Bate M. and Martinez-Arias A.). Cold Spring Harbor, New York: Cold Spring Harbor Laboratory Press. pp.1363–1491

Melamed, J. and Trujillo-Cenóz, O. (1975). The fine structure of the eye imagina disks in muscoid flies. J. Ultrastruct. Res. *51*, 79–93.

Melnattur, K.V. and Lee, C.-H. (2011). Visual circuit assembly in Drosophila. Dev. Neurobiol. *71*, 1286–1296.

Metzger, R.J. and Krasnow, M.A. (1999). Genetic control of branching morphogenesis. Science *284*, 1635–1639.

Mik, E.G., van Leeuwen, T.G., Raat, N.J. and Ince, C. (2004). Quantitative determination of localized tissue oxygen concentration in vivo by two-photon excitation phosphorescence lifetime measurements. J. Appl. Physiol. Bethesda Md 1985 *97*, 1962–1969.

Milosevic, J., Schwarz, S.C., Krohn, K., Poppe, M., Storch, A. and Schwarz, J. (2005). Low atmospheric oxygen avoids maturation, senescence and cell death of murine mesencephalic neural precursors. J. Neurochem. *92*, 718–729.

Misra, T., Baccino Calace, M., Meyenhofer, F., Armenta-Calderón, R., Gorr, T. A., Frei C., Cantera R., Egger, B., Luschnig, S. (2016). A genetically encoded biosensor for visualizing hypoxia responses in vivo (Submitted)

Miyata, T., Kawaguchi, A., Saito, K., Kawano, M., Muto, T. and Ogawa, M. (2004). Asymmetric production of surface-dividing and non-surface-dividing cortical progenitor cells. Dev. Camb. Engl. *131*, 3133–3145.

Mohyeldin, A., Garzón-Muvdi, T. and Quiñones-Hinojosa, A. (2010). Oxygen in stem cell biology: a critical component of the stem cell niche. Cell Stem Cell *7*, 150–161.

Morante, J. and Desplan, C. (2004). Building a projection map for photoreceptor neurons in the Drosophila optic lobes. Semin. Cell Dev. Biol. *15*, 137–143.

Morrison, S.J., Csete, M., Groves, A.K., Melega, W., Wold, B. and Anderson, D.J. (2000). Culture in reduced levels of oxygen promotes clonogenic sympathoadrenal differentiation by isolated neural crest stem cells. J. Neurosci. Off. J. Soc. Neurosci. *20*, 7370–7376.

Mortimer, N.T. and Moberg, K.H. (2013). The archipelago ubiquitin ligase subunit acts in target tissue to restrict tracheal terminal cell branching and hypoxic-induced gene expression. PLoS Genet. *9*, e1003314.

Moulder, J.E. and Rockwell, S. (1987). Tumor hypoxia: its impact on cancer therapy. Cancer Metastasis Rev. *5*, 313–341.

Nambu, J.R., Chen, W., Hu, S. and Crews, S.T. (1996). The Drosophila melanogaster similar bHLH-PAS gene encodes a protein related to human hypoxia-inducible factor 1 alpha and Drosophila single-minded. Gene *172*, 249–254.

Nassif, C., Noveen, A. and Hartenstein, V. (2003). Early development of the Drosophila brain: III. The pattern of neuropile founder tracts during the larval period. J. Comp. Neurol. *455*, 417–434.

Noctor, S.C., Martínez-Cerdeño, V., Ivic, L. and Kriegstein, A.R. (2004). Cortical neurons arise in symmetric and asymmetric division zones and migrate through specific phases. Nat. Neurosci. *7*, 136–144.

Nohe, A., Keating, E., Knaus, P. and Petersen, N.O. (2004). Signal transduction of bone morphogenetic protein receptors. Cell. Signal. *16*, 291–299.

Noirot-Timothée, C., Graf, F. and Noirot, C. (1982). The specialization of septate junctions in regions of tricellular junctions. II. Pleated septate junctions. J. Ultrastruct. Res. *78*, 152–165.

Nurse, C.A. and Vollmer, C. (1997). Role of basic FGF and oxygen in control of proliferation, survival, and neuronal differentiation in carotid body chromaffin cells. Dev. Biol. *184*, 197–206.

Nwaigwe, C.I., Roche, M.A., Grinberg, O. and Dunn, J.F. (2000). Effect of hyperventilation on brain tissue oxygenation and cerebrovenous PO2 in rats. Brain Res. *868*, 150–156.

Olivotto, M. and Paoletti, F. (1981). The role of respiration in tumor cell transition from the noncycling to the cycling state. J. Cell. Physiol. *107*, 243–249.

Olivotto, M., Arcangeli, A., Caldini, R., Chevanne, M., Cipolleschi, M.G. and Dello Sbarba, P. (1984). Metabolic aspects of cell cycle regulation in normal and cancer cells. Toxicol. Pathol. *12*, 369–373.

O'Neill, E.M., Rebay, I., Tjian, R. and Rubin, G.M. (1994). The activities of two Ets-related transcription factors required for Drosophila eye development are modulated by the Ras/MAPK pathway. Cell *78*, 137–147.

Orihara-Ono, M., Toriya, M., Nakao, K. and Okano, H. (2011). Downregulation of Notch mediates the seamless transition of individual Drosophila neuroepithelial progenitors into optic medullar neuroblasts during prolonged G1. Dev. Biol. *351*, 163–175.

Panchision, D.M. (2009). The role of oxygen in regulating neural stem cells in development and disease. J. Cell. Physiol. *220*, 562–568.

Pardal, R., Ortega-Sáenz, P., Durán, R. and López-Barneo, J. (2007). Glia-like stem cells sustain physiologic neurogenesis in the adult mammalian carotid body. Cell *131*, 364–377.

Parmar, K., Mauch, P., Vergilio, J.-A., Sackstein, R. and Down, J.D. (2007). Distribution of hematopoietic stem cells in the bone marrow according to regional hypoxia. Proc. Natl. Acad. Sci. U. S. A. *104*, 5431–5436.

Parnas, D., Haghighi, A.P., Fetter, R.D., Kim, S.W. and Goodman, C.S. (2001). Regulation of postsynaptic structure and protein localization by the Rho-type guanine nucleotide exchange factor dPix. Neuron *32*, 415–424.

Patra, K.C., Wang, Q., Bhaskar, P.T., Miller, L., Wang, Z., Wheaton, W., Chandel, N., Laakso, M., Muller, W.J., Allen, E.L., et al. (2013). Hexokinase 2 is required for tumor initiation and maintenance and its systemic deletion is therapeutic in mouse models of cancer. Cancer Cell *24*, 213–228.

Pereanu, W., Spindler, S., Cruz, L. and Hartenstein, V. (2007). Tracheal development in the Drosophila brain is constrained by glial cells. Dev. Biol. *302*, 169–180.

Pistollato, F., Chen, H.-L., Schwartz, P.H., Basso, G. and Panchision, D.M. (2007). Oxygen tension controls the expansion of human CNS precursors and the generation of astrocytes and oligodendrocytes. Mol. Cell. Neurosci. *35*, 424–435.

Raymond, J. and Segrè, D. (2006). The effect of oxygen on biochemical networks and the evolution of complex life. Science *311*, 1764–1767.

Reichman-Fried, M. and Shilo, B.Z. (1995a). Breathless, a Drosophila FGF receptor homolog, is required for the onset of tracheal cell migration and tracheole formation. Mech. Dev. *52*, 265–273.

Reichman-Fried, M. and Shilo, B.Z. (1995b). Breathless, a Drosophila FGF receptor homolog, is required for the onset of tracheal cell migration and tracheole formation. Mech. Dev. *52*, 265–273.

Reichman-Fried, M., Dickson, B., Hafen, E. and Shilo, B.Z. (1994). Elucidation of the role of breathless, a Drosophila FGF receptor homolog, in tracheal cell migration. Genes Dev. *8*, 428–439.

Reubinoff, B.E., Pera, M.F., Fong, C.Y., Trounson, A. and Bongso, A. (2000). Embryonic stem cell lines from human blastocysts: somatic differentiation in vitro. Nat. Biotechnol. *18*, 399–404.

Rister, J., Pauls, D., Schnell, B., Ting, C.-Y., Lee, C.-H., Sinakevitch, I., Morante, J., Strausfeld, N.J., Ito, K. and Heisenberg, M. (2007). Dissection of the peripheral motion channel in the visual system of Drosophila melanogaster. Neuron *56*, 155–170.

Romero, N.M., Irisarri, M., Roth, P., Cauerhff, A., Samakovlis, C. and Wappner, P. (2008). Regulation of the Drosophila hypoxia-inducible factor alpha Sima by CRM1-dependent nuclear export. Mol. Cell. Biol. *28*, 3410–3423.

Roy, S., Khanna, S., Wallace, W.A., Lappalainen, J., Rink, C., Cardounel, A.J., Zweier, J.L. and Sen, C.K. (2003). Characterization of perceived hyperoxia in isolated primary cardiac fibroblasts and in the reoxygenated heart. J. Biol. Chem. *278*, 47129–47135.

Saito, A., Maier, C.M., Narasimhan, P., Nishi, T., Song, Y.S., Yu, F., Liu, J., Lee, Y.-S., Nito, C., Kamada, H., et al. (2005). Oxidative stress and neuronal death/survival signaling in cerebral ischemia. Mol. Neurobiol. *31*, 105–116.

Saltzman, D.J., Toth, A., Tsai, A.G., Intaglietta, M. and Johnson, P.C. (2003). Oxygen tension distribution in postcapillary venules in resting skeletal muscle. Am. J. Physiol. Heart Circ. Physiol. *285*, H1980-1985.

Samakovlis, C., Hacohen, N., Manning, G., Sutherland, D.C., Guillemin, K. and Krasnow, M.A. (1996). Development of the Drosophila tracheal system occurs by a series of morphologically distinct but genetically coupled branching events. Dev. Camb. Engl. *122*, 1395–1407.

Sanes, J.R. and Zipursky, S.L. (2010). Design principles of insect and vertebrate visual systems. Neuron *66*, 15–36.

Scadden, D.T. (2006). The stem-cell niche as an entity of action. Nature *441*, 1075–1079.

Schofield, R. (1978). The relationship between the spleen colony-forming cell and the haemopoietic stem cell. Blood Cells *4*, 7–25.

Sepp K. J. and Auld V. J. (1999). Conversion of lacZ enhancer trap lines to GAL4 lines using targeted transposition in Drosophila melanogaster. Genetics *151*, 1093-1101.

Seylaz, J. and Pinard, E. (1978). Continuous measurement of gas partial pressures in intracerebral tissue. J. Appl. Physiol. *44*, 528–533.

Shilo, B.Z., Gabay, L., Glazer, L., Reichman-Fried, M., Wappner, P., Wilk, R. and Zelzer, E. (1997). Branching morphogenesis in the Drosophila tracheal system. Cold Spring Harb. Symp. Quant. Biol. *62*, 241–247.

Shonat, R.D. and Johnson, P.C. (1997). Oxygen tension gradients and heterogeneity in venous microcirculation: a phosphorescence quenching study. Am. J. Physiol. *272*, H2233-2240.

Shonat, R.D., Wilson, D.F., Riva, C.E. and Pawlowski, M. (1992). Oxygen distribution in the retinal and choroidal vessels of the cat as measured by a new phosphorescence imaging method. Appl. Opt. *31*, 3711–3718.

Shonat, R.D., Richmond, K.N. and Johnson, P.C. (1995). Phosphorescence quenching and the microcirculation: An automated, multipoint oxygen tension measuring instrument. Rev. Sci. Instrum. *66*, 5075–5084.

Simon, M.C. and Keith, B. (2008). The role of oxygen availability in embryonic development and stem cell function. Nat. Rev. Mol. Cell Biol. *9*, 285–296.

Simsek, T., Kocabas, F., Zheng, J., Deberardinis, R.J., Mahmoud, A.I., Olson, E.N., Schneider, J.W., Zhang, C.C. and Sadek, H.A. (2010). The distinct metabolic profile of hematopoietic stem cells reflects their location in a hypoxic niche. Cell Stem Cell *7*, 380–390.

Slack, J.M.W. (2008). Origin of stem cells in organogenesis. Science *322*, 1498–1501.

Snodgrass, R.E. (1939). The Principles of Insect Physiology. Science *90*, 159–159.

Sonnenfeld, M., Ward, M., Nystrom, G., Mosher, J., Stahl, S. and Crews, S. (1997). The Drosophila tango gene encodes a bHLH-PAS protein that is orthologous to mammalian Arnt and controls CNS midline and tracheal development. Dev. Camb. Engl. *124*, 4571–4582.

Sousa-Nunes, R., Yee, L.L. and Gould, A.P. (2011). Fat cells reactivate quiescent neuroblasts via TOR and glial insulin relays in Drosophila. Nature *471*, 508–512.

Southall, T.D., Gold, K.S., Egger, B., Davidson, C.M., Caygill, E.E., Marshall, O.J. and Brand, A.H. (2013). Cell-type-specific profiling of gene expression and chromatin binding without cell isolation: assaying RNA Pol II occupancy in neural stem cells. Dev. Cell *26*, 101–112.

Storch, A., Paul, G., Csete, M., Boehm, B.O., Carvey, P.M., Kupsch, A. and Schwarz, J. (2001). Long-term proliferation and dopaminergic differentiation of human mesencephalic neural precursor cells. Exp. Neurol. *170*, 317–325.

Studer, L., Csete, M., Lee, S.H., Kabbani, N., Walikonis, J., Wold, B. and McKay, R. (2000). Enhanced proliferation, survival, and dopaminergic differentiation of CNS precursors in lowered oxygen. J. Neurosci. Off. J. Soc. Neurosci. *20*, 7377–7383.

Sutherland, D., Samakovlis, C. and Krasnow, M.A. (1996). branchless encodes a Drosophila FGF homolog that controls tracheal cell migration and the pattern of branching. Cell *87*, 1091–1101.

Takubo, K., Goda, N., Yamada, W., Iriuchishima, H., Ikeda, E., Kubota, Y., Shima, H., Johnson, R.S., Hirao, A., Suematsu, M., et al. (2010). Regulation of the HIF-1alpha level is essential for hematopoietic stem cells. Cell Stem Cell *7*, 391–402.

Tannock, I.F. (1968). The relation between cell proliferation and the vascular system in a transplanted mouse mammary tumour. Br. J. Cancer *22*, 258–273.

Technau, G.M. (2009). Brain Development in Drosophila melanogaster (Springer Science & Business Media).

Teicher, B.A. (1994). Hypoxia and drug resistance. Cancer Metastasis Rev. *13*, 139–168.

Tennessen, J.M., Baker, K.D., Lam, G., Evans, J. and Thummel, C.S. (2011). The Drosophila estrogen-related receptor directs a metabolic switch that supports developmental growth. Cell Metab. *13*, 139–148.

Thomson, J.A., Itskovitz-Eldor, J., Shapiro, S.S., Waknitz, M.A., Swiergiel, J.J., Marshall, V.S. and Jones, J.M. (1998). Embryonic stem cell lines derived from human blastocysts. Science *282*, 1145–1147.

Tøndevold, E., Eriksen, J. and Jansen, E. (1979). Observations on long bone medullary pressures in relation to arterial PO2, PCO2 and pH in the anaesthetized dog. Acta Orthop. Scand. *50*, 645–651.

Tubiana, M., Dutreix, J. and Wambersie, A. (1990). Introduction to radiobiology (United Kingdom: Taylor and Francis).

Uv, A., Cantera, R. and Samakovlis, C. (2003). Drosophila tracheal morphogenesis: intricate cellular solutions to basic plumbing problems. Trends Cell Biol. *13*, 301–309.

Vander Heiden, M.G., Cantley, L.C. and Thompson, C.B. (2009). Understanding the Warburg effect: the metabolic requirements of cell proliferation. Science *324*, 1029–1033.

Wang, G.L. and Semenza, G.L. (1995). Purification and characterization of hypoxia-inducible factor 1. J. Biol. Chem. *270*, 1230–1237.

Wang, H., Chen, X., He, T., Zhou, Y. and Luo, H. (2013). Evidence for tissue-specific Jak/STAT target genes in Drosophila optic lobe development. Genetics *195*, 1291–1306.

Wang, W., Liu, W., Wang, Y., Zhou, L., Tang, X. and Luo, H. (2011). Notch signaling regulates neuroepithelial stem cell maintenance and neuroblast formation in Drosophila optic lobe development. Dev. Biol. *350*, 414–428.

Ward, P.S. and Thompson, C.B. (2012). Metabolic reprogramming: a cancer hallmark even warburg did not anticipate. Cancer Cell *21*, 297–308.

Welch, W.J., Baumgärtl, H., Lübbers, D. and Wilcox, C.S. (2001). Nephron pO2 and renal oxygen usage in the hypertensive rat kidney. Kidney Int. *59*, 230–237.

Weng, M., Haenfler, J.M. and Lee, C.-Y. (2012). Changes in Notch signaling coordinates maintenance and differentiation of the Drosophila larval optic lobe neuroepithelia. Dev. Neurobiol. *72*, 1376–1390.

Whalen, W.J., Riley, J. and Nair, P. (1967). A microelectrode for measuring intracellular PO2. J. Appl. Physiol. *23*, 798–801.

White, K. and Kankel, D.R. (1978). Patterns of cell division and cell movement in the formation of the imaginal nervous system in Drosophila melanogaster. Dev. Biol. *65*, 296–321.

Wigglesworth, V. B. 1954. Growth and regeneration in the tracheal system of an insect, Rhodnius prolixus (Hemiptera). Quart J. Micr. Sci. 95, 115-137.

Wild, J.M., Fichele, S., Woodhouse, N., Paley, M.N.J., Kasuboski, L. and van Beek, E.J.R. (2005). 3D volume-localized pO2 measurement in the human lung with 3He MRI. Magn. Reson. Med. *53*, 1055–1064.

Wilk, R., Weizman, I. and Shilo, B.Z. (1996). trachealess encodes a bHLH-PAS protein that is an inducer of tracheal cell fates in Drosophila. Genes Dev. *10*, 93–102.

Wölfle, D. and Jungermann, K. (1985). Long-term effects of physiological oxygen concentrations on glycolysis and gluconeogenesis in hepatocyte cultures. Eur. J. Biochem. FEBS *151*, 299–303.

Wong, D.M., Shen, Z., Owyang, K.E. and Martinez-Agosto, J.A. (2014). Insulin- and warts-dependent regulation of tracheal plasticity modulates systemic larval growth during hypoxia in Drosophila melanogaster. PloS One *9*, e115297.

Yasugi, T., Umetsu, D., Murakami, S., Sato, M. and Tabata, T. (2008). Drosophila optic lobe neuroblasts triggered by a wave of proneural gene expression that is negatively regulated by JAK/STAT. Dev. Camb. Engl. *135*, 1471–1480.

Yin, T. and Li, L. (2006). The stem cell niches in bone. J. Clin. Invest. *116*, 1195–1201.

Young, I.S. and Woodside, J.V. (2001). Antioxidants in health and disease. J. Clin. Pathol. *54*, 176–186.

Young, W.K., Vojnovic, B. and Wardman, P. (1996). Measurement of oxygen tension in tumours by time-resolved fluorescence. Br. J. Cancer. Suppl. *27*, S256-259.

Yu, D.-Y. and Cringle, S.J. (2005). Retinal degeneration and local oxygen metabolism. Exp. Eye Res. *80*, 745–751.

Zeng, W., Wan, R., Zheng, Y., Singh, S.R. and Wei, Y. (2011). Hypoxia, stem cells and bone tumor. Cancer Lett. *313*, 129–136.

Zhang, J., Niu, C., Ye, L., Huang, H., He, X., Tong, W.-G., Ross, J., Haug, J., Johnson, T., Feng, J.Q., et al. (2003). Identification of the haematopoietic stem cell niche and control of the niche size. Nature *425*, 836–841.